

Lehrstuhl für Ergonomie
der Technischen Universität München

Vertical interior cooling system for passenger cars:
Trials and evaluation of feasibility, thermal comfort and energy efficiency

Paul E. B. Stuke

Vollständiger Abdruck der von der Fakultät für Maschinenwesen
der Technischen Universität München
zur Erlangung des akademischen Grades eines
Doktor-Ingenieurs (Dr.-Ing.) genehmigten Dissertation.

Vorsitzender: Univ.- Prof. Dr.-Ing. Veit St. Senner

Prüfer der Dissertation:

1. Univ.-Prof. Dr. phil. Klaus Bengler
2. Univ.-Prof. Dr.-Ing. Markus Lienkamp

Die Dissertation wurde am 22.06.2016 bei der Technischen Universität München
eingereicht und durch die Fakultät für Maschinenwesen am 18.10.2016
angenommen.

Acknowledgements and Thanks

First and foremost I want to express my thanks to my supervisors and mentors Dr. Daniel Gleyzes and Prof. Dr. phil. Klaus Bengler for their support, help and guidance during my work on the vehicle project and the dissertation.

Thank you Prof. Dr.-Ing. Markus Lienkamp for not only being the second corrector of my thesis, but also for having presented me with the possibility to join the research programme TUM CREATE in the first place, providing me with the environment and funding for the present thesis.

Thanks to all my colleagues at TUM CREATE and TUM for their input and the discussion on the present topic, foremost, but not exclusively, Marius Janta and Christoph Futter.

Thanks to all my students for their exceptional work and support, also the ones that were not mentioned by name in this thesis.

Thanks go to all participants in the experiments for sweating or freezing for a couple of hours in a plywood cage.

Heribert Hart and Michael Arzberger from the LfE workshop provided invaluable help with the whole experiment setup and everything regarding the climate chamber. Many thanks!

My father Ulrich Stuke deserves abundant thanks for support on all things electrical and the loan of several pieces of equipment for the experiment setup.

Last but not least, someone who deserves not only my thanks, but also deserve every reader's gratitude; my stepfather Bernard Doran did the meticulous proof reading and correction of multiple horrid English sentences.

Table of contents

1	Introduction.....	1
1.1	Motivation.....	1
1.2	Outline of thesis.....	2
2	Fundamentals and state of the art.....	3
2.1	Thermodynamic basis.....	3
2.1.1	Psychrometrics.....	3
2.1.2	Heat transfer.....	5
2.2	Human thermal physiology.....	6
2.2.1	Metabolic rate.....	6
2.2.2	Thermoregulation.....	7
2.2.3	Thermal perception.....	8
2.3	Thermal comfort.....	9
2.3.1	Clothing.....	10
2.3.2	Thermal comfort models.....	11
2.3.3	Local thermal comfort.....	15
2.3.4	Draught.....	17
2.3.5	Temperature gradients.....	18
2.3.6	Scales for thermal perception and thermal comfort.....	20
2.3.7	Standards for thermal comfort.....	22
2.4	Vehicle heating ventilation and air conditioning.....	22
2.4.1	History of vehicle HVAC.....	22
2.4.2	State of the art HVAC control.....	24
2.4.3	State of research in future vehicle HVAC.....	26
3	Procedural methods and research questions.....	30
4	Technical solution of new concept for interior cooling.....	31
4.1	HVAC concept in the prototype.....	31
4.2	Air path.....	33
4.2.1	HVAC unit.....	33
4.2.2	Air distribution box and air ducts.....	34
4.3	Ventilated seats.....	37
4.4	Control strategy: Comfort oriented HMI.....	38
4.5	Lessons learned and discussion.....	41
5	Ergonomic studies for local cooling.....	42
5.1	Basic idea and anticipated outcome.....	42

5.2	Experiment environment	44
5.2.1	Experiment room.....	45
5.2.2	Vehicle Mock-up.....	46
5.2.3	Sensors	49
5.2.4	Clothing for the experiments.....	54
5.2.5	Questionnaire and evaluation scales	54
5.3	Experiment 1: Overhead Cooling	55
5.3.1	Pre-test for Experiment 1.....	55
5.3.2	Test sequence Experiment 1	56
5.3.3	Participants Experiment 1.....	57
5.3.4	Results Experiment 1.....	58
5.3.5	Discussion Experiment 1	61
5.4	Experiment 2: Seat ventilation.....	62
5.4.1	Pre-test for Experiment 2	63
5.4.2	Test sequence Experiment 2.....	63
5.4.3	Participants Experiment 2	64
5.4.4	Results Experiment 2.....	65
5.4.5	Discussion Experiment 2.....	68
5.5	Experiment 3: Combined overhead cooling and seat ventilation.....	69
5.5.1	Pre-tests for Experiment 3.....	69
5.5.2	Test sequence Experiment 3.....	70
5.5.3	Participants Experiment 3	70
5.5.4	Results Experiment 3.....	71
5.5.5	Discussion Experiment 3.....	73
6	Evaluation of energy efficiency	75
7	Discussion and outlook.....	81
7.1	RQ1: Is local, vertical cooling feasible in an automotive context?	81
7.2	RQ2: Does local, vertical cooling improve comfort and efficiency?.....	81
7.3	RQ3: What are the operative limitations of such a system?.....	82
7.4	How can the calculation be optimised?	82
7.5	How can the technical solution be optimised?	83
7.6	What should be considered for future work?	84

List of abbreviations and symbols

Abbreviations

ABS	acrylonitrile butadiene styrene
AC or A/C	air conditioning
ACC	automatic climate control
CFD	computational fluid dynamics
CP-50	category partitioning scale
DBT	dry bulb temperature
ECI	equatorial climate index
ET	effective temperature
ET*	new effective temperature
FAT	Forschungsvereinigung Automobiltechnik e.V.
FH	Fachhochschule
FPC	Fiala's thermal physiology and comfort model
GUI	graphical user interface
HMI	human-machine interface
HV	high voltage
HVAC	heating ventilation and air conditioning
ibp	Institut für Bauphysik (Fraunhofer)
IR	infrared
LfE	Lehrstuhl für Ergonomie (TUM)
LV	low voltage
NAFTA	Northern American Free Trade Agreement states
NEA	National Environment Agency Singapore
NTC	negative temperature coefficient
OEM	original equipment manufacturer
PD	percentage of dissatisfied
PD	persons dissatisfied
PE	polyethylene
PMV	predicted mean vote
PPD	predicted percent dissatisfied
PTC	positive temperature coefficient
r.h.	relative humidity
RWTH	Rheinisch Westphälische Technische Hochschule
ROW	rest of world
RQ	research question
SLS	selective laser sintering

TUM	Technische Universität München
US	United States
WW	western world

Symbols

A	area
A_D	body surface area (DuBois area)
c_p	specific heat capacity of air
C	convection loss
E_{diff}	evaporation heat loss due to vapour diffusion through the skin
E_{resp}	respiration latent heat loss
E_{rsw}	heat loss due to evaporation of regulatory sweating from the skin
f_{cl}	ratio of clothed to exposed body surface
h_c	convection conductance
h	specific enthalpy
\dot{H}	enthalpy
I	current
I_{cl}	insulation of clothing
K	heat transfer from skin to clothing surface
L	dry respiration loss
\dot{m}	mass flow
$\dot{m}_{air\ moisture}$	mass flow of water contained in air flow
$\dot{m}_{condensate, evap}$	water condensing at evaporator
M	metabolisms energy
N	number of collected data
n_{pass}	number of occupants
p	pressure
P	power
\dot{Q}	heat flow
\dot{Q}_{body}	heat flow by the warmed car body due to solar irradiation
\dot{Q}_{pass}	thermal radiation of occupants
R	radiation loss
R_{th}	thermal resistance
r_w	specific enthalpy of vaporisation
T	temperature
U	coefficient of heat transmission
U	voltage

v_{air}	mean air velocity
x	specific humidity
$x_1 \dots x_N$	collected data set
\bar{x}	arithmetic mean of collected data set
Σ_{12}	radiation constant
ρ_{air}	density of air
σ	standard deviation
η	mechanical efficiency
φ	relative humidity

Indices

<i>air</i>	air
<i>amb</i>	ambient
<i>cabin</i>	inside cabin
<i>cl</i>	on clothing surface
<i>el</i>	electrical
<i>evap</i>	after evaporator
<i>fa</i>	fresh air
<i>i</i>	control variable
<i>in</i>	into cabin
<i>loc</i>	at local outlet
<i>max</i>	maximum
<i>mean</i>	mean
<i>min</i>	minimum
<i>neutral</i>	neutral
<i>out</i>	out of cabin
<i>outlet</i>	at outlet
<i>persp</i>	perspiration
<i>rec</i>	recirculation
<i>sat</i>	at state of saturation
<i>vap</i>	vapour

Non-SI units

<i>clo</i>	clothing value
<i>met</i>	metabolical rate

List of Figures

- Figure 1: HVAC impact on comfort and energy efficiency (Bubb, 2003; Stuke, 2015)
- Figure 2: Singapore (Changi Airport) hourly temperature and humidity data (NEA Singapore, 2012) in psychrometric chart
- Figure 3: Heat production and heat loss through evaporation and core and skin temperatures respectively at different ambient temperatures (adapted from Klinke et al., 2010).
- Figure 4: Mean distribution of cold and warm receptors on the skin (Klinke et al., 2010; Schmidt, Lang, & Heckmann, 2010)
- Figure 5: Static response of cold and warm receptors (left) (Klinke et al., 2010), warm and cold thresholds depending on initial skin temperature (right) (Schmidt et al., 2010)
- Figure 6: Predicted Mean Vote (PMV) and Predicted Percentage of Dissatisfied (PPD) (Fanger, 1970)
- Figure 7: Singapore temperature data (monthly, 1948-2011) (NEA Singapore, 2012)
- Figure 8: Psychrometric chart, comfort zones and Singapore climate data
- Figure 9: Percentage of dissatisfied (PD) due to draught in ventilated spaces (Fanger & Christensen, 1986)
- Figure 10: Temperature distribution inside vehicle cabin (Kolb, 2004)
- Figure 11: Comfort votes after dynamic exposure to heating and cooling (adapted from Prestel, 2013)
- Figure 12: Air path through the HVAC unit: (1) recirculation flap, (2) blower, (3) filter, (4) evaporator, (5) heater
- Figure 13: Example of a simple manually controlled standard HVAC control panel.
- Figure 14: Example of an advanced HVAC control panel with automatic mode
- Figure 15: The electric taxi EVA by TUM CREATE (TUM CREATE, 2013)
- Figure 16: Seating layout and division in four climate zones in prototype vehicle EVA
- Figure 17: Vertical air flow distribution in prototype vehicle EVA (Stuke & Bengler, 2013)
- Figure 18: HVAC unit, takeover part from a VW Jetta
- Figure 19: Four-zone air distribution box (adapted from Jekelius, 2013)
- Figure 20: Integration of the air distribution box, temperature and mass flow flaps (left), flap motors (right)
- Figure 21: Air ducting for the front and rear left occupants (left), roof outlet [2], ceiling [3] perforated with holes [4], air duct from B-pillar [6] (right)
- Figure 22: Assembly and integration of HVAC unit, air distribution box (left) and air ducts (right) in EVA

- Figure 23: Air velocity (left) and pressure (right) simulation of front left air ducting system
- Figure 24: Ventilated seat (Lutz, 2013) with spacer fabric (Wellcool, 2013) and axial fans (ebm-papst, 2013b)
- Figure 25: The Adaptive Thermal Model's comfort zone (for Singapore) in a psychrometric chart
- Figure 26: Implemented HVAC control on the occupant's smartphone for a purpose-built electric vehicle.
- Figure 27: HVAC control board: HVAC and air flow overview (adapted from Rainer, 2013)
- Figure 28: Test person in the mock-up during the experiment
- Figure 29: Scenarios for local thermal conditioning
- Figure 30: Possible distribution of discomfort votes in section D (heating a cold cabin)
- Figure 31: Experiment setup in the climate chamber
- Figure 32: Setup of the overhead cooling system seat mock-up (compare Figure 28)
- Figure 33: Seat mock-up, modes of operation
- Figure 34: Seat with spacer fabric (operating mode two), segments for seat ventilation (Theissen, 2015)
- Figure 35: Overhead outlet with temperature sensor grid
- Figure 36: Wiring scheme for multiple temperature sensors
- Figure 37: Visualization of grid temperature distribution and mean in Matlab GUIDE
- Figure 38: Measured points for skin temperature (Mitchell & Wyndham, 1969)
- Figure 39: MSR data logger, humidity sensor and "T-3" temperature sensor
- Figure 40: Grid air flow velocity over potentiometer level and velocity distribution over grid area (Theissen, 2015)
- Figure 41: BAPPU-evo and Anemometer-evo
- Figure 42: Discomfort and thermal sensation in the pre-test (test person P1) (Theissen, 2015)
- Figure 43: Chosen cabin temperatures corresponding to a PMV = 0.5, 1.0 and 1.5
- Figure 44: Body and head discomfort votes for overhead ventilation test at 26.5°C (V1.0 - V1.3)
- Figure 45: Discomfort for body and head and thermal perception for head, torso and feet at 26.5°C (V1.0 – V1.3)
- Figure 46: Thermal discomfort over varying cabin and overhead outlet temperatures (interpolated between mean final votes of V1.0 – V1.10)
- Figure 47: Seat modes of operation in the test

- Figure 48: Body discomfort, perception and preference with seat ventilation (V2.1 - V2.4)
- Figure 49: Local thermal discomfort with seat ventilation (V2.1 - V2.4)
- Figure 50: Local thermal perception with seat ventilation (V2.1 - V2.4)
- Figure 51: Experiment 3 – overhead cooling and seat operation mode three
- Figure 52: Body discomfort, perception and preference with seat ventilation and overhead cooling (V3.1 – V3.3)
- Figure 53: Local thermal discomfort with seat ventilation and overhead cooling (V3.1 – V3.3)
- Figure 54: Local thermal perception with seat ventilation and overhead cooling (V3.1 – V3.3)
- Figure 55: Thermodynamic system boundaries and energy flows in a car
- Figure 56: Singapore (Changi Airport) hourly temperature, humidity and enthalpy (NEA Singapore, 2012)
- Figure 57: Cooling power at evaporator for one person or four persons, with and without recirculation
- Figure 58: Thermodynamic system boundaries and energy flows in a car with local outlet

List of Tables

- Table 1: Metabolic rates at different activities (Auliciems & Szokolay, 1997)
- Table 2: Variables affecting thermal comfort (collated from Auliciems & Szokolay, 1997; Fanger, 1970)
- Table 3: Insulating value of clothing elements (based on (ANSI/ASHRAE 55-2010))
- Table 4: Scale for thermal comfort vote by Prestel (2013)
- Table 5: Scale for thermal perception (DIN EN ISO 10551:2001)
- Table 6: Scale for thermal affective vote (DIN EN ISO 10551:2001)
- Table 7: Scale for thermal preference (DIN EN ISO 10551:2001)
- Table 8: CP-50 scale for discomfort (adapted from Ellermeier et al., 1991)
- Table 9: Comparative data of A/C and ACC penetration (Daly, 2006) (Note: NAFTA – Northern American Free Trade Agreement States, ROW – Rest of World, WW – Western World)
- Table 10: User settings, corresponding temperatures and seat ventilation levels (adapted from Lutz, 2013)
- Table 11: Data sheet climate chamber
- Table 12: Data sheet temperature sensor TS-NTC
- Table 13: Data sheet for MSR temperature and humidity sensors
- Table 14: Data sheet for anemometer-evo
- Table 15: Temperature combinations (and resulting overhead outlet temperature) for overhead cooling experiment
- Table 16: Participants main test overhead cooling
- Table 17: Temperature and ventilation setting in the seat test scenarios
- Table 18: Participants main test seat ventilation
- Table 19: Temperature and ventilation settings for experiment 3
- Table 20: Participants with seat ventilation and overhead cooling
- Table 21: Temperatures at evaporator and corresponding air mass flows
- Table 22: Electrical power and energy flow of overhead outlet and seat ventilation in the experiments
- Table 23: Possible energy reduction by raising the cabin temperature

1 Introduction

There is no doubt that future mobility will change. One look at the research fields of relevant universities in this field shows several big trends in automotive development. Both RWTH Aachen and the TUM for example are focusing their research on 'driver assistance', 'vehicle guiding', 'smart mobility', 'vehicle dynamics and control systems', 'lightweight', 'efficiency and energy management' and 'vehicle concepts' (RWTH, 10/1/2016.; TUM, 10/1/2016). The thrust in development is aimed at energy efficient and electric cars, and autonomous driving. Many universities and OEMs have already developed a number of electric cars (e.g. MUE by TUM, BMW i-Series, Tesla) or self-driving cars (e.g. Google, VW and Stanford). However transportation may look like in future, two factors will obviously play a major role in every research field: energy efficiency and driving comfort.

1.1 Motivation

The heating, ventilation and air conditioning (HVAC) system of a car influences both these factors strongly: It controls the thermal wellbeing of the cars' occupants, which is a fundamental parameter according to Bubb's (2003) Comfort Pyramid, while being the biggest secondary consumer in the car (Großmann, 2013).

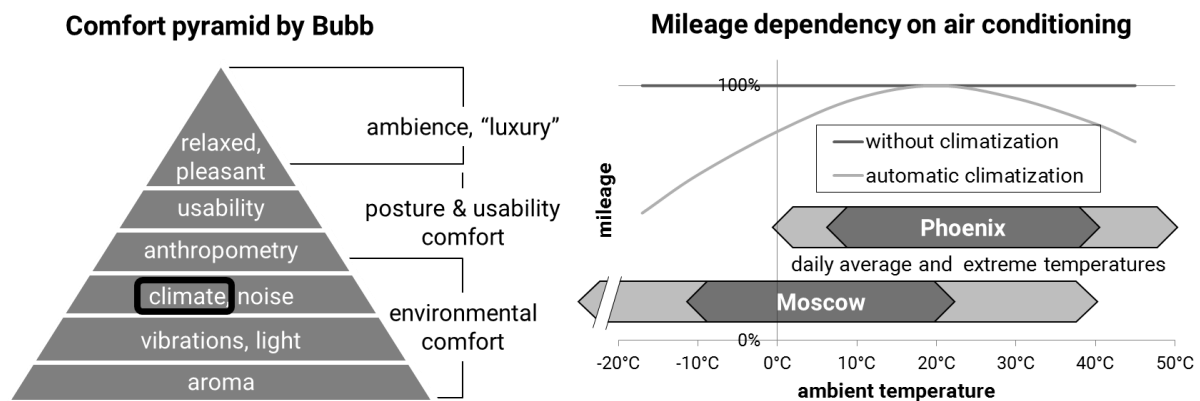


Figure 1: HVAC impact on comfort and energy efficiency (Bubb, 2003; Stuke, 2015)

Until now, thermal management of passenger compartments was developed for vehicles with a combustion engine. The design of heating and air conditioning systems is based on central systems, developed in a time when energy efficiency was not an issue. In the present thesis a new approach will be elaborated: based on human thermo-regulation and perception of thermal wellbeing, a comfort-oriented system will target the occupant only on those parts of the body that need conditioning. The aim: to increase comfort while reducing energy consumption.

1.2 Outline of thesis

The present thesis is divided into seven chapters, including the introduction.

Chapter 2 This chapter outlines the fundamentals necessary to understand heating ventilation and air conditioning in cars and the current state of the art. The thermodynamic basics needed to understand environmental conditions are explained. The basics of human physiology give an introduction on how human beings interact with the environment. Thermal comfort will be introduced as the subjective vote of the resulting human-environment interaction. Additional factors influencing thermal comfort are discussed, phenomena such as temperature gradients, dynamic responses and local thermal comfort are explained. Standards and evaluation scales covering thermal comfort are introduced. Further, the history and state of the art of vehicle air conditioning will be covered. Finally, an overview on the current state of research is given.

Chapter 3 The research idea of a vertical, local cooling application is introduced and three research questions are postulated based on the fundamentals and literature review. The project plan for the research is presented: Technical solution, ergonomic studies, energy efficiency calculation.

Chapter 4 The technical solution is developed and exercised on the EVA electric taxi prototype. This covers the design and dimensioning of the overhead outlets and the air distribution components up to prototyping and manufacture of the parts, as well as the design and the components for seat ventilation. Finally, the embedding of all active systems and sensors into a comfort-oriented control strategy is described, including the development of a customised HMI concept.

Chapter 5 The ergonomic studies in this chapter cover three cooling configurations: overhead cooling, seat ventilation and a combination of the two systems. The experimental environment is described, including the climate chamber used for the experiments, the build-up of the cabin and the system mock-ups. Experiments are conducted with a selected sample of human participants and the results presented and discussed.

Chapter 6 The energy efficiency calculation is carried out to evaluate the potential of the vertical, local cooling application and compared with the measurements taken in the experiments

Chapter 7 The final chapter covers discussion of the results obtained, elaborates lessons learned and provides an outlook on future work.

2 Fundamentals and state of the art

Understanding vehicle air conditioning requires some fundamental knowledge on both the technical side i.e. the car as well as the human side i.e. the driver (or the passengers). This chapter gives an overview on the important terminology and contextual integration in the area of energy systems and heat transfer, physiology, thermal sensation and thermal comfort as well as technical and academic studies and solutions.

2.1 Thermodynamic basis

Conditioning air for a cars' interior is not only raising or lowering the temperature. More than just this factor has to be taken into account, which influence the perception of a climatic condition. "Air conditioning" for human living and working spaces is always the desire to achieve a pleasant and acceptable indoor climate in a surrounding with unfavourable conditions. It is therefore important to know the defining factors of the surrounding and the desired indoor conditions.

2.1.1 Psychrometrics

The atmosphere is a mixture of air and water vapour. Psychrometrics¹ is the analysis of conditions and processes looking at the thermodynamic properties of this mixture (ASHRAE, 2013). Understanding psychrometrics lets us describe and visualise climatic conditions comprehensively. Visualization can be done by the psychrometric chart or the h-x-diagram. Figure 2 shows a psychrometric chart exemplary with the climatic conditions for Singapore in the years 2000 to 2012.

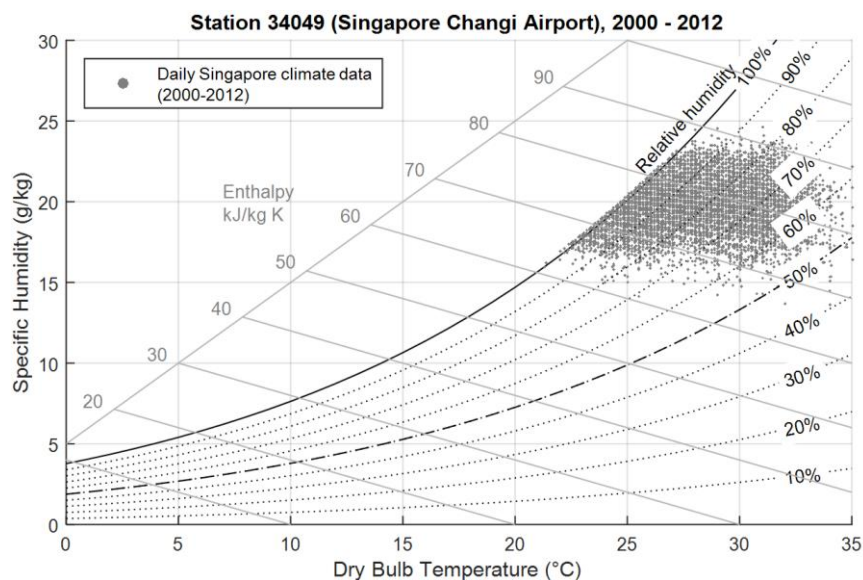


Figure 2: Singapore (Changi Airport) hourly temperature and humidity data (NEA Singapore, 01/12/2012) in psychrometric chart

¹ Not to be confused with Psychometrics, which covers the theory and technique of psychological measurement

Temperature

The horizontal axis of a psychrometric chart is the temperature. Temperature is without doubt one of "the most important climate variables for human comfort and building energy efficiency" (Nall, 2004). When talking about the air temperature it is generally referred to the air's dry bulb temperature (DBT). The DBT is measured by a thermometer exposed to the air, but shielded from moisture and radiation (Gatley, 2013). In contrast, the wet bulb temperature (WBT) takes the moisture of the air into account. It is the temperature the air would have if it was cooled down to the point of saturation (relative humidity of 100%).

Humidity

The content of water vapour in the air can be expressed by the vapour pressure (more accurately the partial pressure of water in the examined atmosphere). Vapour pressure (p_{vapour}) is linearly related to the specific humidity (x) and represents the vertical axis in the psychrometric chart

$$x = 0.622 \frac{p_{vap}}{p_{amb} - p_{vap}} \quad (2.1)$$

With x specific humidity
 p_{vap} vapour pressure
 p_{amb} ambient pressure.

When describing an atmosphere's water content, usually the relative humidity is used. It is the fraction of the vapour pressure to the saturation pressure of the temperature in question.

$$p_{vap} = p_{sat} \varphi \quad (2.2)$$

With p_{sat} pressure at saturation
 φ relative humidity.

Enthalpy

Enthalpy is a thermodynamic state function that is used to calculate energy differences due to temperature changes. Enthalpy is defined as zero at a temperature of 0°C. To find out the enthalpy of moist air, the enthalpies of dry air and vaporized water have to be added (Recknagel & Schramek, 1999).

$$h = c_{p,air} T + x (r_w + c_{p,vap} T) \quad (2.3)$$

With h specific enthalpy
 T temperature
 r_w specific enthalpy of vaporisation
 $c_{p,air}$ specific heat capacity of vapour
 $c_{p,vap}$ specific heat capacity of vapour.

2.1.2 Heat transfer

Heat transfer or heat flow is the movement of heat from a warmer body to a cooler body. Heat can move to and from a body in three ways: conduction, convection and radiation (Jeffus & Fearnow, 2004). In the case of conduction and convection the amount of transferred heat is dependent on the temperature gradient, the contact area and the coefficient of heat transfer (Polifke & Kopitz, 2009).

$$\dot{Q} = UA\Delta T \quad (2.4)$$

With	\dot{Q}	heat flow
	ΔT	temperature gradient
	U	coefficient of heat transmission
	A	area.

Conduction

Conduction is the heat transfer between molecules without movement of the particles themselves. In other words it is heat transfer through solid matter and through the contact surface of two solid bodies. In an automotive context this could be heat transfer from the outside to the cabin through the car body or the heat transfer between body and seat surface. The coefficient of heat transfer is dependant of the thermal resistance of the bodies.

$$U = \frac{1}{A\sum R_{th}} \quad (2.5)$$

With	R_{th}	thermal resistance.
------	----------	---------------------

Convection

Convection is heat transfer between a fluid (liquids and gases, e.g. air) and a solid surface. Forced convection is the heat transfer to and from a fluid that is forced to flow over a surface (e.g. by a fan). In an automotive context this could be heat exchange between the moving cars' body and the surrounding or between the occupant and the HVACs air flow. Free or natural convection occurs through buoyancy forces, e.g. when a parked car is heated up by the sun or an occupant is sitting in a still, cold cabin. The coefficient of heat transfer is a function of the thermal conductivity, viscosity and speed of the fluid, the contact area and shape and the flow regime (laminar or turbulent flow) (Polifke & Kopitz, 2009).

Radiation

Radiation is heat transfer in wave form similar to light. Like light it requires no medium to travel. The best known example for radiation is sun irradiation itself. In the automotive context it can also be a heated occupant or a heated surface (e.g. dashboard in the sun) radiating towards colder surfaces. The temperatures influence the amount of heat transfer by the difference of their respective fourth power. The radiation constant is a function of the

shape and the absorptivity, emissivity, reflectance and transmittance of the emitting and receiving bodies (Polifke & Kopitz, 2009).

$$\dot{Q} = \Sigma_{12} A_1 (T_1^4 - T_2^4) \quad (2.6)$$

With Σ_{12} radiation constant
 A_1 area body one
 T_1 temperature body one
 T_2 temperature body two.

2.2 Human thermal physiology

The human body is constantly producing heat and is therefore in constant thermal interaction with the environment. If exposed to a constant, moderate thermal environment at constant, moderate activity, it can be assumed that the heat production will equal the heat dissipation (Fanger, 1970).

2.2.1 Metabolic rate

On one side of the equation is the metabolic heat production of the body. This heat production can be divided in two categories: basal metabolism and muscular metabolism. The basal metabolism is due to biological processes that keep the body running. As a reference value a 70kg body would have an approximate minimum metabolic rate at rest of about 80W (Klinke, Pape, Kurtz, & Silbernagl, 2010). The muscular metabolism occurs while carrying out work. At continuous power output the metabolic heat production can reach 700W. To simplify matters in calculating thermal comfort, the metabolic rate is usually expressed as a power density, as ‘work per body surface area’ using the unit called *met*.

$$1 \text{ met} \triangleq 58.2 \frac{W}{m^2} \quad (2.7)$$

An average sized male with an approximate body surface of 1.8 m² would produce around 100 W at a seated resting activity of 1 met (Auliciems & Szokolay, 1997).

activity	met	W/m ²
sleeping	0.7	40
reclining, lying in bed	0.8	46
seated, at rest	1.0	58
standing, sedentary work	1.2	70
very light work (shopping, cooking, light industry)	1.6	93
medium light work (house work, machine tool work)	2.0	116
steady medium work (jackhammer, social dancing)	3.0	175
heavy work (sawing, planing by hand, tennis) up to	6.0	350
very heavy work (squash, furnace work) up to	7.0	410

Table 1: Metabolic rates at different activities (Auliciems & Szokolay, 1997)

2.2.2 Thermoregulation

The other side of the equation is the heat exchange with the environment. Heat exchange can occur by

- heat conduction through the clothing,
- conduction, convection and radiation from unclothed skin,
- water vapour diffusion through the skin,
- evaporation of sweat from the skin surface,
- latent respiration heat loss and
- dry respiration heat loss (Auliciems & Szokolay, 1997).

The centre reacting to internal and external changes and regulating the body temperature is located in the hypothalamus (Klinke et al., 2010). It is always trying to maintain an operating core temperature of 36.3 – 37.1°C (Klinke et al., 2010). The actual value can vary inter-individually, is different dependent on the time of day and can also be influenced by several factors such as menstruation cycle or emotions. When exposed to changing climatic conditions, the organism activates different processes to counter rising or falling core temperatures (see Figure 3); vasoconstriction and shivering when cold, vasodilation and sweating when hot. In cold conditions the body keeps blood circulation closer to its core and accepts colder extremities. In hot conditions circulation is accelerated and sweating increased to transport heat from the body.

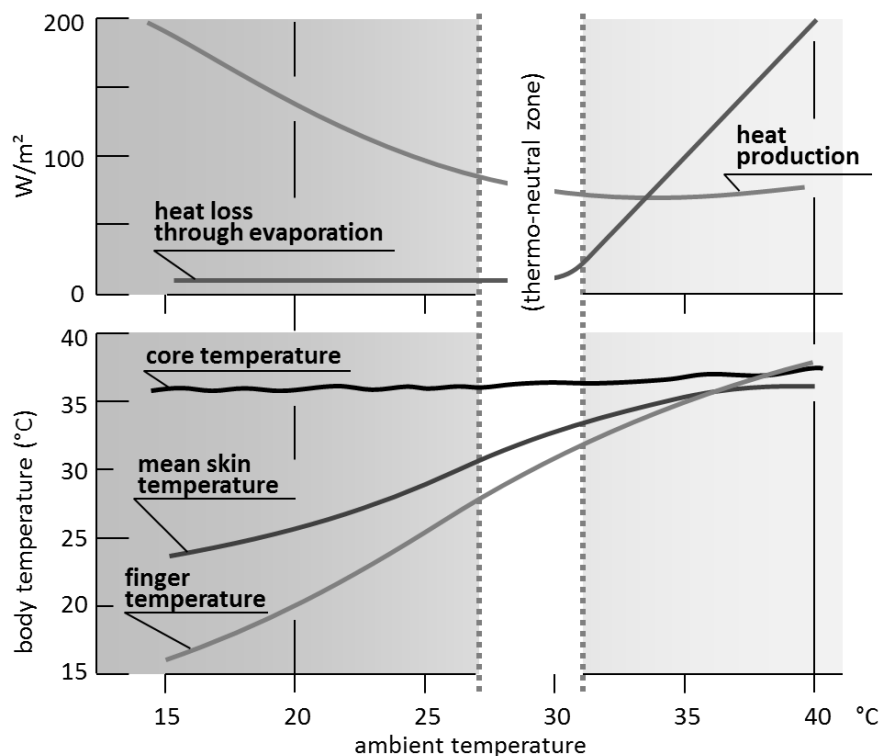


Figure 3: Heat production and heat loss through evaporation and core and skin temperatures respectively at different ambient temperatures (adapted from Klinke et al., 2010).

2.2.3 Thermal perception

The thermal conditions are registered by the body through thermal receptors. Receptors in the hypothalamus register the core temperature while two types of receptors in the skin are able to register warm or cold of the surroundings respectively. The distribution of these peripheral receptors varies over different body parts. Cold receptors for example are sparsely distributed on arms and legs but more densely on neck, nose, face and torso (Figure 4).

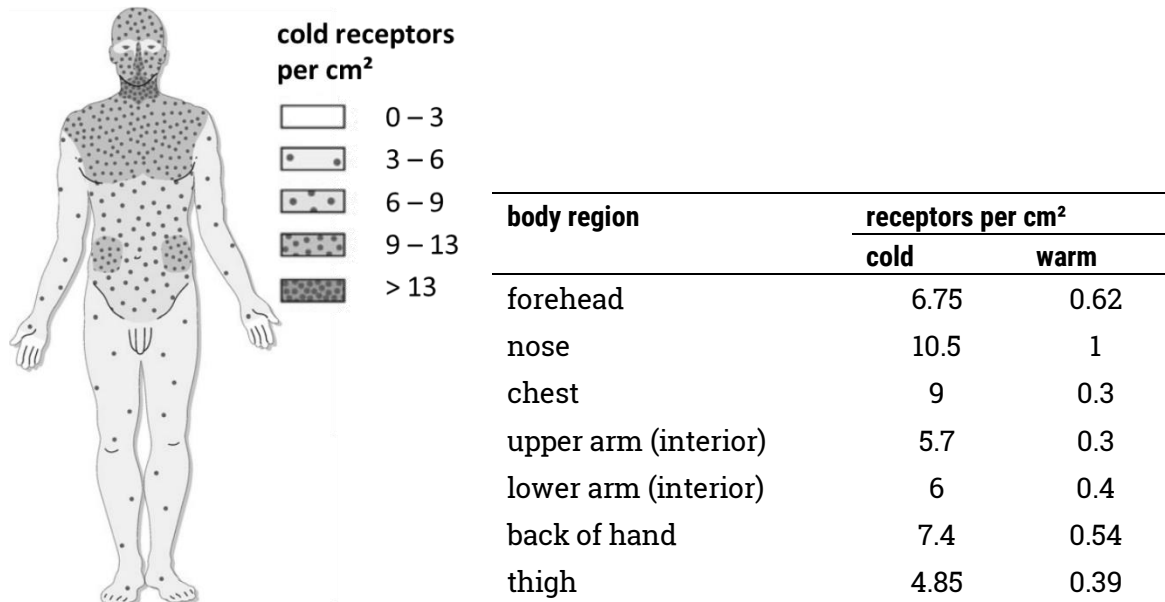


Figure 4: Mean distribution of cold and warm receptors on the skin (Klinke et al., 2010; Schmidt, Lang, & Heckmann, 2010)

Figure 5 (left) shows the mean activity of cold and warm receptors over the mean skin temperature. The anomaly that cold receptors are also active above 45°C can lead to a paradox sensation of cold in extreme heat (e.g. stepping into a hot bathtub).

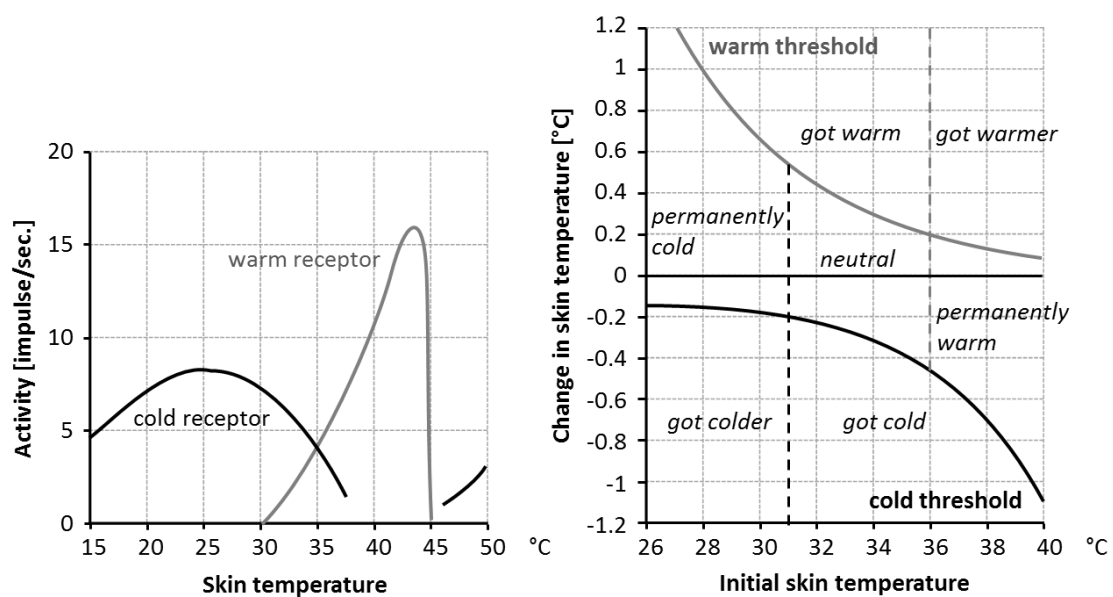


Figure 5: Static response of cold and warm receptors (left) (Klinke et al., 2010), warm and cold thresholds depending on initial skin temperature (right) (Schmidt et al., 2010)

The response of the receptors to dynamic temperature changes is higher than depicted in Figure 5. The signals received by the brain are translated into local and overall thermal sensation, which is generally graded in a seven point scale (cold, cool, slightly cool, neutral, slightly warm, warm, hot) (ANSI/ASHRAE 55-2010). Skin temperatures between about 31°C and 36°C lie inside the zone of indifference and are perceived neutral (Figure 5, right). Everything above and below will trigger a receptor response and is perceived as permanently warm and respectively permanently cold. Depending on the initial skin temperature thermal perception will change if the step of skin temperature change is big enough. A change in temperature that crosses the threshold will trigger a dynamic receptor response.

2.3 Thermal comfort

A person’s thermal perception can then be expressed into a vote of thermal comfort or thermal wellbeing. Thermal comfort has been defined in the ASHRAE (American Society of Heating, Refrigerating and Air-Conditioning Engineers) standard 55 as “that condition of mind that expresses satisfaction with the thermal environment” (ANSI/ASHRAE 55-2010). Conversely, “[t]hermal discomfort may be caused by the body (as a whole) being too warm or too cool but also by a part of the body being too warm or too cool” (Parsons, 2002). It can thus be differentiated between ‘overall’ and ‘local’ thermal (dis-)comfort (see Chapter 2.3.3).

However this definition illustrates clearly the difficulty in identifying thermal comfort since a “condition of mind” is not measurable with sensors. Hence being able to objectively predict thermal comfort, indices, measures and models are needed which are based on and/or evaluated by extensive human subject surveys (see Chapter 2.3.2).

The influencing factors on thermal comfort are mainly environmental factors such as the air temperature or irradiation and human factors such as the activity rate. These factors have been indicated by Fanger (1970) and are used in most standards (ASHRAE and DIN) and measures for thermal comfort as the fundamental influencing factors. But also factors such as gender or the habitual climate zone can have an influence on the vote (Table 2).

fundamental factors		contributing factors
environmental factors	human factors	
air temperature	metabolic rate	food and drink
mean radiant temperature	clothing	age and gender
relative humidity		acclimatization
air velocity		state of health
		psychologic factors
		etc.

Table 2: Variables affecting thermal comfort (collated from Auliciems & Szokolay, 1997; Fanger, 1970)

2.3.1 Clothing

Clothing is a dominant factor in thermal comfort since it is affecting the heat dissipation by insulating the body. For the purpose of expressing thermal comfort, a unit has been devised to be able to express clothing elements in respect to their thermal insulation capacity. The unit is named *clo*.

$$1 \text{ clo} \triangleq 6.45 \frac{W}{m^2K} \quad (2.8)$$

A business suit with cotton underwear has the insulating value of 1 clo (ANSI/ASHRAE 55-2010). Table 3 lists the clo value for a variety pieces of garments. Multiplying the sum of the individual items by 0.82 amounts to the total clo value of an ensemble.

Man		clo	Woman		clo
underwear	singlets	0.06	underwear	bra + panties	0.05
	T-shirts	0.09		half slip	0.13
	briefs	0.05		full slip	0.19
	long-sleeved	0.35		long, upper	0.35
	long-legged	0.35		long, lower	0.35
shirt	light, short sleeve	0.14	blouse	light	0.20
	light, long sleeve	0.22		heavy	0.29
	heavy, short sleeve	0.25	dress	light	0.22
	heavy, long sleeve	0.29		heavy	0.70
waistcoat	light	0.15	skirt	light	0.10
	heavy	0.29		heavy	0.22
trousers	light	0.26	slacks	light	0.26
	heavy	0.32		heavy	0.44
pullover	light	0.20	pullover	light	0.17
	heavy	0.37		heavy	0.37
jacket	light	0.22	jacket	light	0.17
	heavy	0.49		heavy	0.37
socks	ankle length	0.04	stockings	any length	0.01
	knee length	0.10		panty-hose	0.01
footwear	sandals	0.02	footwear	sandals	0.02
	shoes	0.04		shoes	0.04
	boots	0.08		boots	0.08

Table 3: Insulating value of clothing elements (based on (ANSI/ASHRAE 55-2010))

2.3.2 Thermal comfort models

A first mathematical model on the heat balance of a human body was proposed by Gagge (1936). According to the first rule of thermodynamics it was argued, that a neutral state is achieved, when the metabolisms energy M is equal to the gains and losses by convection C , radiation R , evaporation E and the heat stored in or lost by the body ΔS .

$$M \pm \Delta S - E \pm R \pm C = 0 \quad (2.9)$$

Since then this model has undergone many modifications and refinements and now there are several models predicting thermal comfort with either empirical or analytical indices. A detailed overview can be found in "Thermal Comfort" by Auliciems & Szokolay (1997). The two still most widely used models for heat exchange processes of the body today are the "two-node model" from Yale and Fanger's "comfort equation".

Fanger (1970) developed a heat balance equation depending on the six basic parameters in Table 2 (environmental and human factors). Stolwijk & Hardy (1966) developed the empirical two node model of human thermoregulation which is a complex model incorporating in detail heat transfer in the body, properties of body tissue and clothing, heat exchange with the environment and regulatory responses.

Fanger's Predicted Mean Vote (PMV) and Predicted Percent Dissatisfied (PPD)

Fanger's (1970) comfort equation is still one of the most widely accepted models of thermal comfort. The derived indices are the analytical Predicted Mean Vote and the empirical Predicted Percent Dissatisfied. The model is also the basis for the ASHRAE 55 standard as well as for the European/German standard 'Ergonomics of the thermal environment' (DIN EN ISO 7730:2005). Fanger developed a heat balance equation depending on the six basic parameters in Table 2 (environmental and human factors) to calculate the PMV on a scale from -3 to 3, stating thermal comfort according to the thermal sensation scale.

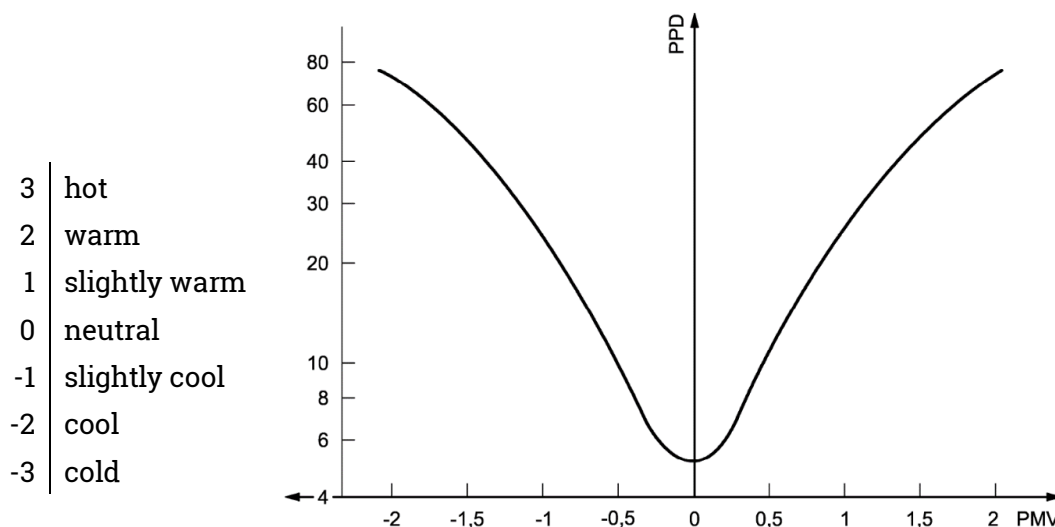


Figure 6: Predicted Mean Vote (PMV) and Predicted Percentage of Dissatisfied (PPD) (Fanger, 1970)

The heat balance equation and the derivation of the PMV can be found in the Appendix. The PPD can be calculated subsequently:

$$PPD = 100 - 95 \cdot e^{(-0.03353 \cdot PMV^4 - 0.2179 \cdot PMV^2)} \quad (2.10)$$

Neutral condition is defined as the optimum. But since the PMV is – as the name says – a mean, there will always be a minimum of 5% that are not content with the surrounding conditions.

Selected Climate Indices

While having been verified for a broad variety of use cases, both the PMV/PPD model and the two-node model do not provide the universal index for every application. An extensive study in Australia by Williamson, Coldicutt, & Riordan (1995) showed for example that the PMV consistently overestimates warm discomfort in tropical climates while overestimating cool discomfort in the cold months of temperate climates. Due to this, several other approaches were developed to objectively express thermal comfort including specific use cases or regions. To name some examples: the Effective Temperature (ET), the New Effective Temperature (ET*) or the Equatorial Climate Index (ECI).

Houghten & Yagloglou (1923) developed the ET which can be visualised as equal comfort lines on a psychometric chart. However ET is overestimating the effect of humidity under both cool and comfortable conditions. ET* has been developed by Gagge, Stolwijk, & Nishi (1971) using the two-node model and is defined as “the temperature of a uniform enclosure at 50% relative humidity, which would produce the same net heat exchange by radiation, convection and evaporation as the environment in question” (Auliciems & Szokolay, 1997). The geometric process underlying the determination of the ET* lines can be found in (Rohles, Hayter, & Milliken, 1975). An approximation is given by the algorithm

$$T_{ET^*,\phi=0} = ET^* + 0.023 (ET^* - 14K) x_{ET^*,\phi=0.5} \quad (2.11)$$

For comparison, the Singapore Index or the Equatorial Climate Index (ECI) was developed by Webb (1959 & 1960) for the use in naturally ventilated buildings close to the equator like in Singapore where climate can be defined by being warm, damp and windless. The resulting comfort values are in much warmer and more humid areas than other indices (see Figure 8).

Adaptive thermal comfort model

While most models can still be used for uniform and steady state conditions, there are a few major shortcomings. In the PMV/PPD model for example, the scales for thermal sensation and thermal comfort are directly correlated (see Figure 6) which might not always be the case (some people might feel comfortable in warmer conditions, some in colder). Also the model is based mainly on physiological, measureable parameters. Furthermore, most studies were based on climate chamber experiments and not on data collected in real life situations.

Studies over the last decades proposed to expand the static models like the PMV model into an adaptive thermal model. Auliciems (1981) research points towards a strong psychological factor on thermal perception and comfort. It is argued that parameters of past cultural climatic experience and expectations should be included. Dear & Brager (1998) confirmed that acclimatisation has a strong impact on thermal perception. People in warmer climates tend to prefer warmer indoor temperatures than people in colder climates (not to be confused with the difference of climate zones of for example ASHRAE 55 and ECI. One is for buildings with HVAC systems, the other for buildings with natural ventilation). This model has been verified for various locations, including Singapore (Dear, Leow, & Foo, 1991), and shows that the static models denying acclimatization are limited to either moderate environments or conditions similar to those they were developed in.

The 'comfort zone'

A comfort zone is defined as "the range of environmental conditions within which the average person would feel comfortable" (Auliciems & Szokolay, 1997). It was first introduced in architecture by (Olgay, 1962) and shown in graphic form in dependence of DBT and relative humidity. Auliciems & Szokolay (1997) provide the following working method based on local climate data.

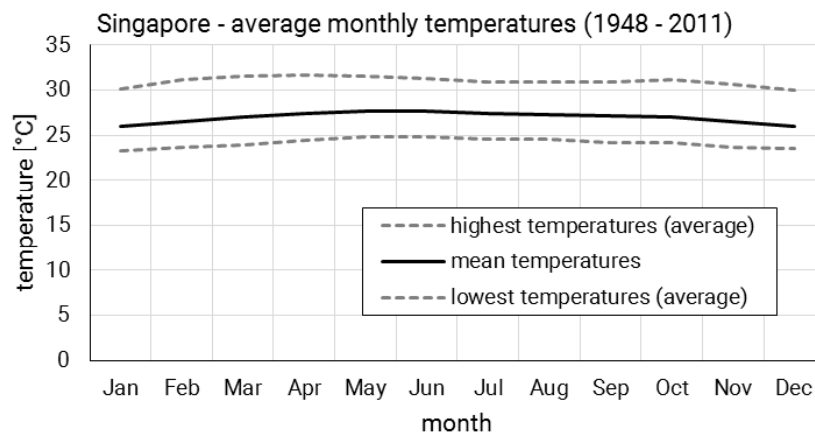


Figure 7: Singapore temperature data (monthly, 1948-2011) (NEA Singapore, 01/12/2012)

This is calculated below on the example of Singapore. The lack of seasonal variation in tropical climates (see Figure 7) leads to a uniform comfort zone over the whole year. First the mean temperature is calculated:

$$T_{mean} = \frac{T_{min} + T_{max}}{2} = 28.1^{\circ}C \quad (2.12)$$

For air conditioned environments, the neutral temperature can be found using Equation (2.13). This value is then marked in the psychrometric chart (Figure 8) on the 50% relative humidity curve.

$$T_{neutral} = 21.5 + 0.11 T_{mean} = 24.6^{\circ}C \quad (2.13)$$

The maximum acceptability (According to PPD: 95%) is along the line that is given by ET^* for $T_{neutral}$. To achieve a higher acceptability, the comfort zone can be expanded with $T_{neutral} \pm 1.2K$ or $T_{neutral} \pm 2K$ and the equivalent ET^* lines through the 50% relative humidity curve. The acceptability at the temperature thresholds is given with 90% or 80% respectively. Reversely, if the occupants can adjust the conditions inside the comfort zone to their liking, the acceptability will be higher than 95% (the exact value cannot be determined due to lack of original data). The lower humidity limit is set to 4 g/kg as it was originally introduced in ASHRAE55 for non-thermal reasons like drying out of the skin or irritation of the eyes and taken out in a later edition (2004). For the human comfort in general these effects are however of great importance, therefore the recommendation has not been changed. The upper humidity limit is set at 12 g/kg (1.9kPa vapour pressure), defined by the vapour pressure at the skin. The upper limit had been defined by the 60% relative humidity curve in the meantime, but has now been reverted to the absolute humidity limit.

The comfort zone of the adaptive thermal model has been established for activity levels of 1.1 to 1.4 met, which corresponds very well with the expected activity levels in the car: the driver driving the car at max. 1.4 met and the passenger at 1 met sitting still, but probably still influenced by previously walking in the warm environment.

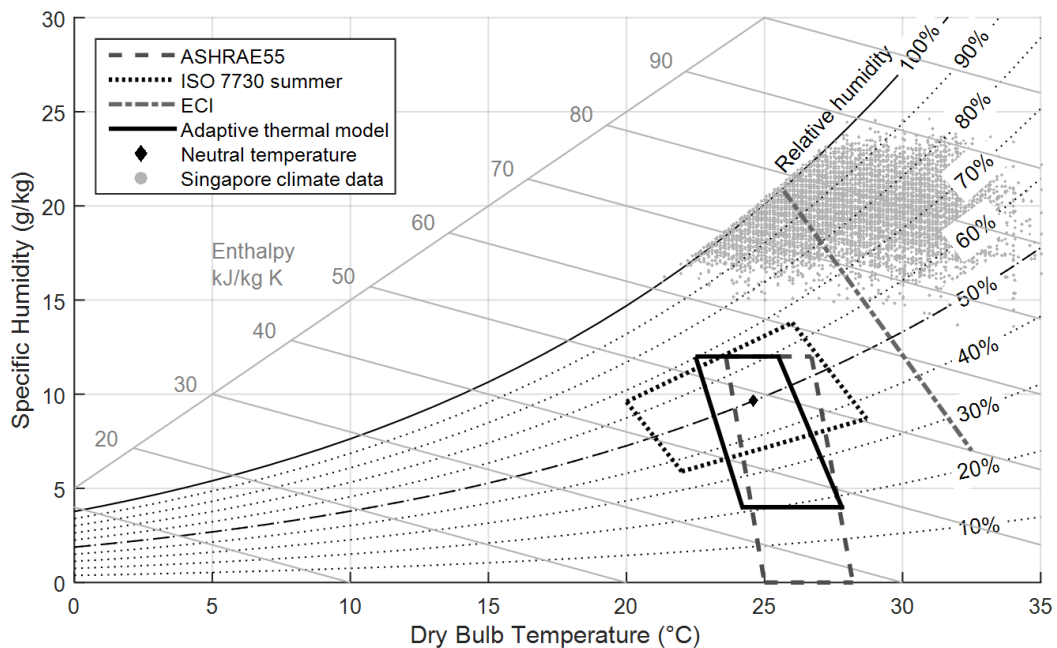


Figure 8: Psychrometric chart, comfort zones and Singapore climate data

The comfort zone of the adaptive model is similar to the summer conditions of the ASHRAE 55 standard which it is generally based upon. The ISO 7730 standard gives an overall wider comfort zone, which is however due to its flaws concerning hot and humid environments. The ECI is shown as an example in Figure 8 to visualize the differences in expectance and preference for air conditioned and naturally ventilated spaces. The

Singapore climate data (NEA Singapore, 01/12/2012) shows the high energetic effort that is needed to condition the air to acceptable indoor conditions.

Complex thermal models

Sophisticated thermal models integrate the principles of heat transfer, human physiology and thermoregulation, combined with anthropometric data, into a mathematical representation of the human body that can predict human thermal responses and the associated thermal sensations. These 'complete' models can be run on a computer and are able to simulate dynamic responses in any environment.

Most models are based on the two-node model by Stolwijk. So is Tanabe's 65-multi-node model (65MN) (Tanabe, Kobayashi, Nakano, Ozeki, & Konishi, 2002) or a mathematical model developed by Fiala (1998) (Fiala's thermal Physiology and Comfort model: FPC). Similar to the two-node-model, it consists of two interacting systems, the passive and the active system. The passive system is a multi-layered, multi-segmented representation of the human body to simulate heat transfers within the body and at its surface and the active system simulates the responses of the human thermoregulatory system. The active system's responses are based on multiple comfort studies carried out over the last decades and all over the world (to be found in detail in (Fiala, 1998)). The Berkeley 'Advanced Human Thermal Comfort Model' by Arens, Huizenga and Zhang (Arens, Zhang, & Huizenga, 2006a; Arens, Zhang, & Huizenga, 2006b; Huizenga, Zhang, & Arens, 2001; Zhang, Arens, Huizenga, & Han, 2010; Zhang, Huizenga, Arens, & Yu, 2005) is equally significant and widely used.

Each model can be used as a standalone product or can be incorporated in simulation software for a multitude of simulated use cases. The FPC, for example, can be activated within the software THESEUS-FE, which in turn can be linked to complex CFD simulations (Fiala et al., 2010). The mentioned complex thermal models are intentionally very detailed, thus providing more information than just an abstract mean vote for a whole room or the whole body. Thermal comfort can in many cases not just be simplified to a single index. The influence of local phenomena has to be determined and included in the models.

2.3.3 Local thermal comfort

When Fanger (1970) developed his heat balance equation, he defined three prerequisites for a person to be defined as in a state of thermal comfort:

- The body is in heat balance
- The sweat rate is within comfort limits
- The mean skin temperature is within comfort limits.

Parsons (2002) adds a fourth condition regarding local thermal discomfort:

- "[. . .] there must be no local thermal discomfort." (Parsons, 2002, p. 284)

These studies show that, to achieve overall thermal wellbeing, it is thus essential to avoid, or at least minimize, local discomfort. Such local uneasiness can be caused by draught, dampness, asymmetrical heat radiation or a too-high temperature gradient over the body. Draught for instance is unpleasant because it causes local undercooling.

The reason for the late inclusion of local thermal comfort is that most research in thermal comfort originates from the building industry where standards and guidelines are strongly influenced by architectural requirements. The goal of building air conditioning is usually to achieve a uniform temperature and humidity in the room concerned. Draught should be avoided as well as bothersome radiative sinks or sources (e.g. solar impact, cold walls...) to achieve an environment inside the building that is mostly steady state and uniform. Standard DIN EN ISO 7730:2005 has already been extended with formulae to calculate a PD (persons dissatisfied) value for cold or heated walls, ceilings or floors.

Thermal comfort in other applications is however even more exposed to dynamic and nonhomogeneous conditions. Examples are air conditioning in aircraft cabins or research in the effect of clothing in combination with high metabolic rates on thermal wellbeing in sports. A lot of findings on thermal comfort are also derived from research and investigations for military combat gear and clothing. Air conditioning in cars is another of these prime examples of applications that are not in a steady state and uniform condition.

A car's interior is a very confined space and a car's body is only lightly insulated. This can result in high temperature gradients. Boarding and alighting from a car exchanges a large proportion of the cabin air volume. Since the car is a moving object, solar irradiation has to be considered not only by time of day. Driving in cities, wooded areas or tunnels may cause irradiation or temperatures to change quickly. These are just some examples, but it can be summarised that air conditioning in cars has to take account of much higher fluctuation in conditions than air conditioning in buildings.

Consequently the same must apply when defining thermal comfort. The indices referred to above for thermal comfort or comfort zones assist in calculating the optimal uniform and steady condition in which a human being will feel comfortable. There is much reference to 'overall' thermal wellbeing, meaning the comfort vote of the body as a whole. But local irritations can affect the comfort vote in a negative way, even if all the influencing parameters combined should, in theory, result in a positive vote. Only sophisticated thermal models are already able to account for comfort phenomena induced by local conditioning.

Local thermal comfort is closely correlated to the local thermal sensation; both are strongly influenced by the local skin temperature and the derivative of the skin temperature. This permits prediction of local comfort based on local sensations and skin temperatures. However, in doing so, the thermal environment and geographical temperature preferences must be considered. Both local sensation and comfort differ greatly in the various parts of

the body, even in the same climatic environment. Furthermore, not all the body's segments have the same impact on the whole-body thermal sensation and overall comfort. Zhang (2003) conducted extensive studies with human participants on the influence of local thermal conditioning. The experiments took place in an office environment (simulated in a climate chamber), in which the body was conditioned locally by cooled or heated air sleeves that were applied to the body part concerned. The study's extensive results provide the database for the calculation of local thermal comfort in advanced thermal models such the Berkeley 'Advanced Human Thermal Comfort Model' or the FPC.

2.3.4 Draught

Draught is defined as "an undesired cooling of the human body caused by air movement" (ANSI/ASHRAE 55-2010, p.3). According to a study by Bolinder, Magnusson, & Nyren (1970) draught is one of the two most annoying environmental factors in workplaces. It can pose a serious problem as it may cause people to turn off a ventilation system or increase the temperature to counteract the cooling effect of the draught. This will in turn increase the energy consumption when the system is in heating mode during cold seasons (Fanger & Christensen, 1986). The cooling effect of draught can be pleasant in hot conditions when heat stress has to be relieved. But it is difficult to control the cooling effect when sweating sets in. People with stronger or prompter perspiration may experience discomfort through excessive evaporative cooling.

Fanger & Christensen (1986) evaluated draught limits in a climate chamber, simulating office conditions with varying air movement. The 'Percentage of Dissatisfied' (PD) due to draught in ventilated spaces can be expressed as a function of air temperature T_a and mean air velocity \bar{v} :

$$PD = 13800 \left[\left(\frac{\bar{v} - 0.04}{T_a - 13.7} + 0.0293 \right)^2 - 0.000857 \right] \quad (2.14)$$

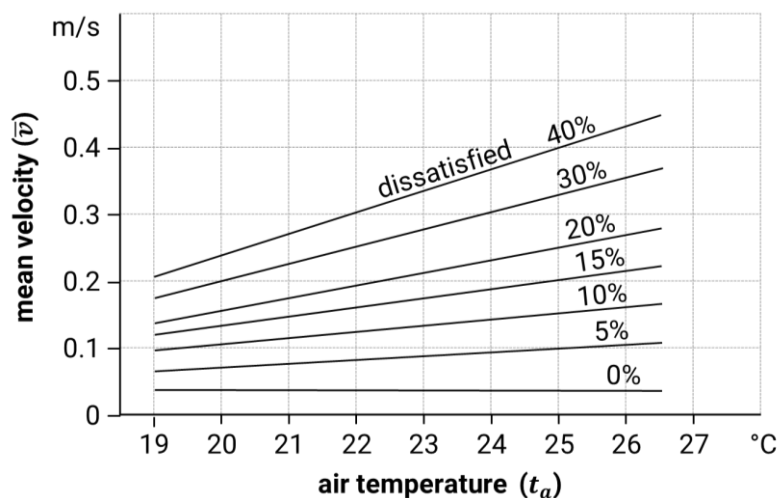


Figure 9: Percentage of dissatisfied (PD) due to draught in ventilated spaces (Fanger & Christensen, 1986)

Draught is experienced to a varying extent in different body parts. The head region and the ankles are most sensitive to air movement. It is also dependant on the degree of turbulence as to where higher turbulence results in more dissatisfied participants. Fanger & Christensen's study maintained a turbulence intensity between 0.4 and 0.6 which correlates to field study measurements in office buildings.

At higher temperatures it can however be beneficial to increase air movement in order to improve comfort (Olesen & Brager, 2004). The new ASHRAE55-2004 standard allows the use of higher air velocities. Use of the PMV model in this standard is validated to air speeds up to 0.2 m/s. But to increase the upper temperature limits of the comfort zone for operative temperatures above 25.5°C, the upper limit to air speed can be pushed to 0.8 m/s for sedentary activities (about 1.2 met) depending on temperature rise and cooling offset. It is however important to add, that in these circumstances individual control of air movement should be provided.

2.3.5 Temperature gradients

Temperature gradients can occur for various reasons. Without external influence a vertical temperature gradient will occur when warm air rises due to lower density. An example of horizontal gradient occurrence in a car application is solar irradiation on windows. While these gradients can cause strong local discomfort, a temperature gradient can in some cases be beneficial. In Figure 10, Kolb (2004) plots temperatures in a passenger cabin for heating and cooling that have evolved in vehicle climate conditioning over the years.

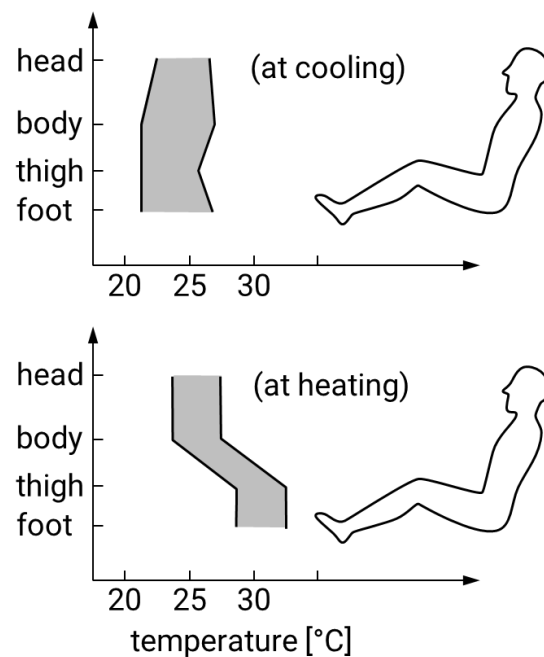


Figure 10: Temperature distribution inside vehicle cabin (Kolb, 2004)

Kolb (2004) states that the temperature distribution while cooling in summer can be between 21°C to 26°C. The mean temperature in the cabin is between 22°C to 25°C. For that the temperature at the outlet has to be set to a temperature between 5°C to 10°C. In winter the temperature in the footwell is approximately 5K higher than at body and head. Even gradients of up to 12K are possible (Großmann, 2013). Mean cabin temperatures range between 25°C and 30°C. The air provided for the footwell is usually between 50°C and 65°C.

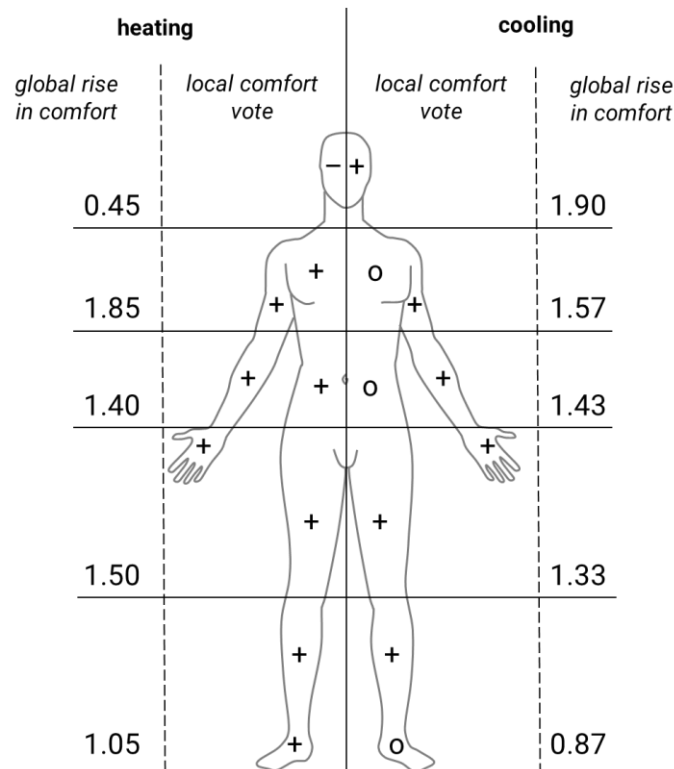


Figure 11: Comfort votes after dynamic exposure to heating and cooling (adapted from Prestel, 2013)

In a preceding study at the Institute of Ergonomics (LfE), TUM, Prestel (2013) exposed test persons locally to heated or cooled air flow after acclimatisation in the climate chamber. They indicated their comfort vote on a six-step rating scale:

very uncomfortable	uncomfortable	slightly uncomfortable	slightly comfortable	comfortable	very comfortable
-3	-2	-1	+1	+2	+3

Table 4: Scale for thermal comfort vote by Prestel (2013)

The participants were seated in uncomfortable cold or warm ambient air conditions and given time to adapt to the temperature. The starting conditions ranged from -1.04 to -2.26. After local exposure to either heated or cooled airflow, the vote for overall comfort changed towards better comfort levels. The results for the dynamic exposure for each body part are summarised in Figure 11. It can be seen that cooling is most efficient in the upper body region, especially at the head, taking the exposed body surface ratio into account. The torso is

however very sensitive to cooling. Overcooling must be avoided. Heating is most efficient at the core but should be avoided to the head, since this leads to a strong local discomfort. The experiments by Prestel present the comfort votes induced by the dynamic thermal receptor response. But the tendencies of the obtained results are also congruent to the static air distribution in a car as proposed by Kolb (2004) and findings by Zhang (2003). Zhang also found out that while heating is most effective at the core, a local undercooling of the extremities has to be avoided because this will lead to a significant rise in local discomfort.

2.3.6 Scales for thermal perception and thermal comfort

Many studies use Fanger's PMV scale to derive votes for thermal comfort. As mentioned, this scale correlates with the vote of thermal perception. This might however not always be useful. Some people prefer warmer or colder conditions to feel comfortable. Therefore a separation of the vote for thermal perception and the thermal comfort/discomfort vote is desirable.

Another question is the definition of comfort and discomfort. The often cited theory by Zhang, Helander, & Drury (1996) states that it is possible to experience both discomfort and comfort at the same time. One example backing this theory is that of a sports car, which can produce discomfort, arising for example through posture or vibration, but also comfort through driving pleasure. These are however different factors influencing perception of comfort (or discomfort). When focusing on just one factor, as in our case thermal comfort, a simultaneous sensation of both comfort and discomfort is contradictory. Therefore it is proposed to use a rating scale where comfort and discomfort lie as opposites on the same axis. Using discomfort and comfort on two independent axes should only be applied as a tool to visualize all factors influencing the perception of a complex system (e.g. a sports car).

A possible scale to determine thermal comfort could be a scale similar to the one used by Prestel (2013) (see Chapter 2.3.5), with discomfort and comfort as opposites on a symmetrical scale. But a second question is whether thermal comfort is just the absence of discomfort or if it can be rated on one side of the full scale. Thermal discomfort is, as discussed in the previous chapters, quite straightforward as negative local or overall thermal stress or irritation. A neutral state would be the absence of thermal discomfort which in terms of skin temperature could be associated with the zone of indifference as presented in Figure 5 (right). Which is in turn (per definition) already a state of thermal comfort. Many researchers believe that a distinct positive sensation of thermal pleasure can only occur with the partial relief of thermal stress and thus thermal discomfort. In other words, a transient stress relief is experienced as more comfortable than uniform, stable, neutral conditions (Zhang, 2003). This is applicable for the dynamic experiments by Prestel. But since no differentiation in thermal pleasure is required in the experiments of this dissertation, it has been decided to use a one sided discomfort scale with 'comfort' at the point of origin.

The relevant standard for assessment of the influence of the thermal environment using subjective judgement scales is DIN EN ISO 10551:2001. Thermal strain can comprehensively be evaluated using five types of assessment: vote of thermal perception, affective vote ('dis-/comfort vote'), thermal preference, personal acceptability and personal tolerance. The experiments in this dissertation will not induce thermal states and skin temperatures that deviate very far from the zone of indifference. Further, evaluation of uncomfortable situations is not sought. Thus the scales for acceptability and tolerance can be neglected.

The vote of thermal perception is congruent to Fanger's PMV scale and can be extended from seven to nine steps ranging from (very) cold (-4) -3 to (very) hot (+4) +3 (Table 5). The affective vote is asked in a five step scale from 0 (pleasant/comfortable) to 4 (most uncomfortable) (Table 6). And thermal preference is either asked in 3 or 7 steps ranging from (much) colder to (much) warmer (Table 7).

very cold	cold	cool	slightly cool	neutral	slightly warm	warm	hot	very hot
-4	-3	-2	-1	0	+1	+2	+3	+4

Table 5: Scale for thermal perception (DIN EN ISO 10551:2001)

comfortable	slightly uncomfortable	uncomfortable	very uncomfortable	most uncomfortable
0	1	2	3	4

Table 6: Scale for thermal affective vote (DIN EN ISO 10551:2001)

much colder	colder	slightly colder	neither warmer nor colder	slightly warmer	warmer	much warmer
-3	-2	-1	0	+1	+2	+3

Table 7: Scale for thermal preference (DIN EN ISO 10551:2001)

The differentiation in the scale for the thermal affective vote is very coarse, having only four steps. When conducting experiments in a close proximity to the zone of indifference, the categories offered can strongly mismatch the stimuli provided, i.e. the differences of the provided changes could all be in the category 'slightly uncomfortable'. An alternative scale that accounts for this flaw is the Category Partitioning Scale (CP-50). It was developed by Heller (1980, 1985, cited from Ellermeier, Westphal, & Heidenfelder, 1991) to evaluate discomfort arising through painful pressure stimuli. Participants are first asked in which verbal category the stimulus falls and then to 'fine tune' inside the category using numbers from 1 to 10. Shen & Parsons (1997) showed that the CP-50 scale proved best in overall reliability and validity after evaluating different scales to rate pressure induced discomfort.

none	very slight	slight	medium	severe	very severe
0	1 – 10	11 – 20	21 – 30	31 – 40	41 – 50

Table 8: CP-50 scale for discomfort (adapted from Ellermeier et al., 1991)

2.3.7 Standards for thermal comfort

An overview of standards in the ISO standard domain is shown in DIN EN ISO 11399:2000. The most important standards for thermal comfort in moderate thermal environments are the already mentioned ANSI/ASHRAE 55-2010 and DIN EN ISO 7730:2005. The scales for evaluating thermal comfort have also been discussed with DIN EN ISO 10551:2001. Denotations, definitions, symbols and units for all that is thermal comfort related can be found in DIN EN ISO 13731:2001.

DIN 1946 deals with ventilation systems located in areas from living spaces to laboratories. The air conditioning of passenger cars and commercial vehicles can be found in part 3 of this standard DIN 1946-3:1962-06. When designing vehicle air conditioning systems standard VDI 6032, which deals with hygiene standards for ventilation technology in passenger vehicles, should also be taken into account.

Instruments and methods for measuring basic physical quantities in thermal environments are covered in DIN EN ISO 7726:2001. DIN EN 27243:1993 gives instructions to estimate the heat stress on a working man, based on the measurement and calculation of the WBGT-index (wet bulb globe temperature). Clothing and its influence in different thermal environments is covered in standards DIN EN ISO 15831:2004 and DIN EN ISO 9920:2009.

In environments outside of moderate conditions, meaning very hot or very cold environments, or where the work entails strenuous activities or high sweat rates, the standards DIN EN ISO 7933:2004, DIN EN ISO 15743:2008 and DIN EN ISO 11079:2007 have to be consulted. When working with thermal radiation, e.g. infrared (IR) heating surfaces, standards DIN EN ISO 13732-3:2008 and DIN EN ISO 13732-1:2008 cover valuation principles for human contact with hot and cold surfaces respectively.

2.4 Vehicle heating ventilation and air conditioning

Before starting to talk about automotive air conditioning, it is important to note that a full air conditioning unit is able to ventilate, heat, cool, humidify and dehumidify air. A car's 'air conditioning (A/C)' unit is strictly speaking only a 'partial air conditioning' unit, since humidifying air is not possible (Großmann, 2013). But since the term 'A/C' is most commonly used for just the cooling (and dehumidification) system, it will be used in this context as well. The term HVAC will subsequently be used for the car's air conditioning system.

2.4.1 History of vehicle HVAC

Early automobiles in the end of the 19th century followed the design of a horse drawn carriage. The cabin space was open to the environment and climate control had to be achieved by adjusting the clothing to changing conditions. With higher speeds possible, the first closed-cabin vehicles were introduced, and ventilation, heating and cooling became necessary. Ventilation was achieved by simple measures such as opening and closing the

windows or tilting the windscreen. Heating and cooling started with straightforward solutions such as using heated bricks or letting a block of ice melt inside the cabin. Later developments introduced vents and air ducts, electric blowers, heat exchangers fuelled by heat of the engine, additional electric heaters and cabin coolers using evaporative cooling (Daly, 2006).

Heating systems became mandatory in the US in 1968 (Bhatti, 1999). The first A/C system was introduced in the USA in around 1940 and was adopted in production vehicles in 1953. Since the 1990s the proportion of newly registered cars with A/C has risen radically. The same goes for the introduction of automatic climate controls (ACC). First automatic controls came up in the USA during the 1950s. In Germany, ACCs are being integrated since the 1970s. Table 9 shows the rise of newly registered cars with A/C and/or ACC.

A/C rate			ACC rate		
	2004	2010		2004	2010
NAFTA	97%	97%	NAFTA	48%	58%
Europe	72%	82%	Europe	50%	67%
Japan	98%	98%	Japan	68%	72%
China	84%	94%	China	40%	61%
ROW	46%	57%	ROW	13%	23%
WW	77%	82%	WW	43%	53%

Table 9: Comparative data of A/C and ACC penetration (Daly, 2006) (Note: NAFTA – Northern American Free Trade Agreement States, ROW – Rest of World, WW – Western World)

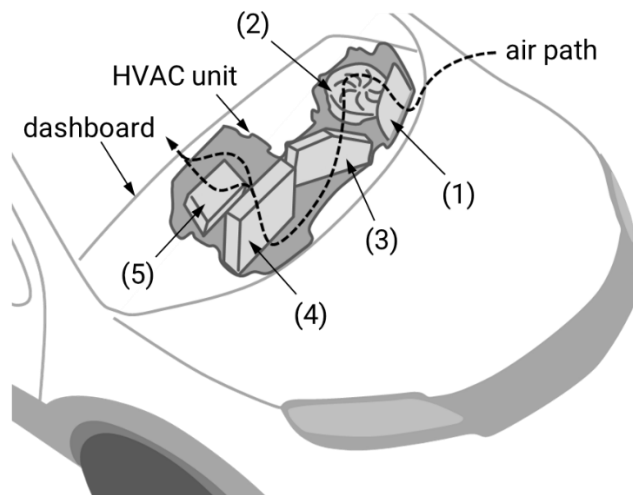


Figure 12: Air path through the HVAC unit: (1) recirculation flap, (2) blower, (3) filter, (4) evaporator, (5) heater

State of the art vehicle HVAC systems consist of a usually centrally located HVAC unit under the dashboard (Figure 12). The air intake is between engine bonnet and windscreen, after that the air passes through a water separator. Prior to the blower (2) is the recirculation flap (1) with which the ratio of fresh air and recirculated cabin air can be set. After the blower the air is led through a dust and pollen filter (3). The cleaned air then passes through the cooling systems' evaporator (if installed) for cooling and dehumidification (4). The ratio of air led

through the subsequent heater (5) (supplied by engine waste heat to provide thermal energy – in case of diesel engines an additional PTC heater might be implemented) is regulated by temperature control flaps. The thus cleaned, dehumidified and tempered air is then channelled through an air distribution box where flaps regulate the flow ratio to the outlets. Outlets are usually located in the dashboard and are directed at the occupant's torso, the windshield and into the footwell.

A two-zone HVAC system in which left and right sides can be controlled individually is already standard for every new car on the market. Premium class vehicles often provide an individual air zone treatment of four zones. Two-zone AC systems distinguish between left and right side of the car whereas four-zone AC systems also provide different settings for front and rear seats. A four-zone AC system is usually implemented by two HVAC units, one for the front, and one for the rear (Volkswagen, 2002).

Until this point in time, heating ventilation and air conditioning was provided centrally for the whole cabin. Energy crises and ecological awareness started to push technologies that reduce energy consumption and in many cases also increase thermal comfort. Passive measures include better insulation of the car body, IR-reflective windows and car finish or reduction of thermal masses inside the cabin. First active measures are waste heat recovery, solar driven parking ventilation or efficient use of recirculation with the help of a CO₂-sensor. Other active measures are local application of heat sources or sinks. One of the first and most widely installed local applications was the electrically heated seat, followed by ventilated seats, electrically heated surfaces or IR-emitters (Großmann, 2013).

The first seats with integrated ventilation and cooling entered into series-production vehicles in the late 1990s, for example the active 'climate seat' in the Mercedes-Benz S-Class (ebm-papst, 2/12/2015). One example for interior heating with IR-emitters is BMWs development of a footwell heating system (GoingElectric, 2/12/2015). Many other OEMs and suppliers are working on localised systems, for example a compact, thermo-electrically driven heating and cooling unit for seats (Gentherm, 2/12/2015). The goal is always to be able to provide faster, more dynamic heating or cooling and to increase the comfort at reduced energy consumption.

2.4.2 State of the art HVAC control

The control panel is normally located in the middle of the dashboard or on the centre console. It comprises a variety of push buttons, levers and adjustment controls. The same functions can also be designed into a digital panel or in combination with one. Operation modes can either be fully automatic, fully manual or any combination of automatic and manual modes.

Historically, the first HVAC controls only had to manage a few functions and human machine interfaces (HMI) were kept simple. The controllable devices and functions are as follows:

- air mass flow / fan speed
- temperature
- fresh air / recirculation
- defrost / defog rear windshield
- distribution (footwell / panel / windscreen)

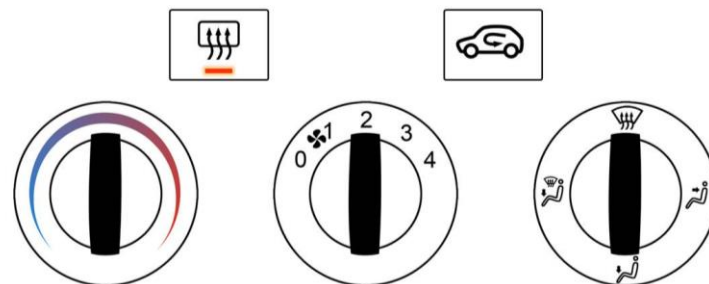


Figure 13: Example of a simple manually controlled standard HVAC control panel.

With the introduction of ever more devices, functions and technologies to improve energy efficiency and comfort, the HMI gained in complexity. This does not only include hardware solutions, but also strategies and sophisticated model-based controls. These new technologies and strategies may include:

- automatic mode
- heat radiation (e.g. heater/IR mats in foot well)
- convective surface heating or cooling (e.g. steering wheel)
- seat ventilation / heating / cooling
- localized / spot heating or cooling
- Peltier elements (heating and cooling possible)
- heat pump
- cooling adaptive to sun radiation and angle

The challenge in designing the overall AC control system lies now in the integration of these features into a coherent manual or (semi-) automatic climate control unit as well as in an easy to use and comprehensible HMI panel design. Newest cars on the market such as the BMW X6 feature a multitude of these functions (BMW AG, 11/11/2015). The interface allows the user to manipulate each system as well as setting the degree of automation.

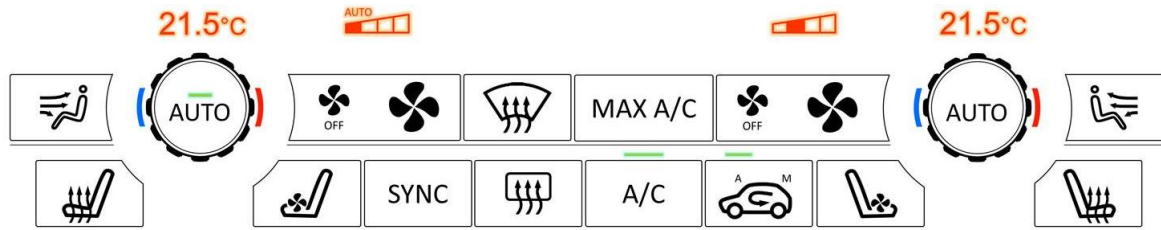


Figure 14: Example of an advanced HVAC control panel with automatic mode

The closed loop control for HVAC automatics is generally temperature driven. Sophisticated controls account for a multitude of input parameters, such as ambient temperature, humidity and irradiation, mean interior and outlet temperatures, seat occupation, driving speed and many more. But most of these advanced control systems are still dependent on the driver's temperature selection. Closed loop controls in series-production vehicles rely generally on characteristic curves or diagrams that have evolved over the years based on feedback and input from test operators and development engineers. This empirical approach is widespread, since it is very difficult to determine and monitor all relevant parameters for a stable mathematical or physical model.

Until now, only a few additional technologies have been integrated in the closed loop control of an HVAC automatic. In general, an automatic control modulates the 'basics' according to the input parameters: air temperature, air speed and air distribution. 'New' functions such as seat heating still have to be switched on and modulated manually. This is mostly the case because no or very few studies exist to cover the operation and interdependency of such a function for all possible use cases. And even less is known on the implications of such an interaction on human thermal comfort.

2.4.3 State of research in future vehicle HVAC

Many studies exist on the effects of local thermal phenomena on overall wellbeing. The works by Zhang already mentioned are a prime example in this field. However, while having shown great progress in understanding the interaction between local and overall comfort, the findings often cannot be translated to specific applications. Zhang conducted experiments in an office environment and conditioned locally with air sleeves. But the combined or differing effect of convective, conductive and radiated heat transfer could not be differentiated in this study. Therefore, every combination of heat transfer especially in transient conditions has to be tested separately in extensive environmental chamber or field tests. The Al-Othmani, Ghali, & Ghaddar's (2009) study, for example, covers the transient thermal comfort response in convective and radiative environments (again in a simulated office environment).

In a confined space such as a car interior, interferences or air flow patterns are high, irregular and also difficult to replicate in a general experiment. Creating a universally valid model for human thermal comfort that is generally applicable in all transient and dynamic conditions

and for all use cases is well on its way as shown in Chapter 2.3.2, but the collection of data is an extensive and time consuming task; and it is far from finished. The best approach is still to use the present findings to build a feasible and intelligent system solution, and to conduct detailed comfort experiments with it, the results of which can in turn be fed into simulation models.

IAV worked on comfort-oriented, energy saving, selective heating (Brinkkötter & Ackermann, 2010), Bertrand proposed a decentralised system utilizing climate seats, ventilated seatbelts and outlets in the door panel, Daimler Benz presented an overall 'environmental comfort' concept of the new S-Class (Frisch, Schanda, Engelhardt, Geisel, & Lasi, 2013) or the new C-Class (Reimund & Haupenthal, 2014) including holistic thermal management, climate-control seats and fragrant and ionising air treatment. Erhard Mayer, of the Institut für Bauphysik (ibp) at the Fraunhofer Institute has filed patents on individual, draught-free overhead cooling to be used in passenger vehicles or aircraft (0312557 B1, 1989; 1064194 B1, 2001). An in-house study by the 'SeatComfort Sàrl' company showed the benefits to microclimatic conditions in car seats by the use of three-dimensionally woven, air permeable spacer fabric (Hauer, 2013). While many manufacturers or suppliers are engaged in the development of such systems, the academic standard of the published material is not high. A paper addressing the seat development by IAV and BMW supports a more coherent research approach. In developing a ventilated seat, the investigation of the local comfort of the contact area between occupant and seat is being undertaken. An understanding of the microclimate is being achieved by simulation. The recommendation for hot conditions is: "The use of cooling seat ventilation systems is desirable, specifically for the summer load case when a warm vehicle is entered" (Paulke & Kreppold, 2008, p. 20), because even the resulting local long-term comfort vote (for trips of one hour and longer) will be "Too warm".

Academic studies include research at the FH Munich exploring "How users perceive the climate comfort of vehicle seats" (Morena, Krah, & Kurz, 2012) using a portable, thermo-hygrographic measuring set-up combined with subjective votes on the microclimatic conditions on a car seat. Factors influencing thermal wellbeing on car seats have been examined from a medical view point in (Schmitz, 2003). Test subjects were exposed to varying thermal states (ergometer, ventilated seat, radiative heat source) in a climate chamber conditioned to 22.2°C. A study at the University of Berkeley explores the influence of heated or cooled seats on thermal wellbeing in an office environment (Pasut, Zhang, Arens, & Zhai, 2015). It is not in an automotive environment, but basic findings might well be translated into car seat designs. The same goes for a similar study on office chairs by (Watanabe, Shimomura, & Miyazaki, 2009). Both studies show a benefit in comfort when conditioning locally, but limited in respect of growing temperature gradients. The study by Bartels (2003) is also in a different but transferrable environment. A small sample of healthy young men evaluated thermal comfort on aircraft seats with varying cover and cushion

materials. At a cabin temperature of 20.5°C, a significant improvement was shown when wool-polyamide fabric was selected rather than leather and three dimensionally knitted spacer fabric over moulded foam.

Lorenz (2015) developed a coupled simulation model to reduce heating loads and predict window fogging in cold conditions. The coupled simulation combined a model for window fogging, a CFD model of the cabin interior, a 1D-model of the vehicle structure and the Fiala FPC model for thermoregulation and thermal comfort. The parameters for the simulation were established by conducting experiments in a climate chamber.

The influence of local heating in an automotive surrounding was trialled in two very recent consecutive FAT (Forschungsvereinigung Automobiltechnik e.V.) studies at the RWTH Aachen. In (Schmidt, Praster, Wölki, Wolf, & van Treeck, 2013), the researchers look at the influence of heated car seats on occupant wellbeing. Several surveys with test persons compared various heating settings at three temperatures (22°C, 17°C and 14°C) with a variety of clothing. In addition, these scenarios were also run in a computer simulation in which the heat loss was monitored. It was confirmed that a state of thermal comfort could not be reached, especially at lower temperatures even though the seat heating and the subjects' heat loss were mathematically in equilibrium. Seat heating will improve the thermal comfort of a person sitting in cold conditions only to a certain extent. As was verified again in (Schmidt, Veselá, Nabi Bidhendi, Rudnick, & van Treeck, 2015), heating only the core and neglecting the extremities leads to a thermo-physiological reaction of the body. The resulting temperature gradients are high and perceived as distinctly uncomfortable. In the second study the seat heating was thus extended to include a heated steering wheel and heated surfaces in the footwell as well as on the sides (door and middle console). Where the first study was conducted with stand-alone seats in a climate test chamber, the second study used wooden cabin mock-ups. It was shown that using multiple local heat sources could rectify the thermal sensation in cooler cabin temperatures. In the best-rated scenarios regarding discomfort, at least three sources were active. The heated steering wheel proves to have the biggest influence, if not activated. This shows that thermoregulation through vasoconstriction in cold environments has a high impact on thermal wellbeing and asymmetry.

To sum up the major findings of the state of research:

- There is a lot of research to be found in various industries and applications regarding thermal comfort, but mostly for living and working spaces in buildings.
- The focus on thermal comfort research in cars is on heating in cold conditions. Little to no work regarding cooling in hot and humid conditions is being conducted.

- When looking at thermal comfort in a highly dynamic and heterogeneous application such as a car, local thermal comfort becomes a major influencing factor on overall thermal wellbeing
- Local heating is preferred at the torso and the extremities. The head should not be heated.
- Local cooling has the most positive impact when applied to the head and the upper torso. When sitting, the microclimate between body and seat should be monitored to avoid accelerated sweat production.
- There is sparse research on the different impacts of convective, conductive and radiative heat transfer on human thermal comfort.
- Experiments to measure human responses to thermal conditions and changes are extensive and time consuming.

3 Procedural methods and research questions

Both the FAT studies and most commercial concepts and design studies for alternate HVAC concepts, tend to focus on heating in cold conditions. This focus has ensued mostly because heating poses a bigger impact on energy consumption, especially in the ongoing change from combustion engines to electric cars (see Figure 1, right). In a tropical climate heating is superfluous however and the cooling system is still the biggest secondary consumer.

The goal is to develop a coherent concept to cool and condition occupants in hot (and humid) climates. Deriving from the research, a comfort oriented, individually conditioned and locally applied system is desirable. The focus for cooling seems to lie on the head and the upper torso, while the micro-climate on the seat contact area should be moderated by seat cooling and/or ventilation.

- In a first step, a concept for local, vertical interior cooling and conditioning is developed based on the assumption that local conditioning leads to improved thermal comfort at lower energy consumption. The system is then designed and integrated into a working vehicle prototype to prove feasibility of the system. Automotive boundary conditions have to be considered and manifold automotive requirements met, especially at the interfaces with interior and exterior design, vehicle package, electrical supply (HV and LV) and function development.
- In a second step, the major elements of the interior cooling system are physically simulated in system mock-ups to enable testing of operability limits. Explorative climate comfort studies in a controlled climate chamber are conducted with these parts of the system to determine the impact on local and overall human thermal wellbeing.
- Thirdly, results are assessed to give an estimation of the system energy efficiency in respect of achieved thermal comfort. This can be discussed further in regard to feasibility, weight and package impact of various cooling approaches.

Thus the research questions (RQ) that require answers are:

- RQ1: Is local, vertical cooling technically feasible in an automotive context?
- RQ2: Does local, vertical cooling reduce discomfort and improve efficiency?
- RQ3: What are the operating limitations of such a system?

4 Technical solution of new concept for interior cooling

The new system for cabin cooling was generated as part of the development of the electric taxi EVA. EVA is a fully operable prototype that was built as a project in the course of the research programme TUM CREATE in Singapore. The prototype was presented at the Tokyo Motor Show in 2013. A summarised overview of the project can be found in (Bender et al., 2013). The electric prototype is a purpose built vehicle for use as a taxi in tropical megacities. The main conclusion for thermal management is a strong focus on component and cabin cooling. Heating the cabin does not have to be taken into account.



Figure 15: The electric taxi EVA by TUM CREATE (TUM CREATE, 1/12/2014)

The backbone of the interior cooling systems is a standard refrigeration cycle with R134a as the operating refrigerant. The refrigeration cycle is linked to the battery cooling cycle via a chiller and to the interior air conditioning system via the evaporator in the central HVAC unit. While most thermal management components are modified state of the art systems, the overall concept for the interior conditioning was designed anew.

4.1 HVAC concept in the prototype

The concept of the HVAC system derives from the same principles that were applied on the FAT studies for localised heating (Schmidt et al., 2013 & Schmidt et al., 2015). Namely, that the major shortcomings of current systems are both energy and comfort related:

- Regulation is by mean cabin temperature,
- local conditioning is minimal and most often targets the whole cabin,
- air flow is horizontal (front to back), and
- airflow speeds are often very high.

The result can be a sub-optimal thermal comfort at an energetically adverse state. Thus a concept was developed to improve the climate system by making it more user friendly and comfort oriented. Additional information of the whole thermal management system can be found in (Stuke & Bengler, 2013).

The thermal conditioning of the occupants is aimed to be as close to the body as possible without creating an unfamiliar and unwanted nuisance. The two major areas of interest are the seat (seating surface and backrest) as well as the head area and upper torso. The most important design fundamentals for the overall concept were: individual climate zones for each occupant, local, close to body conditioning and focus on the scientifically proven most effective areas.

- Climate zones:

The taxi is a four-seater and accordingly the cabin is virtually divided into four climate zones (Figure 16), one for each seat. Climate control is designed to be adapted individually, so the HVAC system has to be able to provide the individual adjustments without influencing other occupants. This has the additional advantage that an unoccupied zone can be turned off when not in use and energy consumption can be minimized.

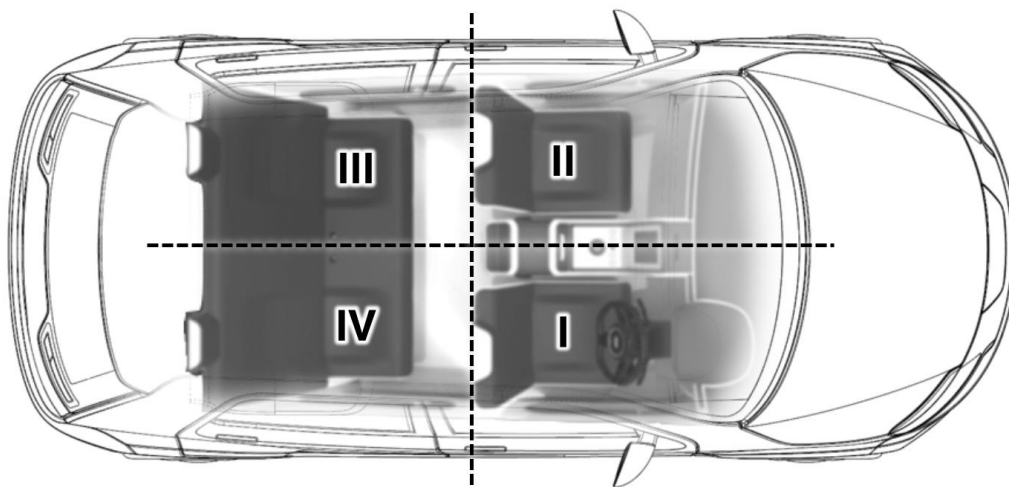


Figure 16: Seating layout and division in four climate zones in prototype vehicle EVA

- Overhead outlets:

According to Zhang (2003) and Prestel (2013) cooling the head has a significantly positive effect on the overall wellbeing. So instead of a horizontal airflow the air is guided vertically through the cabin (Figure 17) with outlets as close to the head as possible. This is accomplished by directing the majority of conditioned air through overhead outlets.

- **Ventilated seats:**

Ventilators in seat surfaces, that draw the air away from the occupant, support this vertical air movement. Thus the microclimatic conditions of the contact area between occupant and seat is improved as has been discussed in Pasut et al. (2015) & Watanabe et al. (2009).

This vertical routing of air flow has another positive effect in the resulting layering of air temperature. A heat accumulation in the head area is avoided since forced vertical flow counteracts warm air rising through natural convection.



Figure 17: Vertical air flow distribution in prototype vehicle EVA (Stuke & Bengler, 2013)

4.2 Air path

Fresh air inlet, recirculation and pressure outlet are analogue to a state of the art vehicle and were integrated with minor adaptations to the vehicle package. The air path into the HVAC unit as depicted in Figure 12 is also state of the art up until the air flow is split in the temperature flaps after the evaporator. The air distribution box containing temperature flaps, heater and mass flow flaps was newly designed. Also, a new development was that air ducting leads through the car body structure to the overhead outlets. To counteract the high heat-load scenarios such as the initial cooldown at the start of a trip on a hot summer day (that cannot be handled by overhead outlets alone), additional outlets directed at the occupants' torso had to be included.

4.2.1 HVAC unit

The main part of the HVAC system, the HVAC unit itself, was a takeover part from a Volkswagen Jetta (Figure 18). The choice fell to this unit, because the taxi's interior has a similar volume as the Jetta and the unit is designed to cope with similar heat loads. The air inlet and mounting system were custom built.



Figure 18: HVAC unit, takeover part from a VW Jetta

4.2.2 Air distribution box and air ducts

The Jetta air distribution is a two-zone system which was not sufficient for the requirements of EVA. To be able to provide individually conditioned air in four zones, the air distribution box and the ducting into the cabin had to be designed anew. This work was supported by the student Friederike Jekelius. Additional information can be found in the resultant diploma thesis (Jekelius, 2013).

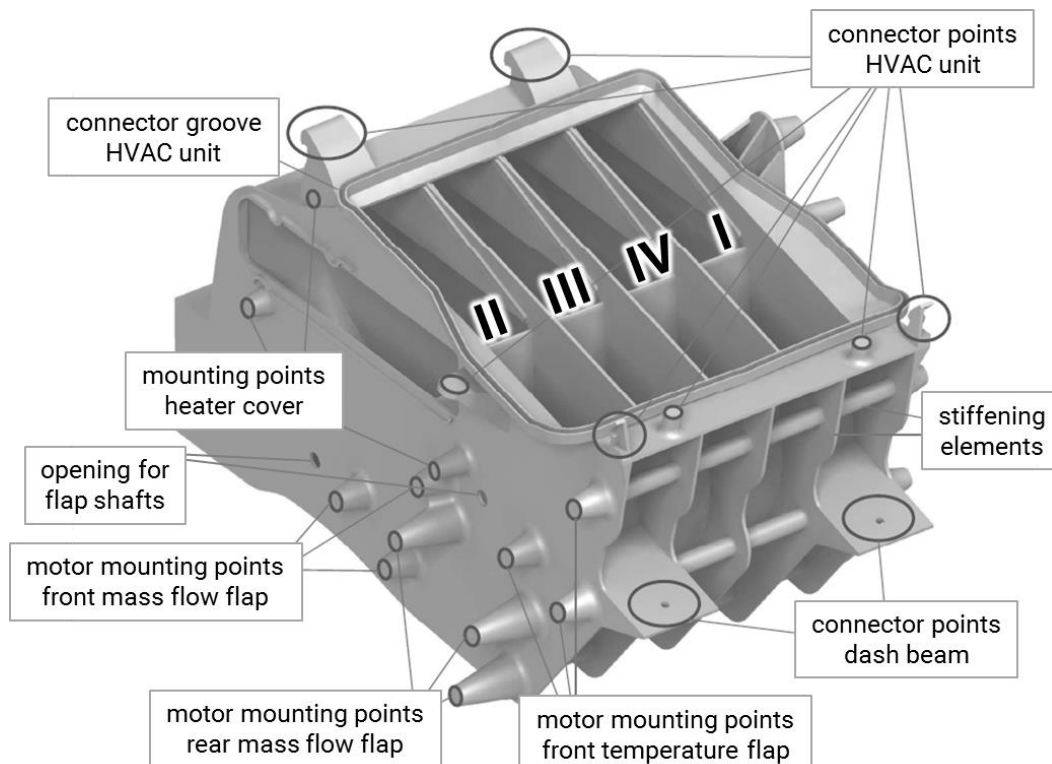


Figure 19: Four-zone air distribution box (adapted from Jekelius, 2013)

Deviating from the approach of Volkswagen in the Touareg (Volkswagen, 2002) that introduced a second HVAC unit for the rear passengers, all four zones of EVA's interior were supplied by one central HVAC unit. Air enters the air distribution box after having been cooled in the evaporator. The air distribution box has two functions: the apportionment of air led through the heater and the distribution of mass flow for each zone.

The new air distribution box is divided vertically into four identical air paths, each with its own temperature and mass flow flap (Figure 19). Each flap is driven by an original Volkswagen step motor. The levers were adjusted and the shafts for flaps (2) and (3) led through hollow shafts of flaps (1) and (4) respectively. The air distribution box with the externally mounted motors is embedded under the dashboard (Figure 20). For manufacturing, the housing of the air distribution box was sectioned in multiple segments, CNC milled in acrylonitrile butadiene styrene (ABS) and glued together. The connection to the air ducts protrudes into the encasement of the centre console between driver and front passenger.

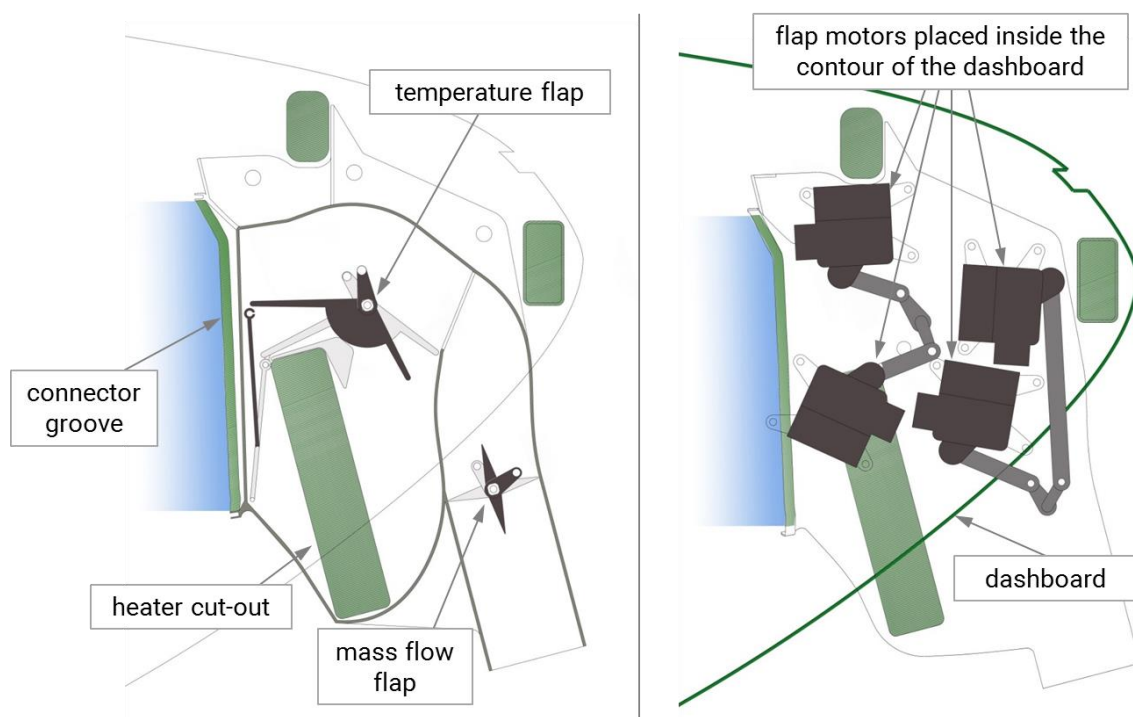


Figure 20: Integration of the air distribution box, temperature and mass flow flaps (left), flap motors (right)

The air is then guided into the air ducting system. The branch for each zone is forked into ducts that lead to the overhead outlet and ducts that lead to the auxiliary front outlet (Figure 21). For manufacturing and assembly purposes, the ducts were split into 42 parts and can be connected by flanges. The geometrically simple parts of the air ducts are produced by thermoforming polyethylene (PE). More complex parts are products of selective laser sintered (SLS) nylon plastic.

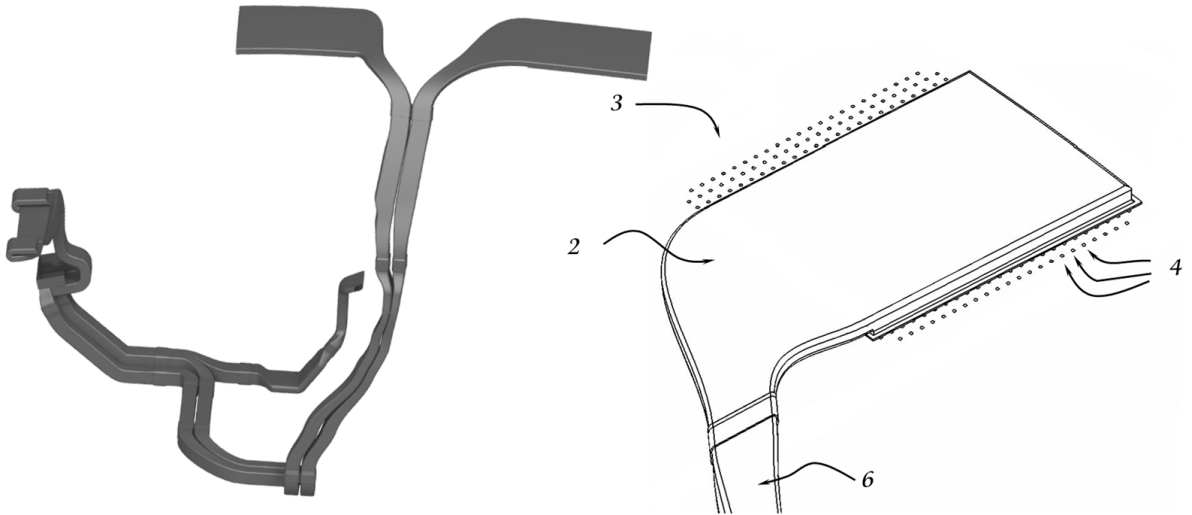


Figure 21: Air ducting for the front and rear left occupants (left), roof outlet [2], ceiling [3] perforated with holes [4], air duct from B-pillar [6] (right)

The air distribution box is mounted on the front firewall and the dash beam. The air ducts are integrated in tight fit inside the central console and under the seats in a way that a dislocation is not possible. Since the ducts inside the B-pillar lead through supporting vehicle structure, additional adhesive was applied to keep them in exact location. The overhead outlets are glued between the insulated vehicle structure of the roof and the headliner. The air is led through a perforated roof with a cross section of 300mm x 350mm. The occupant will experience a 'cold shower' without exceeding draught limits.

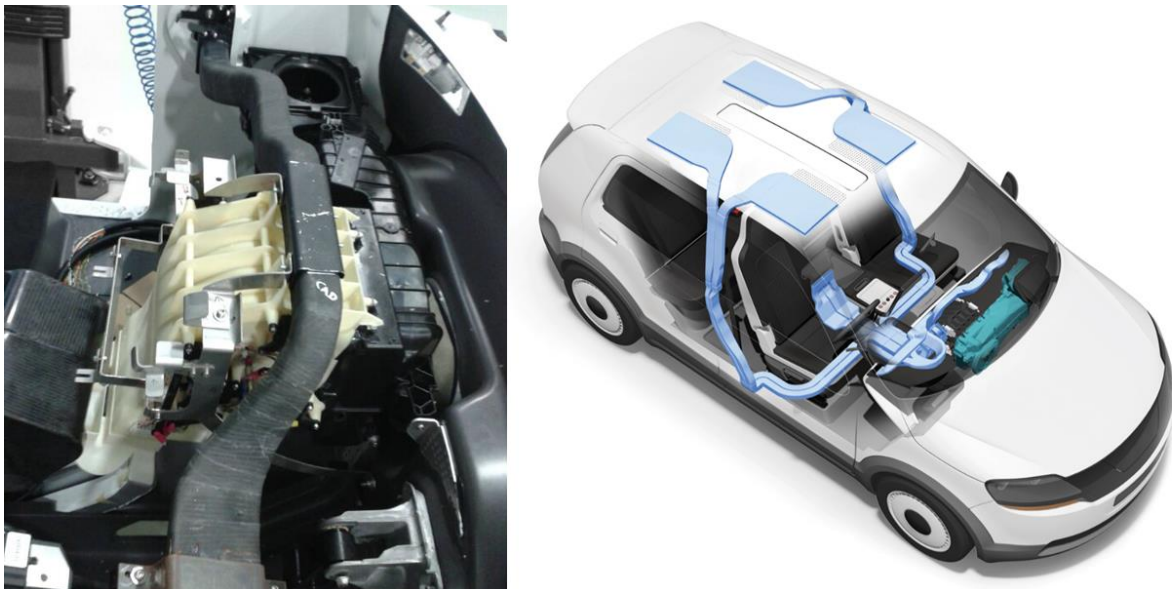


Figure 22: Assembly and integration of HVAC unit, air distribution box (left) and air ducts (right) in EVA

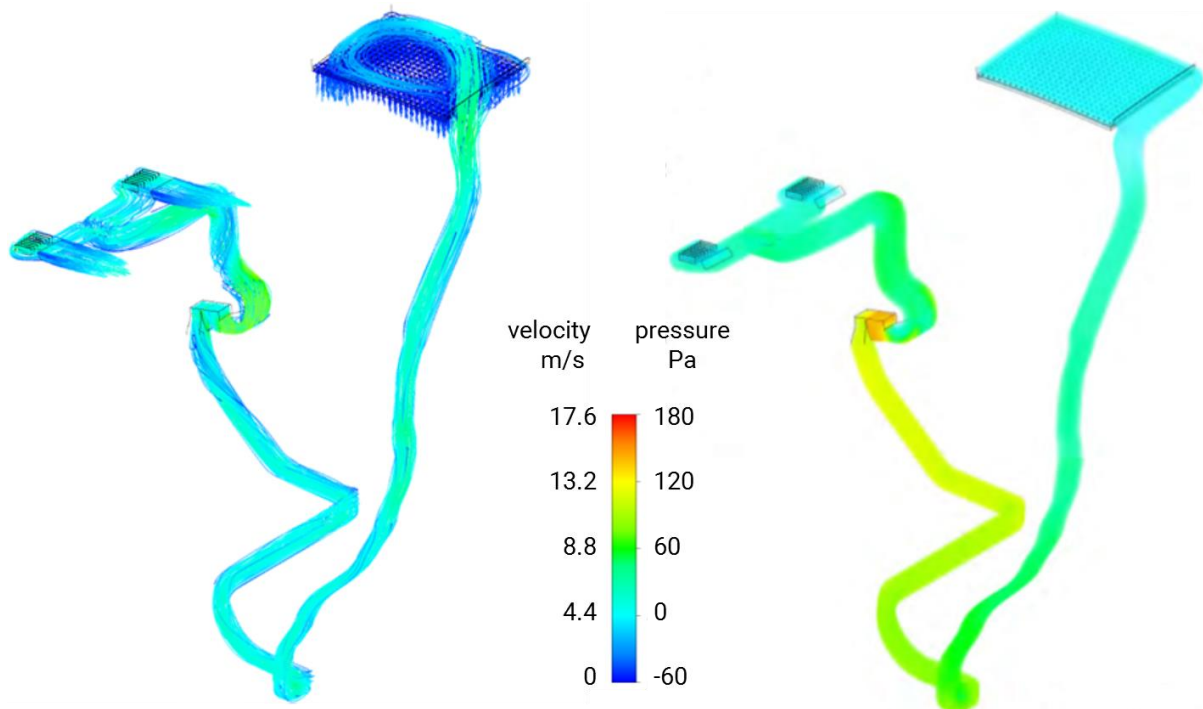


Figure 23: Air velocity (left) and pressure (right) simulation of front left air ducting system

The dimensioning of the air ducts had to be large enough to provide sufficient airflow while minimising both pressure loss and noise generation. According to (DIN 1946-3:1962-06), a typical maximum air mass flow to the cabin of 5 kg/min is required for cooling and ventilating in passenger cars. The guideline to noise-related limits for air velocity inside the ducts was taken from the building industry and defined as 5m/s (Monteur, 2011). A simulation with ANSYS Fluent helped in designing the air ducts in accordance with the mass flow, pressure loss and maximum velocity requirements (Figure 23).

4.3 Ventilated seats

When entering the car from a tropical surrounding, the occupant is likely to have an increased sweat rate. Sitting down on a leather or fake-leather seat traps the heat and moisture between occupant and seat and creates an uncomfortable moist and hot microclimate. The seats in the prototype are equipped with fans and feature breathable spacer fabric to avoid this. The six fans per seat are axial fans by ebm-Papst and have a power consumption of up to 1W per fan (Figure 24, right). The spacer fabric by Wellcool is a 3D-knitted highly breathable material that can be used as a foam replacement (Figure 24, left). The design and the integration of the ventilated seats into the prototype was aided by Markus Lutz. A more comprehensive description can be found in the resulting term paper (Lutz, 2013). Preliminary tests with several seat mock-ups have shown that great care has to be taken to obtain a uniform flow pattern and to avoid spots of high velocity and overcooling.

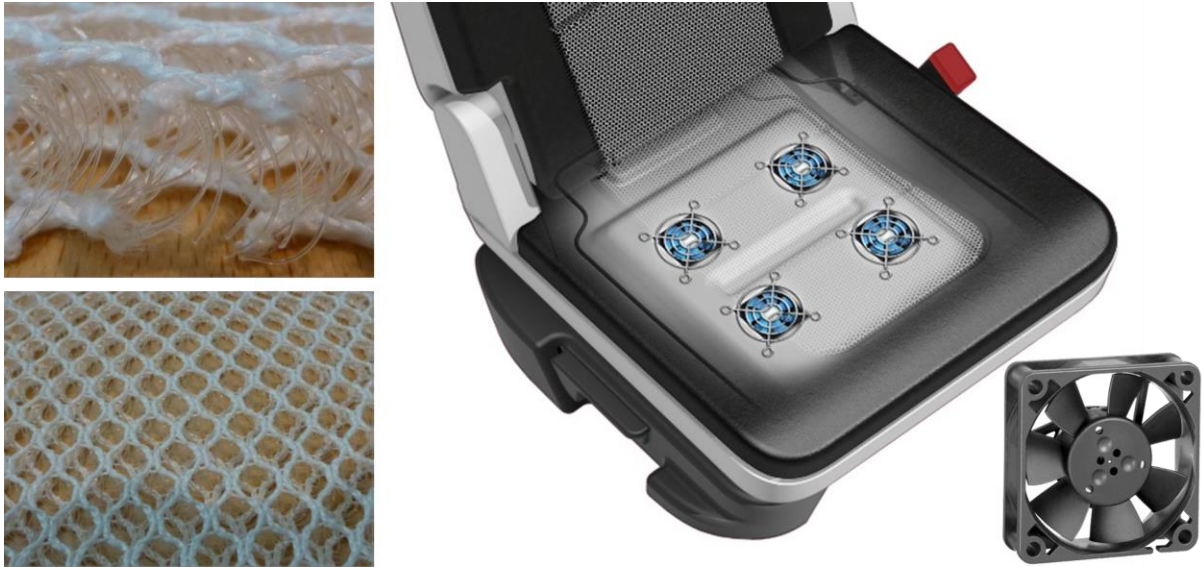


Figure 24: Ventilated seat (Lutz, 2013) with spacer fabric (Wellcool, 2/12/15) and axial fans (ebm-papst, 4/1/2016)

The decision to draw air away rather than to blow air towards the occupant was founded on preliminary tests and on thermodynamic considerations. In the preliminary tests between five and ten people in varying clothing and with varying thermal conditioning (having been in the workshop for more than two hours, coming in from outside tropical climate, coming in after exercise) sat down and adapted the fan speed in both blowing and drawing mode. The preference vote fell decidedly to drawing air away. The thermodynamic consideration is that the degree of perspiration cannot reliably be measured in the car and thus the cooling effect of evaporating sweat is difficult to control. Drawing the air, and with it the moisture, away diminishes the risk of local overcooling that is more likely to occur when air is blown towards the body.

4.4 Control strategy: Comfort oriented HMI

The choice for the HVAC control fell to an intelligent climate automatic rather than a user controlled manual one. This advanced system regulates cabin cooling, overhead outlets and seat ventilation and follows the same two major principles that provided the basis for the overall system: thermal comfort and energy efficiency. Considering the mutual interference between these two principles, it is debatable whether a user is able simultaneously to match his thermal comfort experience with energy efficiency demands. It was thus assumed that reducing the users' degree of HVAC adjustment freedom is a valuable aid in meeting the two principles at the same time. It was further expected that this reduced degree of freedom will not detrimentally influence user acceptance of the HVAC system. To investigate this assumption a new HVAC system HMI concept was designed, which was optimized for the electric prototype vehicle.

The basic idea behind the new HMI is a change in the control strategy. Instead of demanding a temperature for the automatic control, as is done in state of the art controls, the user inputs his desired state of thermal wellbeing. In a simplified scenario, the cabin is assumed to have a uniform temperature. The HVAC system is set to operate within the calculated comfort zone. Using the adaptive thermal model, the optimal combination of temperature and humidity can be found. Assuming the tropical climate in Singapore for the climate zone as derived in Chapter 2.3.2, and implementing two 1K increases or decreases in mean cabin temperature, this would result in the operational states depicted in Figure 25.

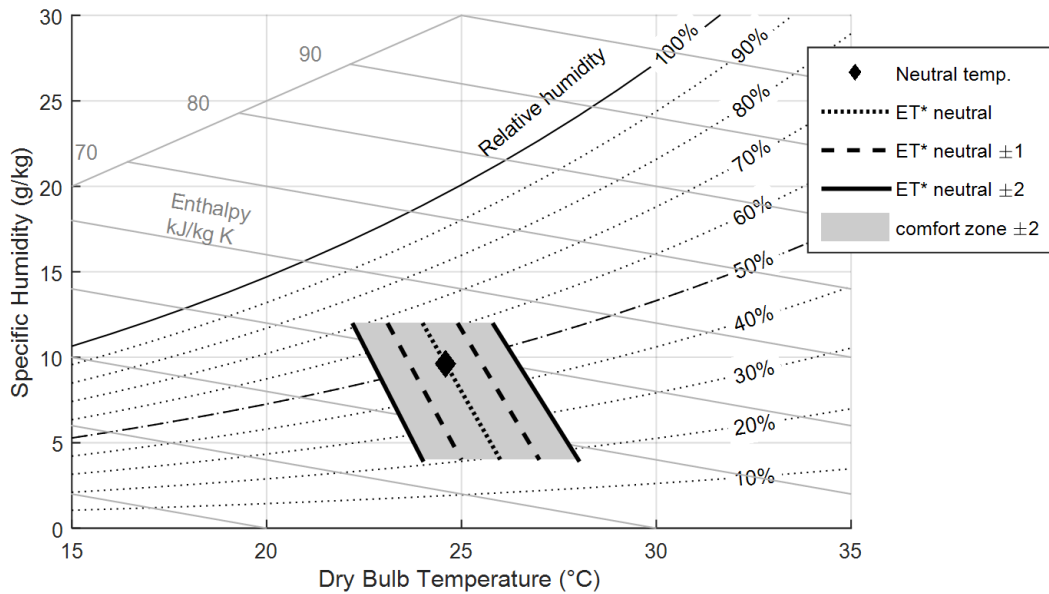


Figure 25: The Adaptive Thermal Model's comfort zone (for Singapore) in a psychrometric chart

The five resulting operational states can then be selected by the user via the 'A/C HMI' (Figure 26). The controls are implemented on a display located in the centre console: the central information screen. The occupant can also activate and deactivate the climate control for his/her seat via smartphone.

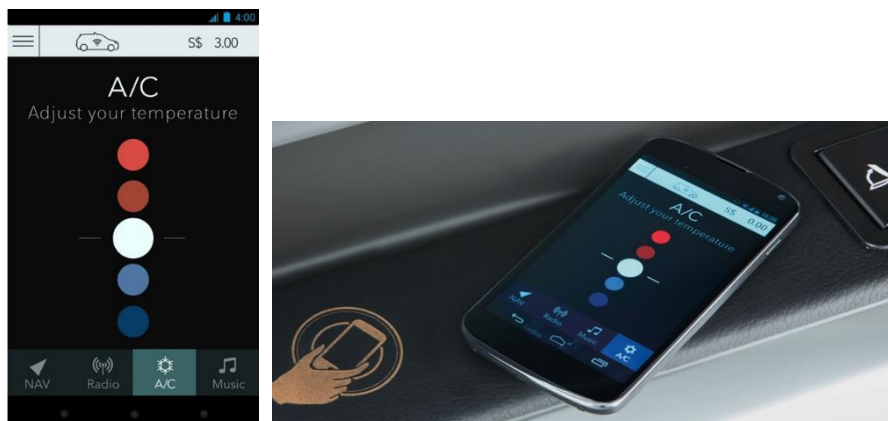


Figure 26: Implemented HVAC control on the occupant's smartphone for a purpose-built electric vehicle.

The default setting is the calculated “neutral comfort” state (‘white’ in Figure 26). The only manual possibility to influence the system is a scale inspired by Fanger’s PMV scale and the thermal preference scale of DIN EN ISO 10551: The occupant can state his thermal preference (slightly warmer/warm, slightly cooler/cool) and the system will adapt output accordingly within the calculated comfort range.

One advantage of this new control interface over a standard interface is that the user cannot interfere with the energy-optimized setting. The decision options given to the occupant are based on perception rather than hard facts (such as air temperature or blower speed), because thermal comfort is, in itself, a perceived state.

The chosen states are achieved by calculating the desired (overhead) outlet airflow, temperature and humidity values taking into account ambient conditions, cabin conditions, occupation level and selected preference. The goal was to develop a model-based control concept. The control model is based on the physical parameters of all thermal management components. The controlled components and influencing sensors are shown in Figure 27. Michael Rainer supported the entire derivation of the control concept, including management of the refrigeration cycle, cooling of both the propulsion system and the high voltage battery, as well as the interaction of thermal management components. All this can be found in the resulting diploma thesis (Rainer, 2013).

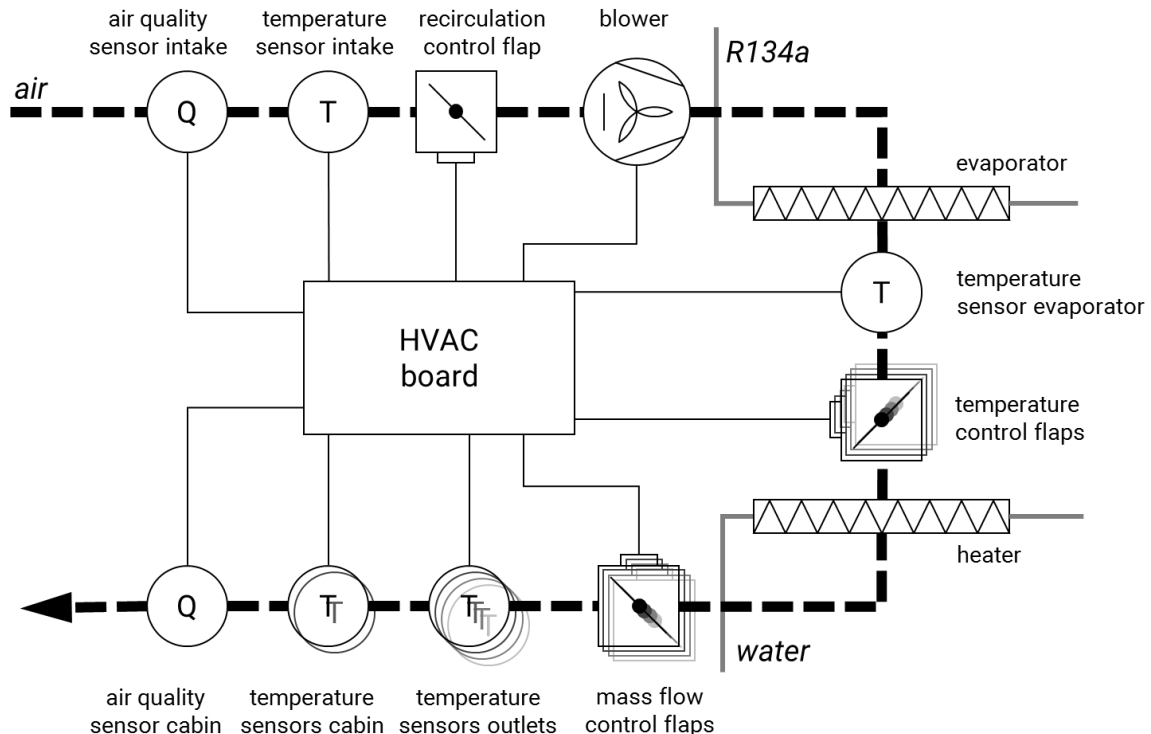


Figure 27: HVAC control board: HVAC and air flow overview (adapted from Rainer, 2013)

The parameter settings for the vehicle prototype were derived from the assumptions based on the Adaptive Thermal Model and the results of the explorative pre-tests on preliminarily ventilated seat prototypes. The corresponding parameter settings for each user choice on the HMI are shown in Table 10. When a passenger (or the driver) enters the taxi in Singapore's hot and humid outside conditions, the initial cooldown is supported by higher integrated seat fan settings. Initial cooldown phase duration has been set arbitrarily and will be evaluated in human subject studies evaluating the dynamic cooldown after ingress.

user setting	equivalent indoor temperature	seat ventilation level	
		initial phase	continuous
MAX	$ET^*_{neutral} + 2 \text{ K}$	1	0
HIGHER	$ET^*_{neutral} + 1 \text{ K}$	1	0
NORMAL	$ET^*_{neutral} = 24.6^\circ\text{C}$	2	1
LOWER	$ET^*_{neutral} - 1 \text{ K}$	2	1
MIN	$ET^*_{neutral} - 2 \text{ K}$	2	2

Table 10: User settings, corresponding temperatures and seat ventilation levels (adapted from Lutz, 2013)

4.5 Lessons learned and discussion

EVA was developed as a fully functioning prototype that can be used as a basis for the design of a commercially produced vehicle. During the design process it was always ensured that all parts of the car can also be produced (if adapted for mass production) in assembly-line production. Part of the EVA project was a fiscal feasibility study as to whether electric taxis can be competitive on the market. It was shown, that the car has the potential to be financially feasible.

The technical challenge demanded that all influencing parameters had to be considered. The interfaces with interior and exterior design, with seat belt and safety system, with the high and low voltage electrical system, the ergonomic guidelines and package-related topics in general raised a number of restrictions in the design and compelled iterative redesign. The result is however a fully functioning system that is feasible in both manufacturing and assembly. Some minor corrections require incorporation in follow-up design, especially for maintenance and service access.

The cooling system is working as intended. However as of now, no comprehensive studies have been conducted with the prototype car. The discussion, as to whether the proposed system, using a centrally supplied cool air source in the HVAC and distribution to the roof through air ducts, is a viable solution, will be taken up again in Chapter 6.

5 Ergonomic studies for local cooling

The prototype primarily provided the means for a feasibility study and research platform to elaborate whether and how the new system is technically possible. This is especially important because in an automotive context the limitations given by interfaces to other domains reduce the degree of freedom in design. The optimal interior cooling system might therefore eventually look different. If the limitations of the interior cooling systems have to be proven by test and especially if they are to be evaluated for scientific purposes, a flexible mock-up is needed.

This chapter initially describes the experimental environment, namely the climate chamber, the mock-up and the measuring equipment used, then three separate but correlating tests that have been carried out. The first two address the influence of overhead cooling and seat ventilation as standalone systems to enhance the occupants' thermal wellbeing. The third test deals with the combined effect of overhead cooling and seat ventilation. The tests were supported by Pablo Theissen, Andreas Rolle and Martin Höchenberger and resulted in three term theses (Höchenberger, 2016; Rolle, 2016; Theissen, 2015).



Figure 28: Test person in the mock-up during the experiment

5.1 Basic idea and anticipated outcome

Figure 29 shows four scenarios for varying ambient air temperature and air flow temperature in a car. The temperature of the cabin interior is plotted on the horizontal axis. The vertical axis represents the delta in temperature between cabin interior and overhead outlet. The

intersection of a vertical line at an interior temperature equivalent to a PMV of 0 (for Singapore at a temperature of around 24°C) divides the area into 4 quadrants.

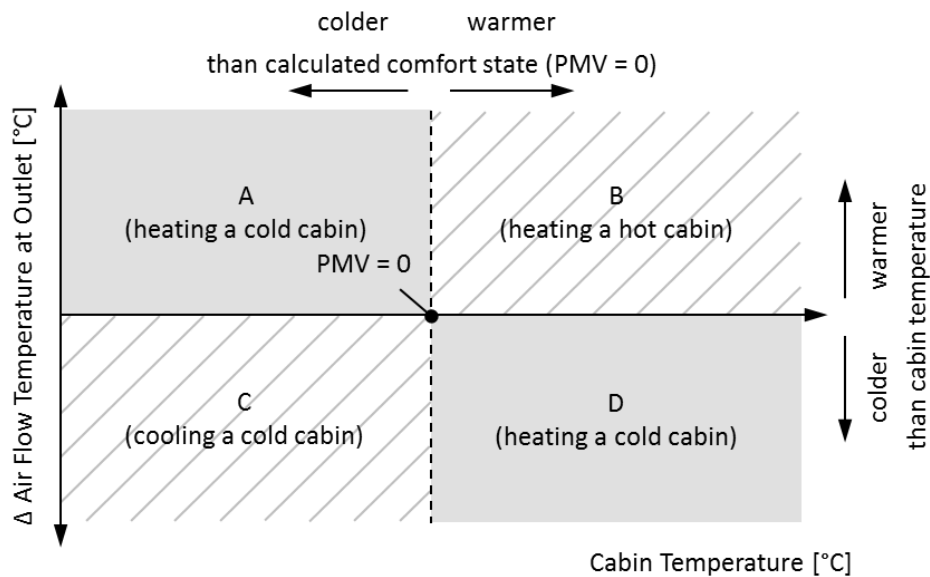


Figure 29: Scenarios for local thermal conditioning

Section B (heating a hot cabin) and C (cooling a cold cabin) can be discarded as being not relevant in vehicle air conditioning. Section A (heating a cold cabin) and D (cooling a hot cabin) require further investigation. Section A will not be discussed in this dissertation (one student thesis showed a positive impact of overhead heating. For details refer to (Hertle, 2015)). The focus of this dissertation is on cooling under hot (tropical) conditions, thus Section D will be discussed in detail.

Based on the hypothesis that local cooling or ventilation has a significant impact on overall thermal comfort, the possible distribution of discomfort in Section D is plotted in Figure 30 based on the example of local overhead cooling.

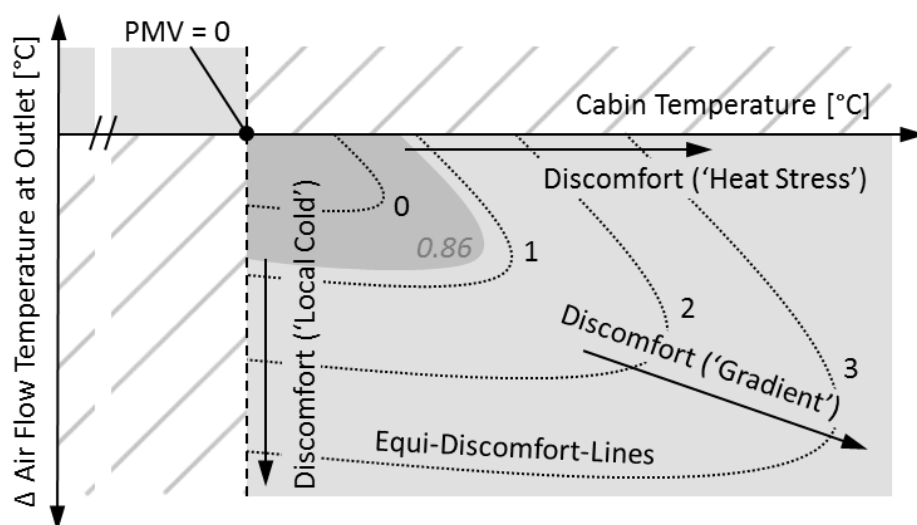


Figure 30: Possible distribution of discomfort votes in section D (heating a cold cabin)

Herein, the z-axis depicts the status of the occupants' overall thermal comfort. The point equivalent to $PMV = 0$ will be taken as the point with the lowest discomfort. Taking the range of thermal indifference into account, an area of discomfort equivalent to a PMV of 0 is expected to protrude elliptically into the temperature field. Raising the cabin temperature will go along with rising thermal discomfort. This discomfort is the result of whole body (overall) heat stress. Activating the overhead cooling at neutral conditions will also result in thermal discomfort. In this case, unnecessary local cooling will result in higher local discomfort and is thus the source of overall discomfort. Activating the overhead cooling in hotter cabin states is expected to at first lower the overall discomfort and rise again with increasing temperature gradients between cabin and outlet as increasing the gradients between body parts too much will again increase the overall discomfort.

As discussed in Chapter 2.3.3, the result of overall discomfort can have various causes. It has also been stated that Fangers' PMV is not the perfect tool to evaluate overall discomfort through local phenomena (gradients, cold spots, moisture at seat surface...). But, for reasons of comprehensibility, Figure 30 shows the lines of theoretical absolute PMV values. Connecting the points of the same absolute level of discomfort (for example equivalent to a PMV of +2 due to overall heat stress and equivalent to -2 due to local 'cold spots') will result in so called 'equi-discomfort-lines'. If for example an acceptance of 80% is deemed sufficient (which results in a PMV of about 0.86), the overhead cooling could be operated inside the dark grey area in Figure 30.

The goal of the experiments is to establish whether the behaviour of the equi-discomfort lines is indeed as predicted. If so, the function of minimal discomfort over cabin temperatures is of interest. The experiments are explorative. Sample sizes of around ten people are not enough for a valid statistical analysis. This would require a sample size of minimum 25 participants per data point.

5.2 Experiment environment

The experiments were conducted in a climate test chamber under controlled conditions. Controlled conditions are important, since fewer variables mean easier reproducibility and more uniform results. This includes the controlled thermal parameters in the climate chamber and the mock-up, the preassigned experimental procedure as well as the selection of the test person sample. It is furthermore important to reduce to acceptable or negligible, stable values all discomfort-inducing influences such as odour, light, sound and vibration, seat pressure and posture.

The schematic of the experiment setup is depicted in Figure 31. The operators' room with the chamber controls and the PC for the driving simulation is on the left. The climate chamber can be monitored through a window behind the operators' workplace and entered through an insulated door. The vehicle mock-up and a big television screen for the driving simulation

are in the chamber. The PC for the temperature sensors and the controls for the overhead and seat fans are on a ledge attached to the rear of the mock-up. The chamber can also be accessed from the hallway through an insulated door wide enough for the mock-up assembly.

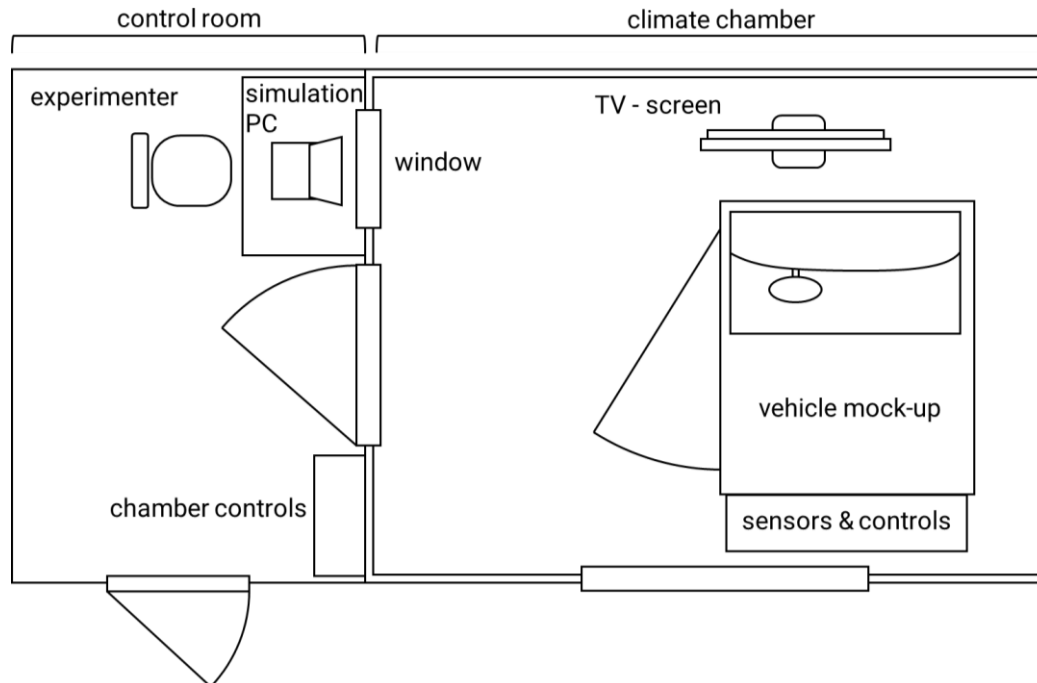


Figure 31: Experiment setup in the climate chamber

5.2.1 Experiment room

The test chamber of the Lehrstuhl für Ergonomie (LfE, institute of ergonomics) of the Technische Universität München was made available for this project. An excerpt of the datasheet is provided in Table 11. The air is led into the chamber via a perforated ceiling. Outlets are positioned on the bottom of one side wall. The ventilation of the room was set to the lowest possible setting to keep the general air speed low while still being able to maintain the desired thermal conditions. Discomfort through draught caused by the chamber ventilation could thus be minimized.

Climate Chamber	
Model	SB 32' / 30 – S
Test space dimensions	H: 2300mm
	W: 3000mm
	D: 4000mm
Temperature range	+10°C ... +60°C
Temperature deviation over time	±1K
Humidity range	10 ... 95% r.h.
Humidity deviation over time	±(3 ... 5)% r.h.

Table 11: Data sheet climate chamber

5.2.2 Vehicle Mock-up

The mock-up consists of the hardware for the simulated driving environment, the replicated plywood vehicle interior, the hardware for the overhead outlet and the modified vehicle seat.

Cabin mock-up

The wooden car model had to be spacious enough to replicate a real car interior and small enough to pass through the climate chambers doors. The dimensions of a small two-seater interior were chosen, comparable to the interior dimensions of the electric car MUTE by the TUM. The thickness of the plywood and the acrylic glass was calculated to resemble a real car's thermal values. The mock-up was utilised without windows in the present studies, but glazing was considered in anticipation of follow-up studies. According to Großmann (2013), the heat conductivity of a car can be calculated by summarizing the conductivity of the elements of the car body:

$$k \cdot A = \sum_{n=1}^n \frac{A_n}{\frac{1}{\alpha_{i,n}} + \left(\frac{\delta}{\lambda_n}\right) + \frac{1}{\alpha_{a,n}}} \quad (5.15)$$

Grossmann also gives a reference value for standard cars with a volume of ca. 2.5m³: $k \cdot A = \text{ca. } 60 \frac{W}{K}$. With the following equation this value can be approximated for interiors with a different volume.

$$k \cdot A_1 = k \cdot A_2 \cdot \left(\frac{V_2}{2.5}\right)^{\frac{2}{3}} \quad (5.16)$$

The insulation of car bodies varies for each model and manufacturer, but with a plywood thickness of 12mm and acrylic glass with a thickness of 1.5mm the present mock-up is at least in a comparable range in terms of heat conductivity.

Overhead outlet

An outlet for the cold air flow resembling a perforated ceiling is installed above the test subject seated in the car model. The outlet is a 30 cm × 34 cm grid with 20 × 23 = 460 holes, each 4mm in diameter. The dimensions were adopted from the EVA prototype. Air is drawn from the chamber and the air flow is created above of the grid by three fans that were contributed by Gentherm. A cooler with a water cycle cools the air flow in a heat exchanger between fans and perforated ceiling (Figure 32). In the first part of the experiments a thermostat by LAUDA was used. Since the cooling power was fairly poor and the cooldown took more time than deemed acceptable (up to 6min/K), in the latter part of the experiments the cooler was fed by the climate chambers water connectors (temperature: 0°C – 80°C, temperature change rate: min. 1K/min).

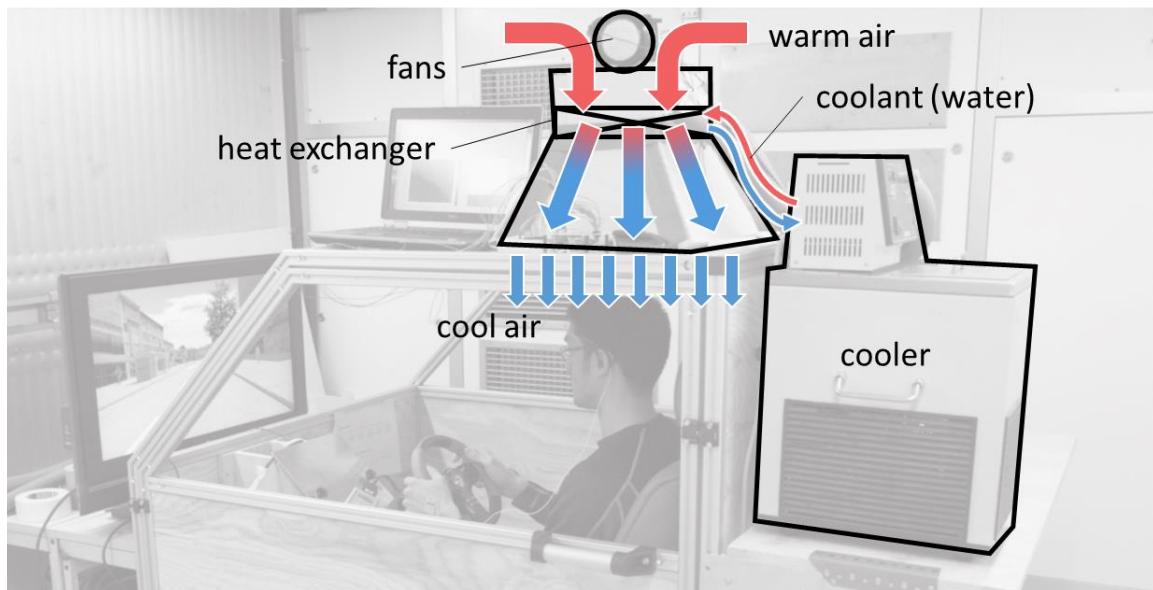


Figure 32: Setup of the overhead cooling system seat mock-up (compare Figure 28)

An original car seat was modified to the required specifications for the mock-up seat. The seat had to be able to ventilate and cool the occupant. In a first step, only convective cooling was considered. Conductive cooling could easily be integrated for example with a detachable water cooled mat. The desired modes of operation are depicted in Figure 33 from left to right:

- one: unmodified seat (faux leather cover)
- two: passive ventilation (spacer fabric)
- three: active ventilation (suction mode)
- four: active ventilation (blowing mode)
- five: active cooling in blowing mode

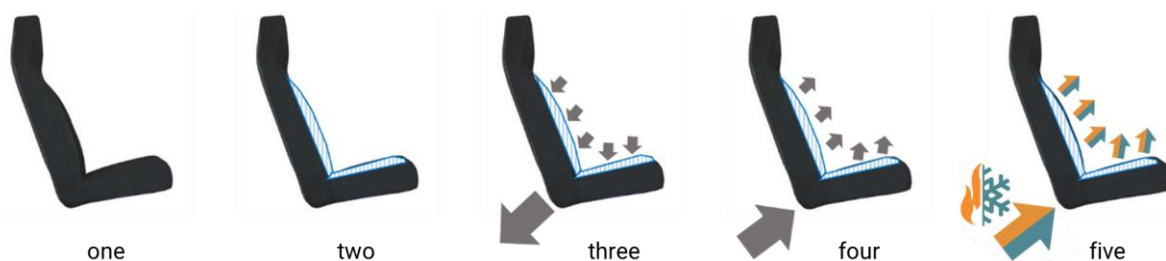


Figure 33: Seat mock-up, modes of operation

Mode one was the original seat with the original faux leather cover. For Mode two, the faux leather was removed and the foam replaced with air permeable spacer fabric. Ventilation for Mode three to five was managed by fans contributed by Gentherm. Seat surface and backrest were separated into two sections each (upper [I] and lower [II] backrest as well as back [III] and front [IV] seating area, see Figure 34) to allow fine tuning of the airflow. This was done primarily because pre-tests had shown that the lower back around the kidneys is significantly more sensitive to cold air flow than the upper back. Switching between suction

and blowing mode was achieved by reversing a slide-in panel on which the fans are mounted. Active cooling for Mode five can be achieved by cooling a heat exchanger mounted in the air path before the fans. The studies in the present work only used Modes one and three. Modes four and five were implemented in anticipation of future studies. The build-up of the mock-up seat was supported by Vincenz Marschall and the proceedings can be found in detail in (Marschall, 2015).

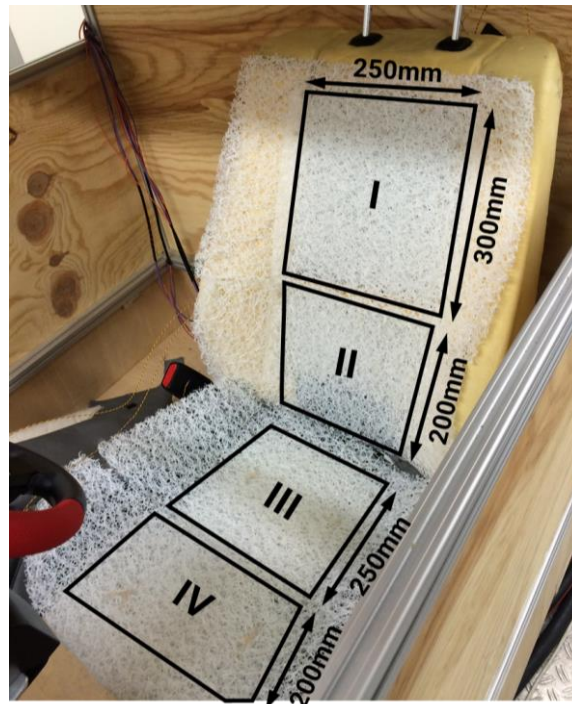


Figure 34: Seat with spacer fabric (operating mode two), segments for seat ventilation (Theissen, 2015)

The seat had the same degrees of adjustment freedom as a car seat and the participants were able to adjust their seating position to a comfortable setting. They were asked whether they were seated comfortably to eliminate discomfort arising through posture.

Driving simulation

Zhang, Arens & Arens (2002) conclude that “computer driving games with steering wheels and pedals can usefully increase the physiological realism of laboratory studies of drivers’ thermal comfort in automobiles” and that “the metabolic level of subjects performing the driving game” are “similar to that of actual driving on the road.” For this reason a simple driving simulator consisting of a single TV screen, steering wheel, and pedals was used in this experiment. The steering wheel and pedal could be adjusted to the participant’s preference. The software SILAB by wivw was used for the driving simulation of the first experiment. This was changed for the follow-up experiments to driving through a landscape of the game gta by Rockstar Games because participants complained about the monotonous route in SILAB. The participants were asked to drive as they would in real life and observe traffic regulations.

5.2.3 Sensors

While the test person was inside the climate chamber, cabin temperature and moisture were monitored, overhead outlet temperatures and air flow were measured, as were the subject's skin and core temperature. Built in sensors were used to measure and maintain chamber air temperature. The air at the outlet was measured by a custom-built setup of 16 sensors via an Arduino board.

Grid Sensors

Temperature measurement at the overhead outlet was achieved by a grid of 16 sensors. The sensors were thermistors of the type TS-NTC-502 by B+B Sensors. The technical specifications are shown in Table 12.

Precision temperature sensor TS-NTC	
Measuring principle	NTC
Measuring range	-60...+150 °C
Nominal resistance at 25 °C	5,00 kΩ ±0,5 %
B-value	3976 K ±0,5 %
Response time T66 in air	15 s
Self-heating	1.2 mW / K
Max. power loss	6 mW
Connection wires	Tinned steel
Dimensions	3.8 x 2.8 x 17 mm

Table 12: Data sheet temperature sensor TS-NTC

Figure 35 shows the arrangement of the sensors in the grid of the overhead outlet. The spacing between sensors was 7-8-7 holes (105-120-105mm) along the x-axis and 6-7-6 holes (90-105-90mm) along the y-axis.

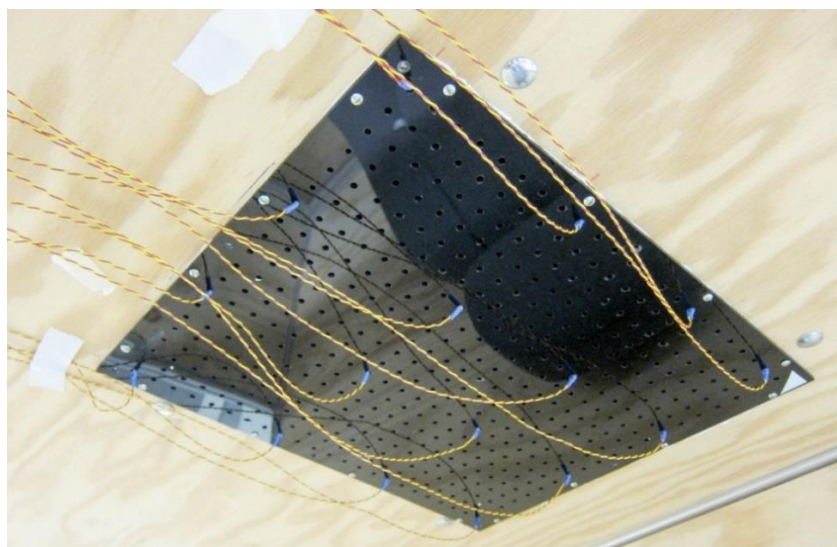


Figure 35: Overhead outlet with temperature sensor grid

The thermistor signals were bundled by a multiplexer and read via an Arduino board. The schematic is shown in Figure 36. The analogue signal $ANALOG_{IN}$ is a value between 0 and 1024 bits and can be transferred to the desired thermistor resistance R_{NTC} by Equation (5.17). The derivation of the formula can be looked up in the appendix.

$$R_{NTC} = 5110\Omega \cdot \left(\frac{1024}{ANALOG_{IN}} - 1 \right) \quad (5.17)$$

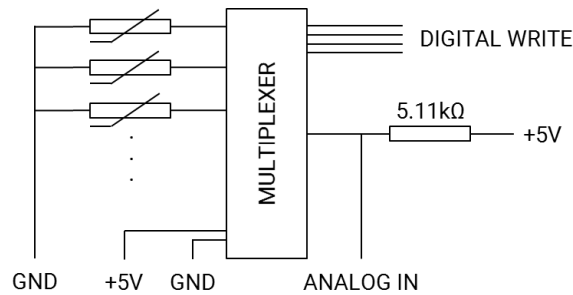


Figure 36: Wiring scheme for multiple temperature sensors

The temperature at the sensors can be derived from the measured/calculated resistance by means of the Steinhart-Hart-Equation (Steinhart & Hart, 1968).

$$\frac{1}{T} = C_1 + C_2 \cdot \ln(R) + C_3 \cdot \ln(R)^3 \quad (5.18)$$

The calibration to determine C_1 , C_2 and C_3 can be done by measuring the resistance of the thermistor in ice water, lukewarm water and boiling water and taking the corresponding temperature with a calibrated temperature sensor. In this case a sensor of the type PT-1000 by GHM-Greisinger was used.

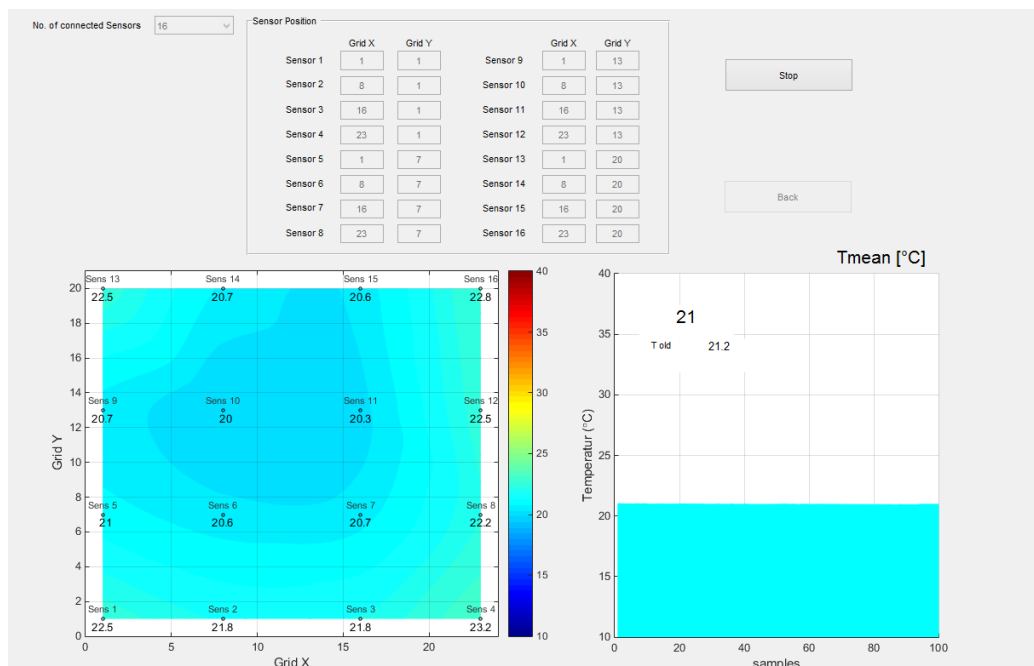


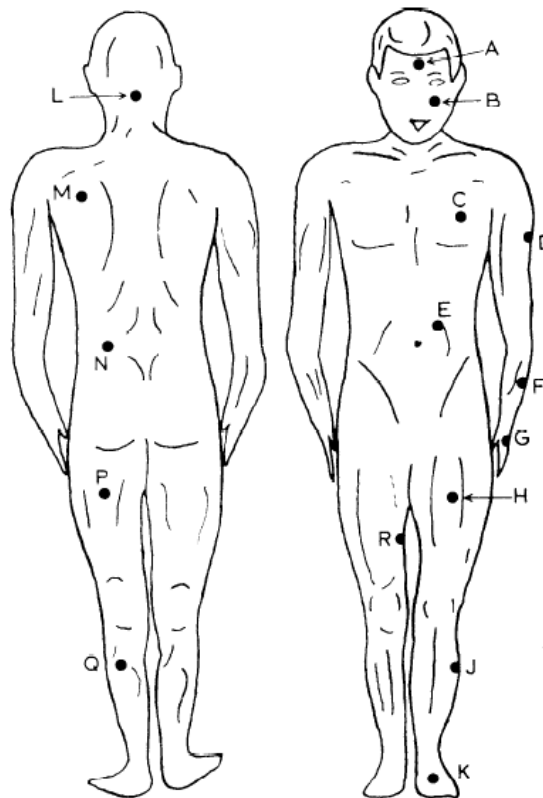
Figure 37: Visualization of grid temperature distribution and mean in Matlab GUIDE

The measured signals are calculated in a Matlab program and displayed both graphically and numerical (Figure 37). The temperature was interpolated and integrated over the grid to get the mean outlet temperature.

In the later experiments sensors of the type TS-NTC-502 were also used to log room temperatures and skin temperatures. With the implementation of another multiplexer, the number of sensors was increased to 32. The GUI was adapted to display all measured temperatures numerically and in real time.

Skin Temperature Sensors

For the first experiment with only overhead cooling active, skin temperature was measured on eight points on the body. The main emphasis was put on the head and torso which led to an adaption of the arrangement of temperature sensors proposed by Hardy & DuBois (1938, cited from Mitchell & Wyndham, 1969). The skin temperature positions that were measured in this experiment are shown in Figure 38.



	Measured skin temperature points							
Sensor	A	C	E	G	H	K	N	Q
Weight	0.07	0.117	0.117	0.19	0.19	0.07	0.117	0.13

Figure 38: Measured points for skin temperature (Mitchell & Wyndham, 1969)

The weighting formula to calculate a mean surface temperature was also adapted from Hardy/DuBois and the weighting factors for each measured point are shown in the table below Figure 38. In the experiments with seat ventilation, the sensor location M and two sensors above and below location P were also logged to get a better resolution of the cooling effect with active ventilation. All sensors were applied to the left body half and secured with surgical tape. The test subjects applied the sensors if possible by themselves (help was regularly needed to position and secure sensor M and sensor N). The experimenter then checked if all sensors were applied properly and started logging.

The data logger used in this experiment was “MSR 12” by MSR Electronics GmbH (Figure 39). It is portable and has sufficient working range and accuracy. An excerpt of the data sheet is displayed in Table 13.



Figure 39: MSR data logger, humidity sensor and “T-3” temperature sensor

	Temperature sensor “T-3”	Humidity sensor “HUM”
Measured parameters	Temperature	Relative Humidity, Temperature
Sensor type	DS18B20	SHT15
Working range	-40°C... +70°C	0%r. h. . . . 100%r. h. -20°C... +60°C
Accuracy	±0.5°C	< ±2%r. h. ±0.5°C
Dimensions sensor	9mm × 4.5mm × 2.5mm	20mm × 5mm × 5mm
Measurement frequency	1/s	1/s

Table 13: Data sheet for MSR temperature and humidity sensors

MSR sensors proved to be prone to breaking wires, however, which resulted in costly and lengthy delays for repairs. This is why, in a later stage of the experiments, the skin temperature was measured with the same sensors and measuring setup that were used for the overhead outlet. Before switching to the latter sensors, the systems were used in parallel to ensure consistent datasets.

Air flow measurement

In the present experiments, the aim was that discomfort should be caused or affected only by the air temperature. This is why the airflow was set to be below the threshold of 0.15m/s (compare Figure 9, max. 10% PD at 26.5°C). The velocity was measured with an anemometer ahead of the first experiments. A similar grid as that used for the temperature was used for this measurement, resulting in 16 measuring points. The air velocity measurements were taken 5cm below the grid to measure a more homogeneous flow; the outlet was surrounded by a 5cm long apron to prevent measuring errors caused by secondary air flows. The apron was discarded for the main experiments.

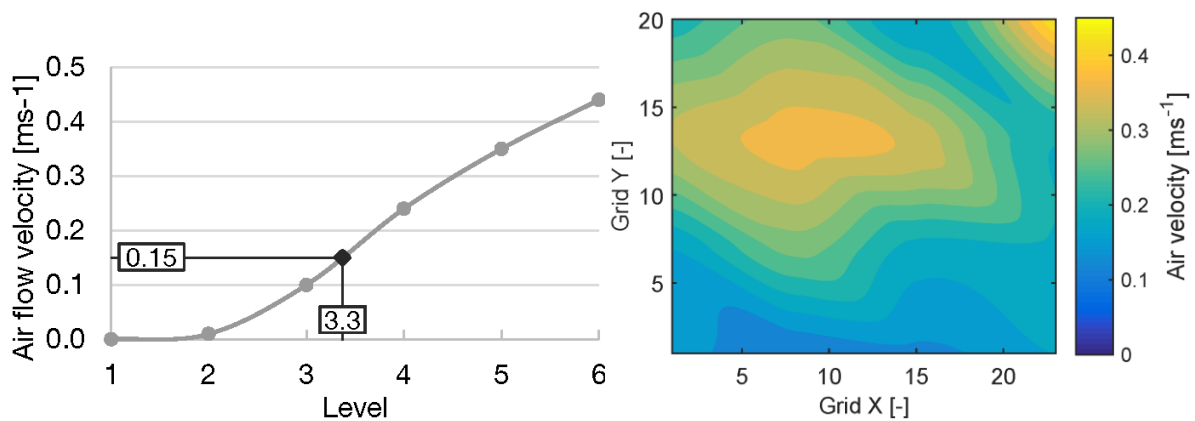


Figure 40: Grid air flow velocity over potentiometer level and velocity distribution over grid area (Theissen, 2015)

The airflow was regulated through a potentiometer and the measurements were used for calibration. Splitting the operating range into six equal segments allows setting the velocity precisely on a near-linear scale. Figure 40 (left) shows the average air flow over the potentiometer levels. The distribution of velocity over the grid is not homogeneous since the fans are slightly slanted and thus superimposing the air flow and leading to higher speeds around coordinate (X = 8, Y = 13) (see Figure 40 right).



Figure 41: BAPPU-evo and Anemometer-evo

During measurement the anemometer was held in place by a custom built tripod. Each point was measured for one minute and the average value logged. The anemometer used was an Anemometer-evo in combination with a BAPPU evo by ELK GmbH, shown in Figure 41. The data sheet is displayed in Table 14.

Anemometer-evo	
Measured parameters	Air velocity and temperature
Working range	0 m/s . . . 5 m/s
Accuracy	0.01 m/s

Table 14: Data sheet for anemometer-evo

5.2.4 Clothing for the experiments

The clothing worn in the experiment had to be standardized for all participants and experiments. Also it had to be realistic, that is to say that it would represent an average clothing ensemble which would be worn in the tested environment. In anticipation of future research, it was decided that the clothing ensemble also be realistic for both heating in cold conditions and cooling in hot conditions. The choice resulted in an ensemble with an insulating value close to 1clo. The participants were asked to wear jeans, normal socks and shoes for the experiments. Because conditioning in the present experiments was done for the upper part of the body, the garments were standardized and provided by the experimenter. After the attachment of the skin sensors, the participants were given a short-sleeved polo shirt and a long-sleeved running sweater worn over the polo. The ensemble results in a clothing value of 0.73 clo (compare with Table 3). The car seat will be seen as a standard office chair, which adds another 0.1 clo to the sum. The final insulating value is thus $I_{cl} = 0.83 \text{ clo}$.

5.2.5 Questionnaire and evaluation scales

Every test person had to fill out a questionnaire before the first test sequence. Additionally to standard demographic data (age, sex, height, weight), the participants were asked if they had already participated in other experiments at the institute. Their state of fitness was asked on a three-level scale (low fitness, neutral, high fitness) as well as their personal tendency towards perception of temperature (I feel cold easily, neutral, I feel warm easily). Finally the hair density on the head was determined on an unlabelled five-level scale.

During the experiments the participants were asked to state their level of discomfort and their thermal perception in five minute intervals. For the overhead cooling experiment the level of discomfort had to be stated locally (at the head) and overall (for the whole body – including the head) on the CP-50 scale. The thermal sensation was expressed separately for the head, the torso and the feet on the nine-level thermal sensation scale (for both scales see Chapter 2.3.6).

In the latter experiments with seat ventilation, both discomfort vote and thermal sensation had to be stated for the back, the seat surface, the head and the entire body. Additionally the thermal preference was asked on a seven-level-scale. The questionnaires can be found in the appendix.

5.3 Experiment 1: Overhead Cooling

As has been shown in Chapter 2.3.3, the head has the biggest impact on overall comfort when only one part of the body is cooled locally. For this reason, the first experiment aimed to evaluate the influence of overhead cooling on the occupants comfort. The experiment was conducted with the cabin mock-up in the climate chamber with activated overhead cooling. The seat stayed in the unmodified operating mode with faux leather cover.

5.3.1 Pre-test for Experiment 1

In pre-tests, possible cabin temperatures and outlet settings were evaluated as well as the minimum time necessary to collect a valid subjective vote from the participants. Two participants were brought in for the pre-test. The cabin conditions were set to hot and humid conditions at temperatures between 28°C to 31°C and a relative humidity of 45%. The outlet temperature was set to 19.5°C at an air velocity of 0.15m/s. The participants sat in the mock-up for one hour. During the experiment core and skin temperatures were logged. Every five minutes the level of discomfort for head and body as well as the thermal sensation of head, torso and feet had to be stated.

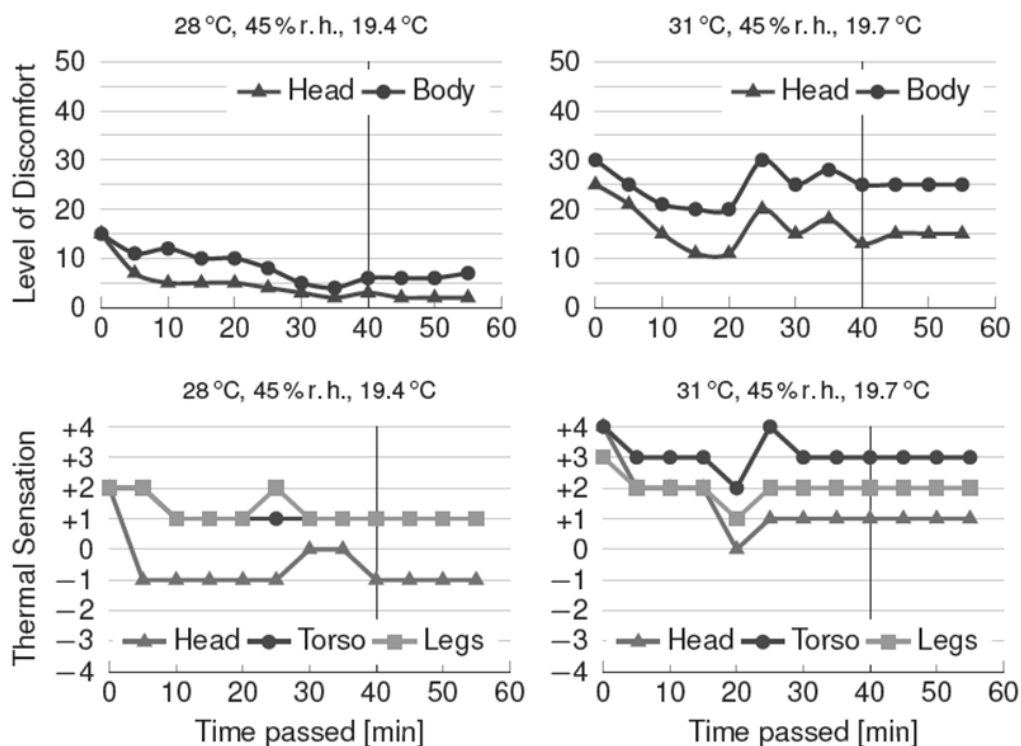


Figure 42: Discomfort and thermal sensation in the pre-test (test person P1) (Theissen, 2015)

The discomfort and thermal sensation votes of test person P1 are representative in showing how the votes of a participant level out after 40 minutes (Figure 42). This value correlates well with the times used in reference publications. Zhang (2003) uses a minimum of 30 minutes for the regeneration periods. The FAT studies are also content with a 30-minute exposure time (Schmidt et al., 2015). In this dissertation, a duration of 40 minutes was chosen to gain more stable results.

The temperature limits for the chamber temperature and the overhead outlet could also be defined. At a cabin temperature of 30°C and higher, mere overhead cooling did not seem able to achieve an acceptable climate. Also, the cooler used for this experiment was not capable of cooling the air flow below a difference of 9K at an average air speed of 0.15m/s.

5.3.2 Test sequence Experiment 1

The overhead cooling was tested at three different ambient temperatures at three different outlet temperatures. With these nine setups it was hoped to cover the section 'cooling a hot cabin' (section D in Figure 29) sufficiently. To acquire a noticeable spread in cabin temperatures, conditions were chosen in a similar approach to (Schmidt et al., 2013) that lead to PMV values of 0.5, 1.0 and 1.5. A cabin humidity of about 45%r.h. was targeted, to stay safely below the suggested humidity limit of 55%r.h., above which mould occurs in a real car (Großmann, 2013). A lower level was not selected, since the present work deals with cooling in tropical conditions and dehumidification, being very energy consuming, has to be kept as low as possible. The corresponding temperatures at 45%r.h. are calculated as 24.1°C, 26.5°C and 28.8°C (Figure 43).

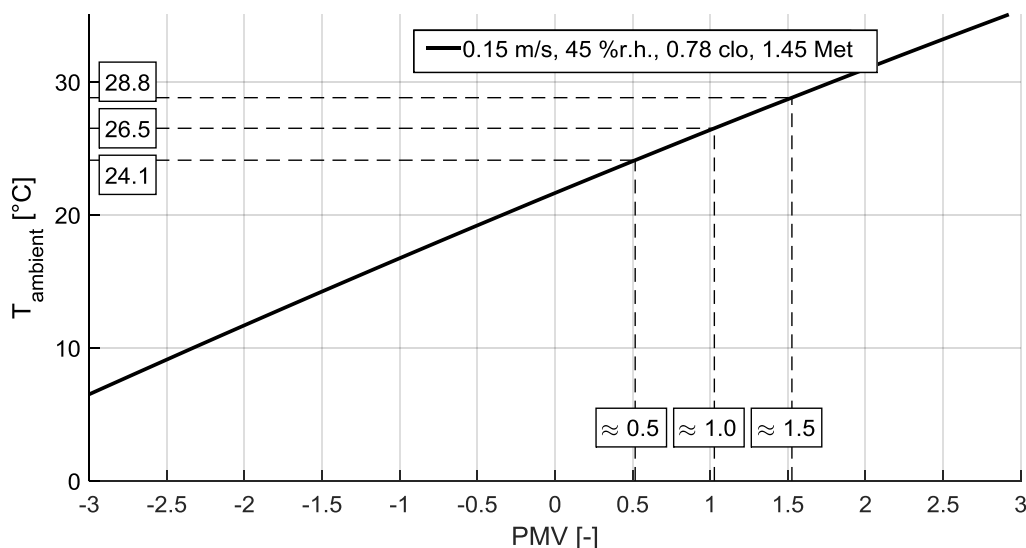


Figure 43: Chosen cabin temperatures corresponding to a PMV = 0.5, 1.0 and 1.5

The steps of the outlet temperature had to evoke a noticeable difference in thermal sensation. According to Figure 5 (right), cooling in initially warm conditions calls for a minimum temperature step of 0.4°C to 0.8°C. To account for temperature inaccuracies and to

cover a wider variance of outlet temperatures, ΔT of -3°C , -6°C and -9°C were chosen. The combination of $24.1^{\circ}\text{C}/-9^{\circ}\text{C}$ could not be tested, because the experimental setup was not capable of maintaining this temperature difference. In a later step the necessity of having a baseline measurement (overhead airflow at surrounding temperature) became obvious. The combination $26.5^{\circ}\text{C}/+0^{\circ}\text{C}$ was collected retroactively. Since the data collection of V1.0 took place later in the year, one random data set of V1.1, V1.2 or V1.3 was measured again to safeguard against variation in comfort votes due to different climatic conditions outside. The resulting means were in every case very close to the originally collected test and showed no dependence of the comfort vote on the change of seasons.

		Cabin temperature		
		24.1°C	26.5°C	28.8°C
ΔT	0K	–	26.5°C (V1.0)	–
	-3K	21.1°C (V1.9)	23.5°C (V1.1)	25.8°C (V1.5)
	-6K	18.1°C (V1.10)	20.5°C (V1.2)	22.8°C (V1.6)
	-9K	–	17.5°C (V1.3)	19.8°C (V1.7)

Table 15: Temperature combinations (and resulting overhead outlet temperature) for overhead cooling experiment

The participants came in for blocks of a maximum of three measurements each. The sequence in which V1.0 to V1.10 was tested was randomised to avoid the influence of sequential conditioning. When the participant had arrived and filled out the pre-test questionnaire, he was asked to step into the climate chamber, remove his sweater and shirt and attach the sensors. The experimenter checked the position of the sensors and helped when necessary. The participant was then given the standardized polo shirt and running sweater, was asked to sit down in the car seat and adjust it so the distance between his head and the overhead outlet was approximately 10cm and he was sitting comfortably. This process took approximately 15-20 minutes. The experimenter started the temperature logging and the first experiment was started. After 40 minutes the experimenter changed the parameters of chamber and outlet to the next combination while keeping the participant oblivious to both whether and what had been altered. During this time the participant was asked to exit the chair and move around a little in the climate chamber. After approximately 20 minutes the next experiment could be started.

5.3.3 Participants Experiment 1

Nine participants took part in the main experiments. To gain a homogenous sample, the participants were aimed to be of similar age, height, weight and state of fitness (see Table 2, influencing parameters on thermal comfort). Only male participants were selected, who were between 20 and 30 years of age, of an average height, reasonably fit, and not bald or shaven. The data of the tested sample is shown in Table 16.

participants	9	age	height	weight	hair	fitness
mean		25.9	183.2 cm	76.5 kg	4.3	2.7
min		24	175 cm	65 kg	3	2
max		29	188 cm	85 kg	5	3
standard deviation		1.7	4.5	7.6	0.9	0.5

Table 16: Participants main test overhead cooling

It became apparent during the evaluation that not all collected data was consistent enough to be used. One participant whose answers diverged greatly admitted to being hungover on at least two measurements. His data had to be discarded. Two participants' answers were at a discomfort value of around zero for all settings. Their being asked about this after evaluation of all data revealed that the reason lay in a false interpretation of the CP-50 discomfort scale. By using the scale, 0 (equal to 'no discomfort') should be interpreted as the best achievable state and 50 ('very high discomfort') as a state barely bearable. Discussion with the participants in question made another possible interpretation obvious. As both participants were familiar with comfort experiments and comfort evaluation at the Chair of Ergonomics (but not the use of CP-50 scale) they were aware of the descriptive differences of comfort and discomfort as stated by (Zhang et al., 1996). The state 0 was not seen as the state of 'best possible comfort', but merely as 'neutral/bearable'. It was assumed that a similarly distributed 'comfort scale' would extend on the other side of the CP-50 (compare with the discussion in Chapter 2.3.6). Thus the data of these two participants also had to be discarded. The remaining participants interpreted the scale as intended.

5.3.4 Results Experiment 1

The means of the collected votes were calculated using Equation (5.19) and the correlating standard deviations for a finite data set with Equation (5.20) (Mittag, 2016).

$$\bar{x} = \frac{1}{N} \sum_{i=1}^N x_i \quad (5.19)$$

$$\sigma = \sqrt{\frac{1}{N} \sum_{i=1}^N (x_i - \bar{x})^2} \quad (5.20)$$

With \bar{x} arithmetic mean of collected data set
 $x_1 \dots x_N$ collected data set (i control variable, N sample size)
 σ standard deviation

In analysing the remaining results, it was apparent that all remaining participants followed a similar pattern. In Figure 44 all four measurements at a temperature of 26.5°C (V1.0, V1.1, V1.2 and V1.3) are depicted. The initial votes start at divergence but converge over the

duration of the experiment. The starting vote is dependent on the sequence of the experiments and the associated preconditioning before each measurement.

The votes of most participants oscillate over time but settle towards a stable final vote. To balance these oscillations, the last three votes at 30, 35 and 40 minutes were averaged with the weighting factors 1, 2 and 3 respectively. These mean votes at the end of the experiments are depicted in Figure 45 for better comparability. The delta in air flow temperature decreases from left to right (V1.3: $\Delta T = -9$, V1.0: $\Delta T = 0$). The votes for overall discomfort without conditioning are in an area of light discomfort (10-20) and medium discomfort (20-30). The mean is located at 17.9. Under conditioning with a temperature delta of -3°C and -6°C , the means drop to 9.3 (V1.1) and 6.8 (V1.2) with a smaller standard deviation. However reducing the overhead cooling temperature further, leads to an increase in discomfort to a mean discomfort vote of 17.4 (V1.3).

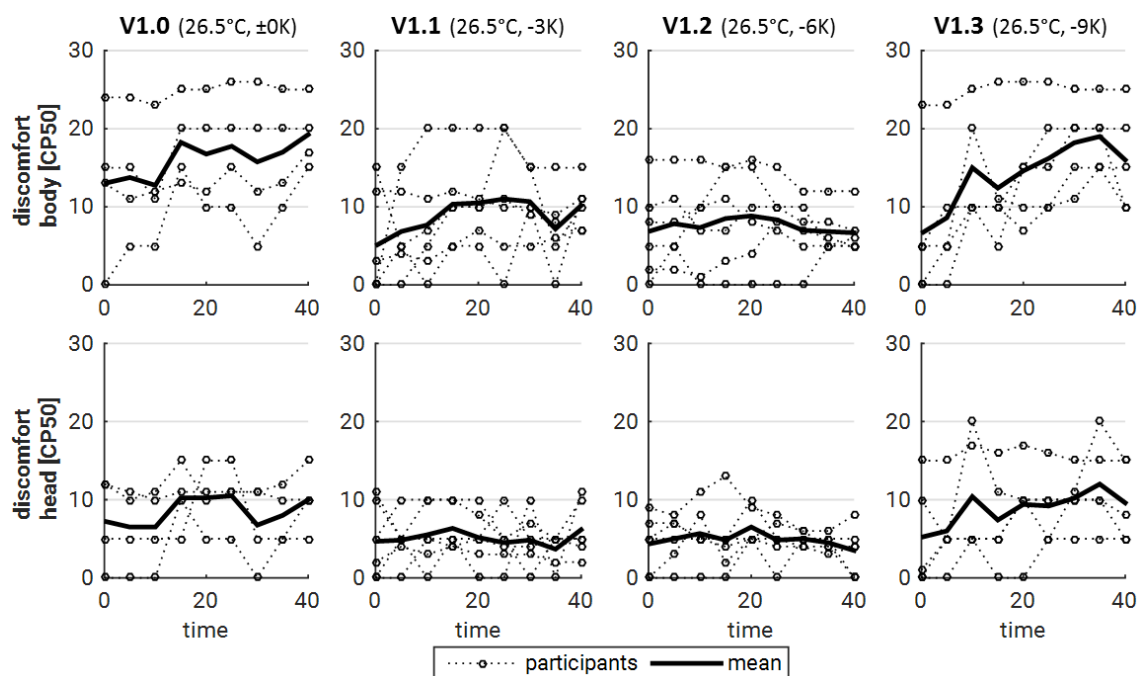


Figure 44: Body and head discomfort votes for overhead ventilation test at 26.5°C (V1.0 - V1.3)

The votes for local discomfort at the head take a course similar to the overall discomfort, but are smaller in magnitude: 8.9 (V1.0), 5.1 (V1.1), 4.1 (V1.2) and 10.5 (V1.3). The final vote for thermal perception for the four experiments is calculated accordingly and is also depicted in Figure 45. The vote for the head is also similarly curved as the discomfort votes. Without additional cooling, the mean vote for the head is at 0.8, cooling with a delta of -3°C and -6°C lowers the thermal vote to a mean of 0.3 and 0.4. It is interesting to note, that cooling with a delta of -9°C does not lower the thermal perception further, but rather increases it to a mean of 0.9. The vote for thermal perception on the torso is at a mean of 2 for V1.0 and is reduced to 1.1 (V1.1), 1.2 (V1.2) and 1.3 (V1.3). The standard deviation in the votes for thermal perception on the feet is very high for V1.1, V1.2 and V1.3. The mean votes are in the range of 1.3 to 1.7.

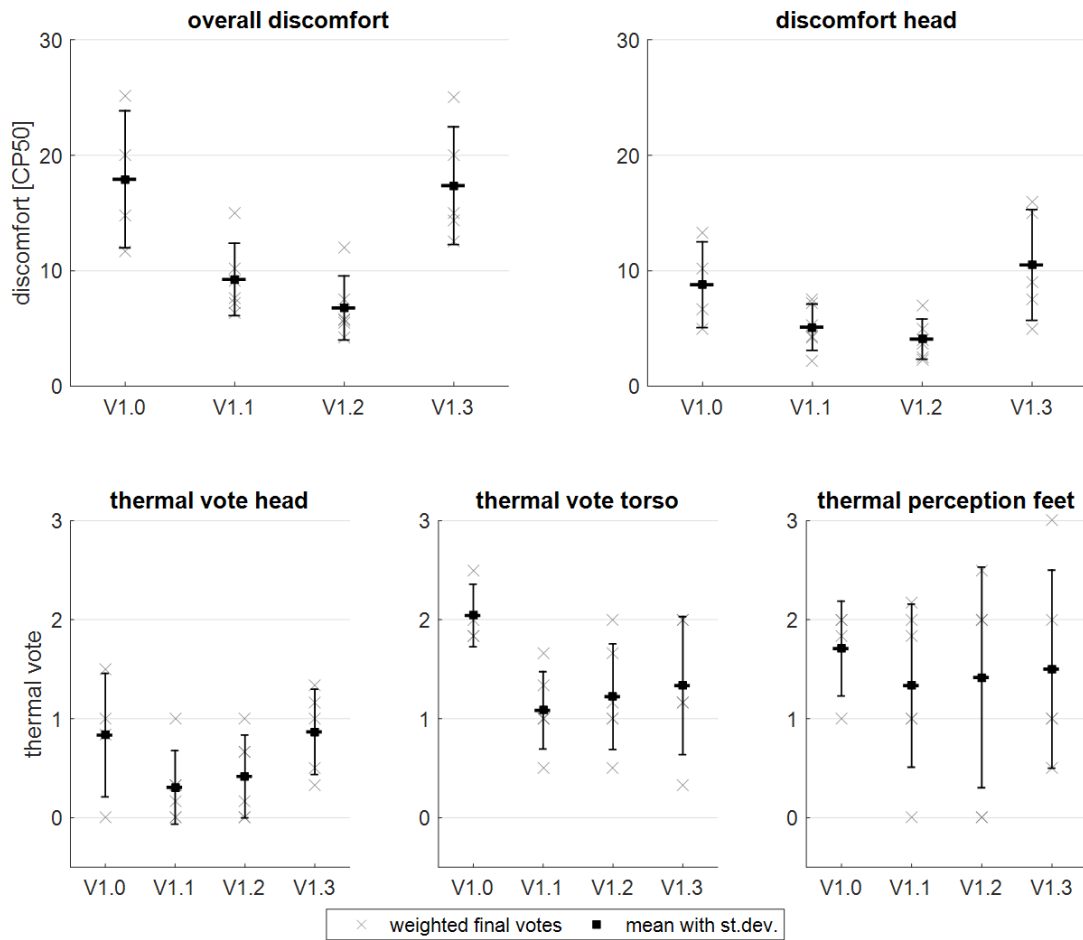


Figure 45: Discomfort for body and head and thermal perception for head, torso and feet at 26.5°C (V1.0 – V1.3)

Finally, if all temperature combinations are taken into account, the results can be used to span the whole area as described in Figure 30.

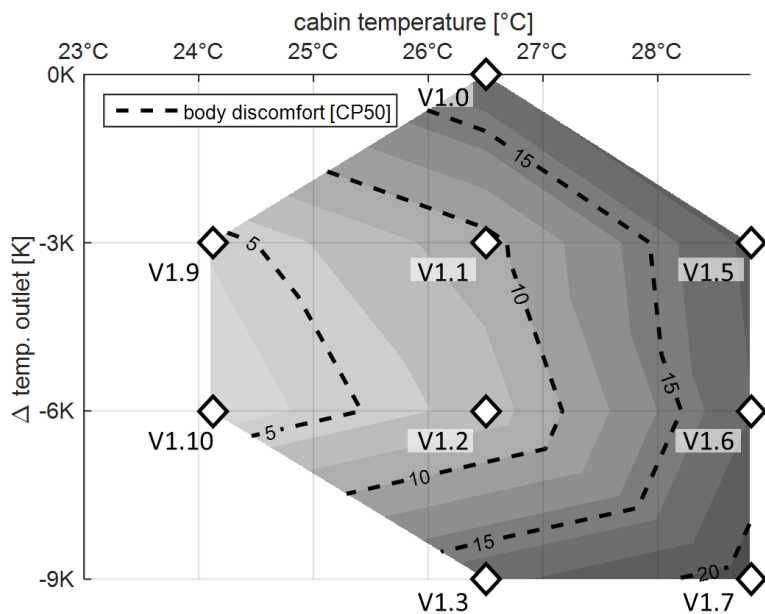


Figure 46: Thermal discomfort over varying cabin and overhead outlet temperatures (interpolated between mean final votes of V1.0 – V1.10)

The final votes of V1.1 to V1.10 are calculated with the help of the aforementioned weighting method. Interpolating between the mean values results in Figure 46. The mean results at cabin temperatures of 24.1°C are below 5 on the CP-50 scale. The mean results for 28.8°C are at 18 or higher on the CP-50 scale. Plotting the lines of equi-discomfort results in a shell-like pattern with a minimum around the outlet temperature delta of -6K.

5.3.5 Discussion Experiment 1

The results of the overhead cooling experiments show good tendencies towards a positive impact. The lines of equal-discomfort in Figure 46 correlate well with the assumption made in Chapter 5.1 and take a course very similar to the expected outcome. The optimal operating range for the overhead cooling in this setup is close to the delta of -6°C.

Analysis of the four experiments at 26.5°C cabin temperature reveals that the expected decrease-increase pattern in body discomfort. V1.0 ($\Delta T_{\text{outlet}} = 0\text{K}$) produces higher values for thermal discomfort. Overall discomfort is lowered if the temperature difference of the overhead cooling is increased. As expected, the discomfort will rise again, if cooling at the head is excessive. It is interesting to note, that discomfort does not arise because the head is perceived as 'too cold'. Figure 45 shows a distinct rise of discomfort for V1.3 at the head as well as on the whole body. But rather than decreasing the vote of thermal perception, the vote rises compared to the 'warmer' outlet temperatures in V1.2 and V1.1. The explanation could be in the thermo-regulatory system of the human body. The blood circulation in the head is always very high, even in cold conditions to maintain the temperature for the brain (Schmidt et al., 2010). If the body notices a drop in temperature at the head as might be the case in V1.3, the thermoregulation works against it by increasing blood circulation.

Even though the answers converge over time, all results - especially when looking at the dynamic responses over time in Figure 44 - are spread with high values of standard deviation. This means that either the participants are anchoring their votes on the CP-50 scale differently, or the overhead cooling in itself - while having a positive impact - is creating different reactions in the participants' thermo-regulation. Also, the oscillations up to the point of reaching a near-steady vote are very high. This might be an indicator that the body's thermo-regulation and thermal perception is 'overshooting' and is not converging properly. The duration of one measurement seems to be almost too tight for a proper convergence, especially under higher heat stresses. This is further influenced by differing starting values. The idea was to precondition the participants in the climate chamber. However, in some setups the heat stress is higher than in others and the convergence to a steady vote in the follow-up experiment seems to take longer when human thermo-regulation is in an elevated state of stimulation.

The applied time for one measuring point of 40 minutes is a minimum that cannot be shortened. In some cases, it even seems to be barely enough time for the body thermo-

regulation to adapt and the participant's comfort vote to level off. If the original plan to span the whole area of possible cabin temperatures and local outlet temperatures is adhered to, participants have to attend for at least ten hours. While revealing the most comprehensive overview, this is a very time consuming approach. The information that is most relevant, however, is only the curve of the optimal settings for every cabin temperature and the base line without conditioning for comparison. The more economic approach would be to identify the optimal settings in a pre-test with fewer participants and conduct the main test with these settings.

The air flow set for the experiment was barely noticeable. When asked whether test subjects perceived air flow over the period of the last five minutes, almost one in two answers was negative. The question whether they thought air flow unpleasant was always answered 'no'. Although the mean air velocity was set to 0.15m/s to stay under the draft limits, the velocity could be higher locally. Some measurements revealed local air velocities of 0.2 - 0.25 m/s at the forehead. These were however not registered as unpleasant. One explanation could be that people expect higher air velocities in a car than in an office environment on which Fanger & Christensen's (1986) draught limits are based.

The operating limit for overhead cooling can be seen in Figure 46: If for example only very slight discomfort is accepted (max. 10 on the CP-50 scale), the mean cabin temperature can be raised to a maximum of 27°C if the local overhead conditioning is operated with an air flow at 21°C.

5.4 Experiment 2: Seat ventilation

In the follow-up experiment, the selective influence of various seat configurations on overall thermal comfort was evaluated. The lessons learned from the first experiment were taken and implemented in test execution. To further economise the experiment, not all possible seat modes of operation were evaluated. The choice fell to evaluate the influence on thermal comfort of mode three (active ventilation in suction mode, see Figure 33 and Figure 47) and compare it with the votes for the unmodified seat with faux leather.

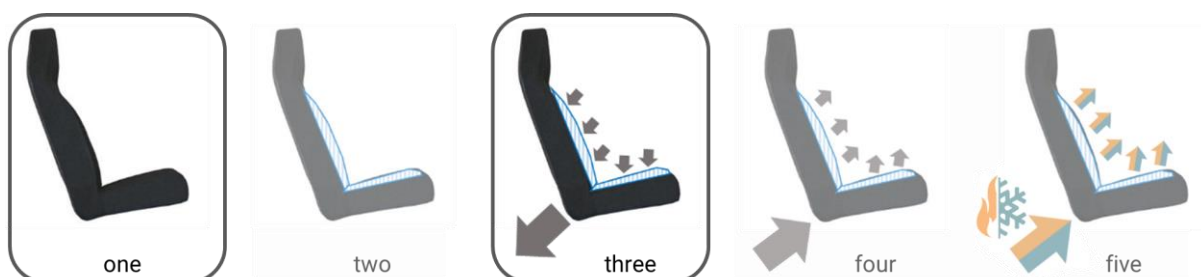


Figure 47: Seat modes of operation in the test

5.4.1 Pre-test for Experiment 2

The goal of the pre-test was the establishment of the optimal settings for the seat fans for increasing cabin temperatures. Since each seat surface and backrest segment can be controlled separately, this entailed the definition of four fan settings. The first setting was chosen by the experimenter himself after sitting down in the simulator. After driving the simulation for 40 minutes he adjusted the settings to his preference. The adjustment process and driving time was repeated until no further alteration was deemed necessary. Three participants were then asked to drive with the final settings for 40 minutes. During the test, thermal discomfort, thermal perception and thermal preference were each asked every 5 minutes. Interacting with the test person gave more details as to where on the seat surface or backrest discomfort arose and why. The experimenter could then readjust the settings as required. Results were achieved in an iterative process. In total, 18 pre-test runs were carried out at three cabin temperatures: 26.5°C, 28.5°C and 30.5°C.

5.4.2 Test sequence Experiment 2

The choice of cabin temperatures was set at 26.5°C and 28.5°C. The third temperature at 30.5°C was discarded, since the pretest showed that even with optimal settings the temperature gradient between the front and back of the body was too high for an acceptable affective vote. The operation of seat ventilation at 30.5°C was not sufficient to reach acceptable discomfort levels. Together with the two tested modes of operation for the seat, this resulted in four combinations (Table 17). The relative cabin air humidity was held at a constant 45%.

	V2.1	V2.2	V2.3	V2.4
cabin temperature	26.5°C	26.5°C	28.5°C	28.5°C
cover	faux leather	spacer fabric	faux leather	spacer fabric
seat ventilation	off	on	off	on
I	-	250 mA	-	400 mA
II	-	0 mA	-	150 mA
III	-	130 mA	-	200 mA
IV	-	125 mA	-	210 mA

Table 17: Temperature and ventilation setting in the seat test scenarios

The fans for seat ventilation were set by potentiometer before each test. The respective electric current for each seat area was evaluated in the pre-tests. The corresponding values are listed in Table 17. It is interesting to note, that the lower back– as is well known about the kidney area (see also the distribution of skin temperature receptors in Figure 4) – is very sensitive to draught and cold. The fan setting in that area (II) was set to zero for a cabin temperature of 26.5°C and to only 150 mA at 28.5°C.

Instead of preparing the test person in the climate chamber, he was asked to stay in the ante-chamber to answer the questionnaire. The application of the skin temperature sensors was also completed before he entered the climate chamber. Between experiments, while the experimenter changed the setup, the participant was asked to regenerate in the anteroom. With this pre-conditioning, it was hoped that a strong divergence of the starting votes could be reduced. The scenarios V2.1 to V2.4 were randomized and tested in either two- or four-hour blocks.

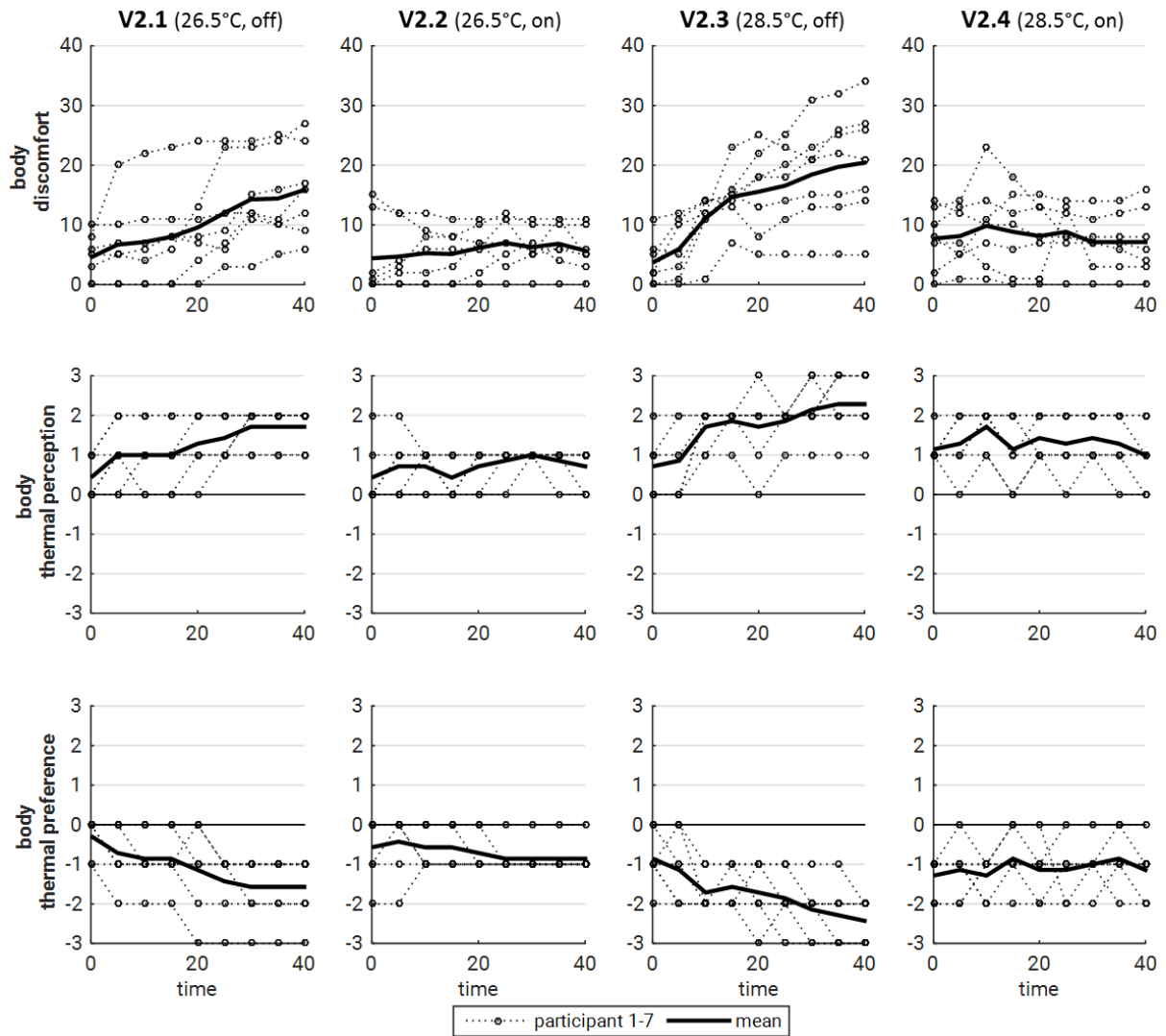
5.4.3 Participants Experiment 2

For the main part of the second experiment cluster seven participants were again specifically selected to gain a homogenous sample. Participants were chosen with the same criteria that have been used in the previous test: They had to be male, between 20 and 30 years of age, of an average height, reasonably fit and not bald or shaven. The data of the tested sample is shown in Table 18.

participants	7	age	height	weight	hair	fitness
mean		23	178.1 cm	74.6 kg	4.4	2.3
min		20	168 cm	65 kg	3	2
max		28	195 cm	85 kg	5	3
standard deviation		2.9	8.9	5.8	0.79	0.49

Table 18: Participants main test seat ventilation

5.4.4 Results Experiment 2

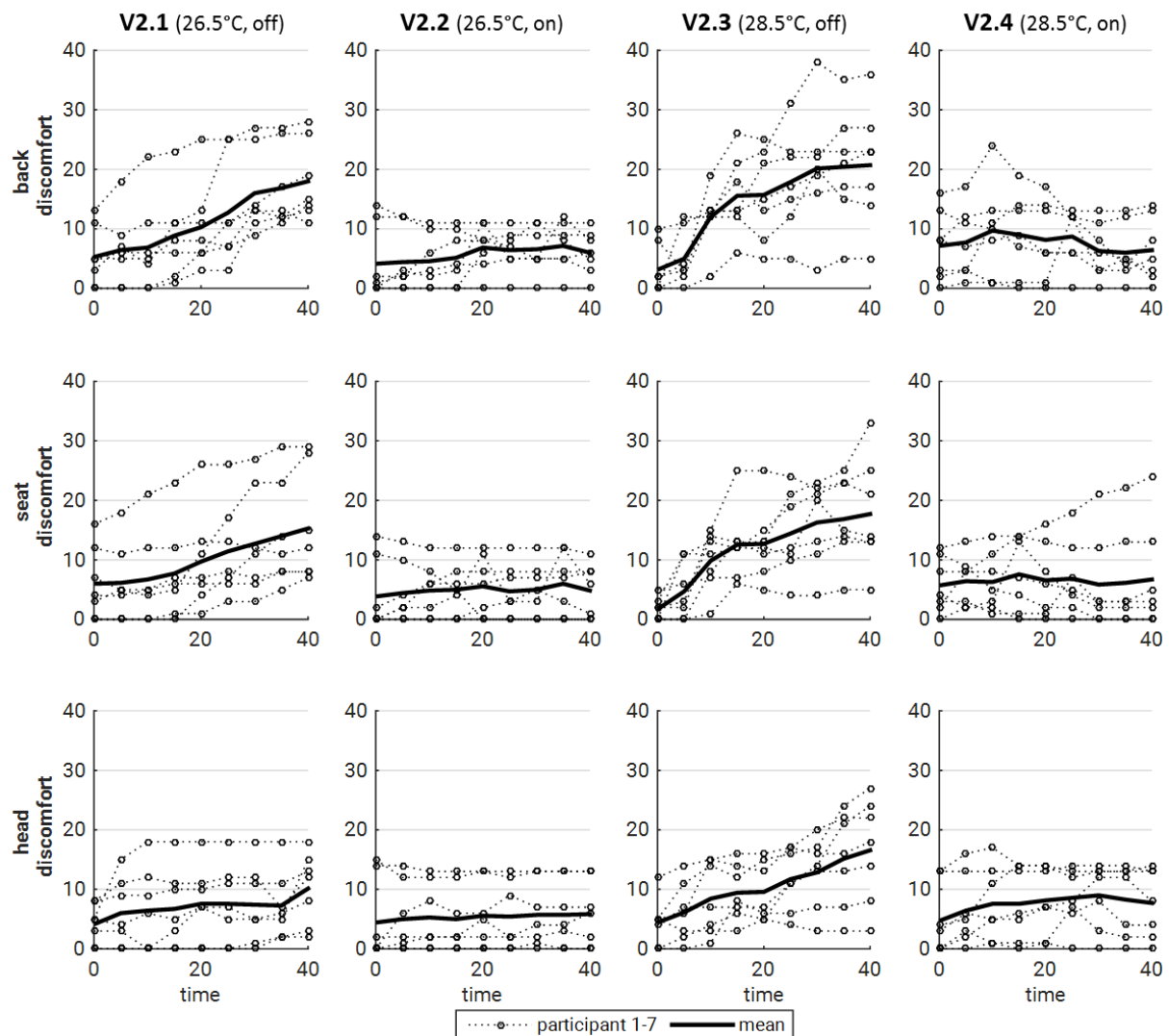


	V2.1		V2.2		V2.3		V2.4	
	\bar{x}	σ	\bar{x}	σ	\bar{x}	σ	\bar{x}	σ
discomfort body	15.9	7.6	5.7	3.8	20.4	9.6	7.1	5.7
perception body	1.7	0.5	0.7	0.5	2.3	0.8	1	0.8
preference	-1.6	0.8	-0.9	0.4	-2.4	0.5	-1.1	0.7

Figure 48: Body discomfort, perception and preference with seat ventilation (V2.1 - V2.4)

Figure 48 shows the results over time for the whole body thermal discomfort votes, thermal perception and thermal preference. The results oscillate much less over time than the votes of the overhead experiments. V2.1 and V2.3 are the two setups on faux leather without ventilation. The discomfort votes do not level out after 40 minutes but still show a positive incline towards a discomfort value of 20 (V2.1) or 30 (V2.3). The standard deviations are high. Comparing V2.1 with the final mean of V1.0 (also 26.5°C, no conditioning) shows matching results. The discomfort votes for V2.2 and V2.4 (with ventilation) level out quickly and also

feature a distinctly smaller standard deviation than the tests on faux leather. The means for whole body thermal perception and thermal preference are inversely congruent. Meaning the sums of the means for every test are always close to zero.

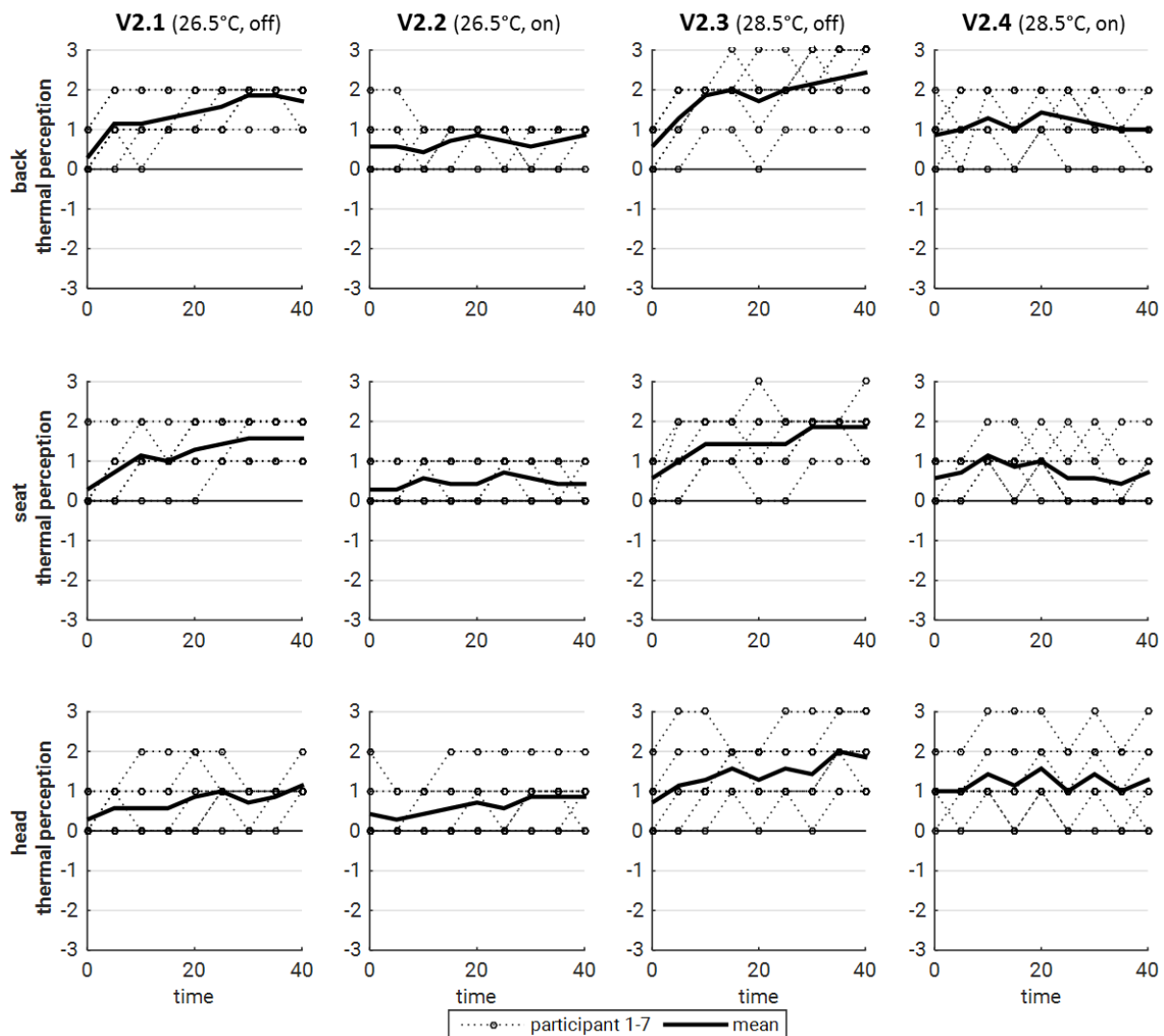


	V2.1		V2.2		V2.3		V2.4	
	\bar{x}	σ	\bar{x}	σ	\bar{x}	σ	\bar{x}	σ
discomfort back	18	6.6	6	3.7	20.7	9.9	6.4	5.4
discomfort seat	15.3	9.4	4.9	4.5	17.7	9.3	6.7	8.8
discomfort head	10.1	6.0	5.9	5.6	16.6	8.8	7.7	5.8

Figure 49: Local thermal discomfort with seat ventilation (V2.1 - V2.4)

Figure 49 shows the separate thermal discomfort votes for the contact area to the backrest, the seat surface and at the head. The mean votes for backrest and seat surface are very similar for every combination. The votes still increase at 40 minutes for the two combinations with faux leather (V2.1 & V2.3) and in two cases reaching a vote over 30 (high discomfort), while the combinations with ventilation (V2.2 & V2.4) level out very early (with

one exception at the seat surface in V2.4). The discomfort votes for the head are also similar with the exception of V2.1. While the discomfort at seat surface and back rest still increases, the discomfort at the head levels out after ten minutes.



	V2.1		V2.2		V2.3		V2.4	
	\bar{x}	σ	\bar{x}	σ	\bar{x}	σ	\bar{x}	σ
perception back	1.7	0.5	0.9	0.4	2.4	0.8	1	0.8
perception seat	1.6	0.5	0.4	0.5	1.9	0.7	0.7	0.8
perception head	1.1	0.4	0.9	0.7	1.9	0.9	1.3	1.1

Figure 50: Local thermal perception with seat ventilation (V2.1 - V2.4)

Thermal perception votes are depicted in Figure 50. Again the votes for seat surface and backrest are very similar. However the votes for the seat area are slightly lower than the votes for the backrest. The thermal perception at the head does not change by much for V2.1 and V2.2 opposed to the votes for the seat. The results of V2.3 and V2.4 show a slight decrease in thermal perception at the head towards neutral in V2.4.

The final mean votes including their corresponding standard deviations are listed in Figure 48, Figure 49 and Figure 50. The weighting of the final votes in the first experiment was conducted to smooth oscillating votes (see Chapter 5.3.4). However, in the seat ventilation experiment, the votes were neither oscillating, nor converging after 40 minutes so the weighting was not only not necessary but would rather have been counterproductive.

The participants' votes for thermal preference (Figure 48) were expressed for the whole body. By interacting with the test person during the test it was also asked if the vote was influenced by a local preference only or if one body part in particular was more in need of a temperature change than the rest of the body. Specific cooler preferences were often expressed for the back and the head or the full torso. Arms, legs and the extremities were not mentioned to be in need of cooling compared to the rest of the body.

5.4.5 Discussion Experiment 2

With help of seat ventilation, the mean cabin temperature can be set higher while still maintaining low values of thermal discomfort. With ventilation, the whole body thermal discomfort can be reduced to mean values of only very slight discomfort (1-10). Both the dynamic votes over time and the final votes show a very stable result for a cabin temperature of 26.5°C. The local discomfort values are well below 10 and the thermal perception does not exceed 'slightly warm'. The discomfort was reduced by at least 10 points on the CP50 scale.

At a cabin temperature to 28.5°C seat ventilation achieves a potential discomfort reduction of almost 20 points on the CP-50 scale. However the mean is close to 10 points (border to slight discomfort) and the standard deviation is still considerably high with a value of 5. Also, the thermal perception on the back and especially the head is tending towards 'warm'. A thermal preference for the whole body of more than -1 is also noticeably high. That is why the limit of operation for the seat ventilation with the chosen parameters is expected to be slightly below 28.5°C cabin temperature.

The low values for discomfort with seat ventilation have proved to be the result of an improved micro-climate on the contact area between body and car seat. However, the head is still perceived 'warm' at the ambient temperature of 28.5°C, with a high standard deviation to the votes. The pre-tests also showed, that increasing the ventilation intensity in the seat will only result in even warmer head temperature perception. The reason here is, that the temperature gradient increases between the seat and the head. Even though the head stays at the same temperature, it is perceived warmer relative to back and upper thigh, while these areas are brought closer to 'neutral'. As a result it can be concluded that, while the seat ventilation is an energy saving and effective cooling method, this is possible only up to a certain cabin temperature below 28.5°C if the head is not conditioned as well.

5.5 Experiment 3: Combined overhead cooling and seat ventilation

The combined effect of overhead cooling and seat ventilation was examined in a final test person survey. The procedure was analogue to the seat ventilation experiment. Rather than spanning the whole field of all settings over all temperatures, one optimal setting was chosen for each cabin temperature. This is even more important for this test, since the combined activation of seat ventilation and overhead cooling introduces more variables and dependencies. The specific parameters for cooling and ventilation were determined in a pre-test, then the test sequences were set and finally the main experiment conducted with a selected sample.



Figure 51: Experiment 3 – overhead cooling and seat operation mode three

5.5.1 Pre-tests for Experiment 3

In the pre-test, the experimenter sat down in the simulator at cabin temperatures of 26.5°C, 28.5°C and 30.5°C. The selection of the temperatures was taken from the preceding experiments. The overhead cooling and seat ventilation were tuned to the optimal settings also found in the two preceding experiments. The experimenter then adjusted the fans and the outlet temperature to his personal preference. The settings were kept and three test people came in to fine-tune the parameters. The participants were asked to sit down in the mock-up and drive for 40 minutes. The thermal discomfort, thermal perception and thermal preference was asked every five minutes. Interacting with the test person gave more details as to where on the body discomfort arose and why. The experimenter then readjusted the settings for the seat areas and the overhead outlet as necessary. The results were found in an iterative process. 15 runs were necessary to set the parameters for all three cabin temperatures.

5.5.2 Test sequence Experiment 3

The three test temperatures for the main test were 26.5°C, 28.5°C and 30.5°C. The choice of these temperatures was mainly due to comparability with the preceding experiments. Overhead cooling proved to suffice at cabin temperature 26.5°C, but not at 28.8°C. Seat ventilation on its own reached its limit below 28.5°C. The temperature of 26.5°C was chosen as a validation and comparison measurement. At a cabin temperature of 28.5°C, the combination of the two systems was also expected to only induce discomfort values of a maximum of very slight discomfort. Pushing the limit further, 30.5°C was chosen as the third cabin temperature to be evaluated. The relative cabin humidity had to be set slightly lower for this temperature to avoid condensation at the overhead outlet. The tests with the corresponding parameters are depicted in Table 19. The participants came in for one three-hour block in which the sequences V3.1 to V3.3 were randomised. The execution of the experiments, including the preparation and regeneration phases were equal to the seat ventilation experiments (see Chapter 5.4.2).

		V3.1	V3.2	V3.3
cabin temperature		26.5°C	28.5°C	30.5°C
cabin rel. hum.		45%	45%	43%
overhead ΔT		-6 K	-6 K	-9 K
overhead v		0.17 m/s	0.3 m/s	0.4 m/s
seat cover		spacer fabric	spacer fabric	spacer fabric
seat ventilation		on	on	on
seat ventilation	I	250 mA	405 mA	1000 mA
	II	0 mA	153 mA	450 mA
	III	130 mA	200 mA	603 mA
	IV	127 mA	215 mA	615 mA

Table 19: Temperature and ventilation settings for experiment 3

5.5.3 Participants Experiment 3

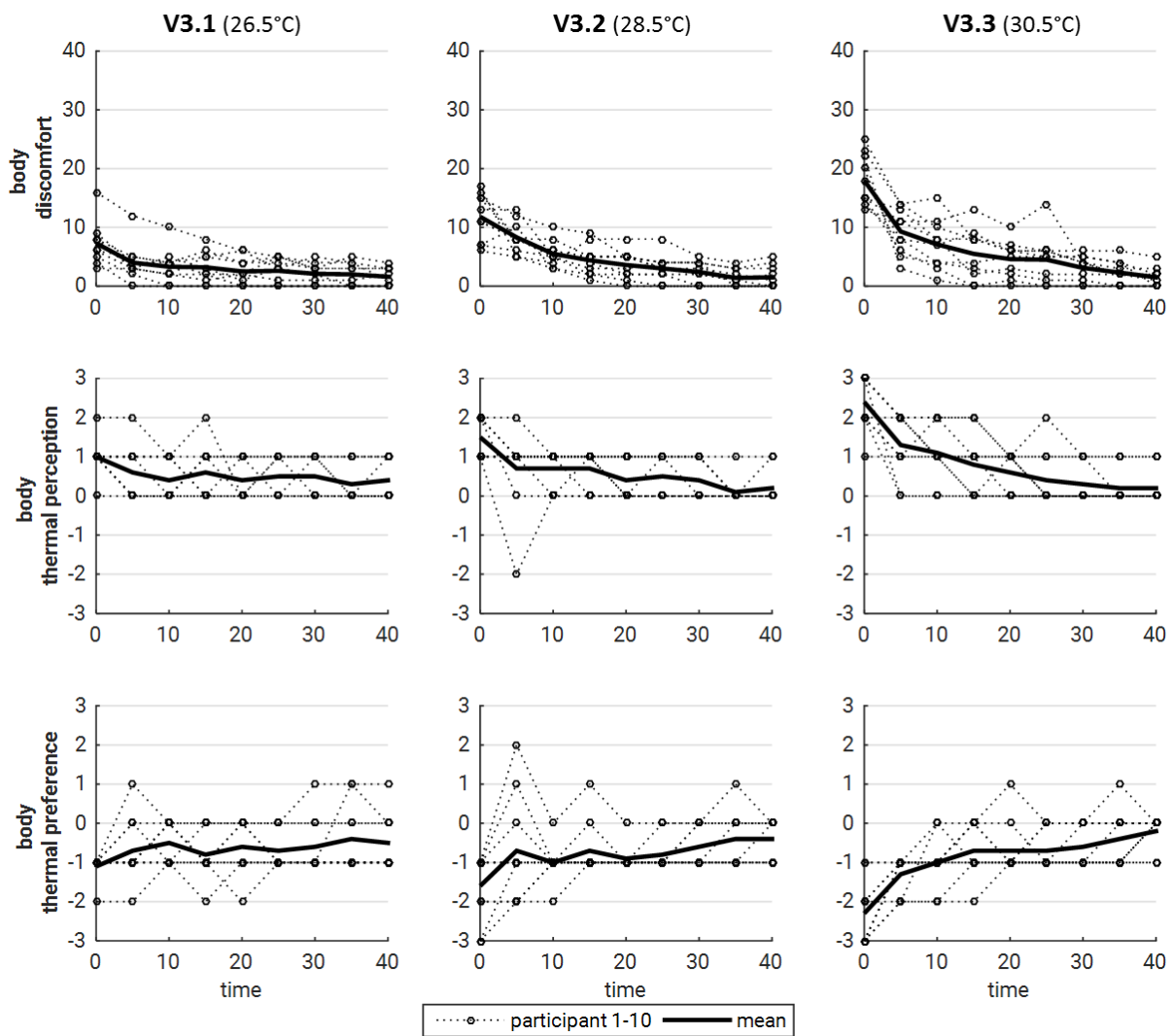
For the third experiment cluster, ten participants were again specifically selected to gain a homogenous sample. Participants were chosen with the same criteria that have been used in the previous tests: They had to be male, between 20 and 30 years of age, of an average height, reasonably fit and not bald or shaven. The data of the sample is shown in Table 20.

participants	10	age	height	weight	hair	fitness
mean		23.9	178.6 cm	73.9 kg	4.8	2.8
min		21	170 cm	64 kg	3	2
max		28	190 cm	81 kg	5	3
standard deviation		2.38	6.2	4.95	0.63	0.42

Table 20: Participants with seat ventilation and overhead cooling

5.5.4 Results Experiment 3

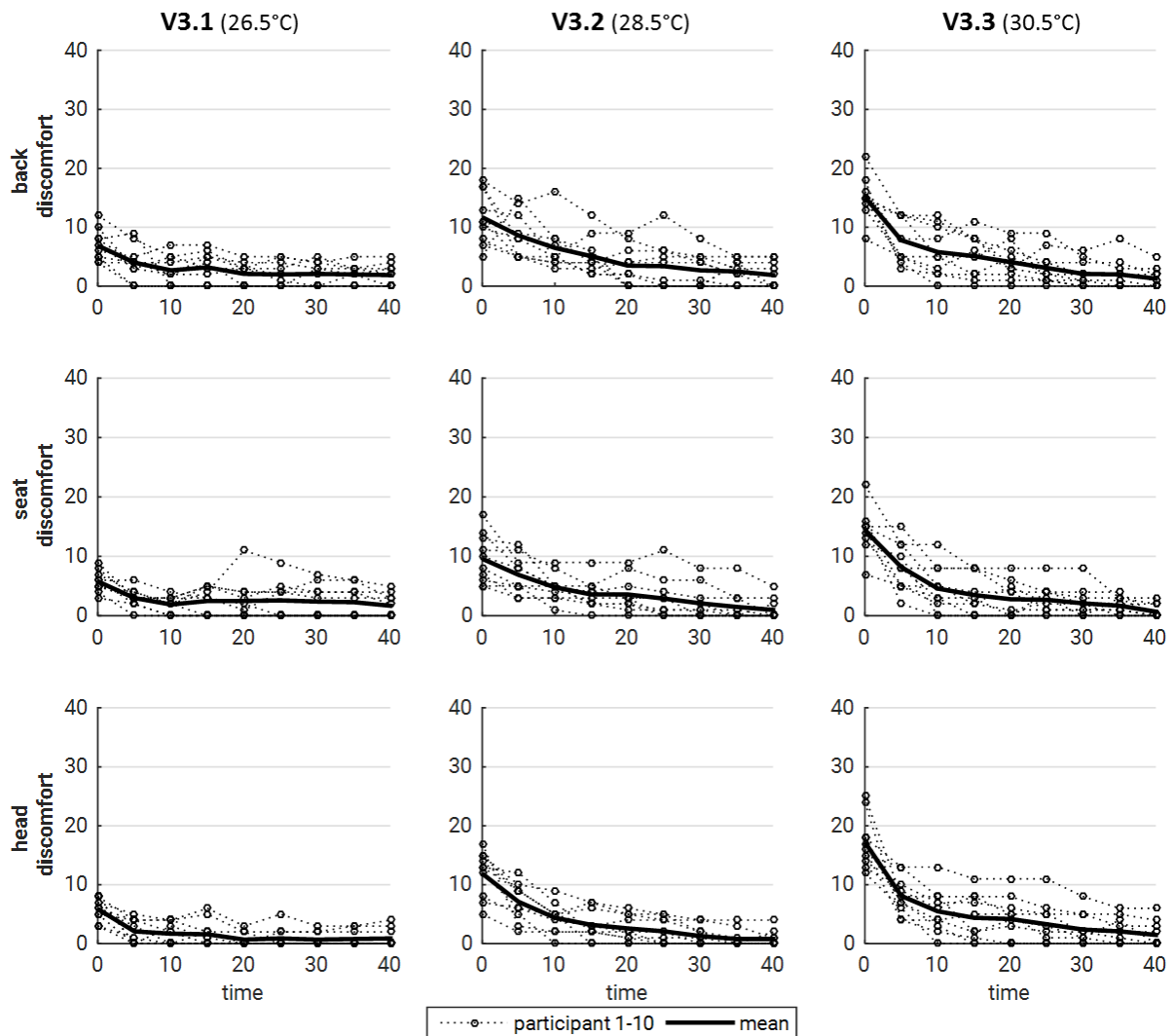
The results for the combined experiment show very good results. The body discomfort votes in Figure 52 equal out quickly to values well below 10. Standard deviations are small and oscillations minimal. Only V3.3 shows some oscillations for one participant before converging with the other votes. The whole body thermal perception also quickly converges to values between 0 and 1, as is the thermal preference with the occasional positive value 1. In V3.2 two participants oscillate with their preference between 'warmer' and 'colder' (especially in the transient first ten minutes) before converging with the other votes. In V3.4, only one participant changes his vote between 0 and 1 twice, before settling on a final vote of 0.



	V3.1		V3.2		V3.3	
	\bar{x}	σ	\bar{x}	σ	\bar{x}	σ
discomfort body	1.6	1.6	1.5	1.9	1.5	1.6
perception body	0.4	0.52	0.2	0.42	0.2	0.42
preference body	-0.5	0.71	-0.4	0.52	-0.2	0.42

Figure 52: Body discomfort, perception and preference with seat ventilation and overhead cooling (V3.1 – V3.3)

In considering the local votes for thermal discomfort in Figure 53, it can be seen that all votes fall quickly below the value 10 and converge to mean values below 2. The standard deviations are also low with a maximum of 2.2. Slight oscillations occur for two participants in the votes for the back in V3.2 and V3.3 and for the seat in V3.1 and V3.2.

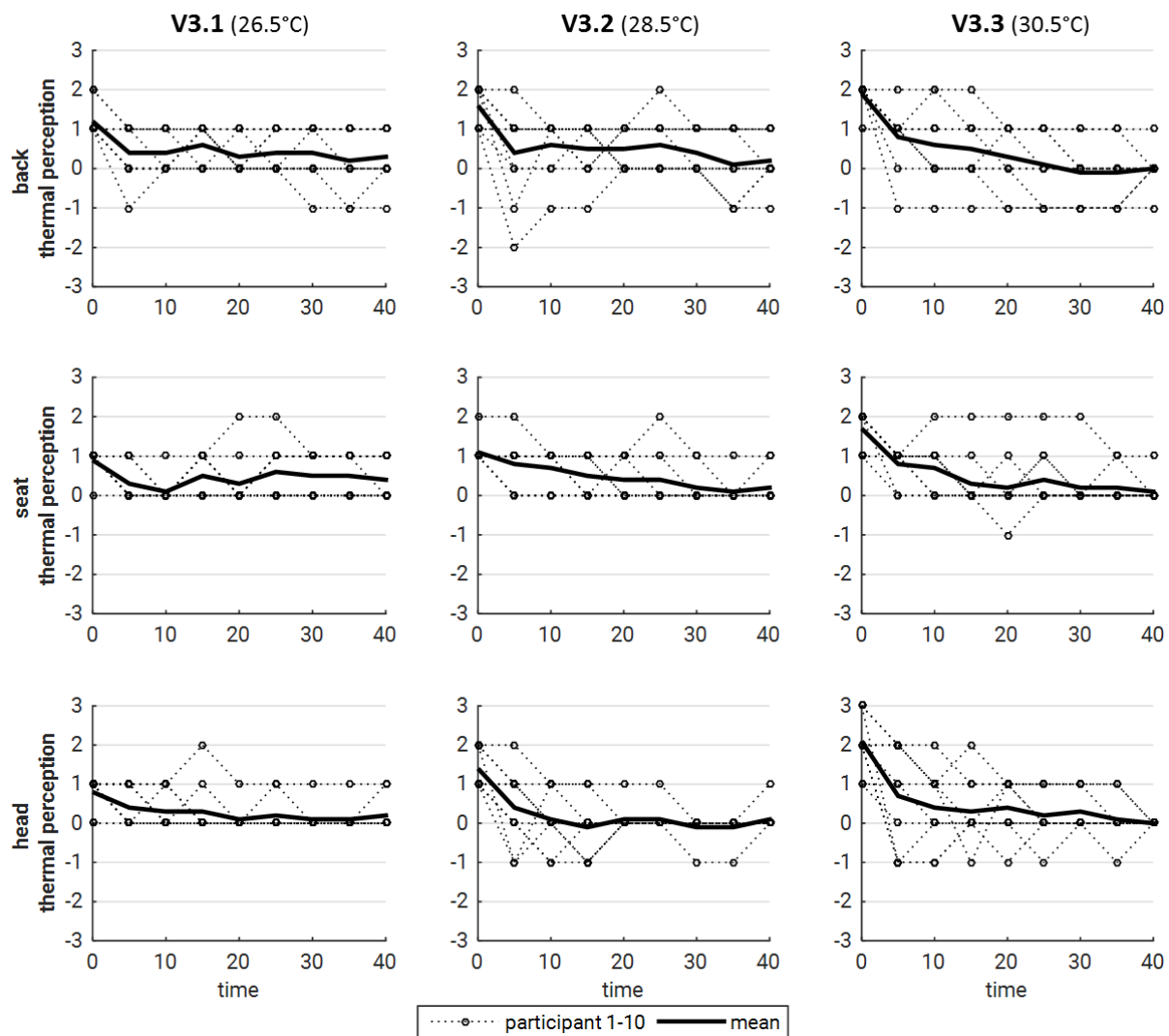


	V3.1		V3.2		V3.3	
	\bar{x}	σ	\bar{x}	σ	\bar{x}	σ
discomfort back	1.9	1.9	1.9	2.2	1.3	1.7
discomfort seat	1.7	1.9	1	1.8	0.7	1.2
discomfort head	0.9	1.5	0.8	1.3	1.5	2.2

Figure 53: Local thermal discomfort with seat ventilation and overhead cooling (V3.1 – V3.3)

The votes for local thermal perception for the back rest contact area, the seat surface and the head are depicted in Figure 54. The mean votes converge very close to zero below a maximum value of 0.4. The final standard deviations of each subtest are always highest for the backrest and lowest for the head. The overshoot in local thermal perception at the back

levelled out to zero in less than five minutes and did not have a noticeable influence in the participant's discomfort vote.



	V3.1		V3.2		V3.3	
	\bar{x}	σ	\bar{x}	σ	\bar{x}	σ
perception back	0.3	0.67	0.2	0.63	0	0.47
perception seat	0.4	0.52	0.2	0.42	0.1	0.32
perception head	0.2	0.42	0.1	0.32	0	0.00

Figure 54: Local thermal perception with seat ventilation and overhead cooling (V3.1 – V3.3)

5.5.5 Discussion Experiment 3

The combined effect of overhead cooling and seat ventilation with the chosen settings shows satisfactory results for all cabin temperatures. With the exception of one participant, all votes drop below the value of 10 with only 'very slight discomfort' after 15 minutes. At a driving time of 30 minutes, even the last vote drops down below ten.

The experiments have been set up to evaluate the influence of local conditioning on steady state conditions. With the results obtained in experiment 3, a first positive prediction can be made towards transient conditioning. Even in very hot conditions at a cabin temperature of 30.5°C, the overall and local mean discomfort votes drop to 'very slight discomfort' within five minutes.

All participants expressed a "remarkably comfortable climate" very quickly. It became apparent that many votes of positive or negative 1 for thermal perception and thermal preference were given even though the perceived state was close to 'neutral' and the thermal discomfort barely noticeable. The reason might lie in the coarse scales for perception and preference, and the eagerness of the participants to diligently report every minor perceived tendency. To obtain finer results a scale similar to the CP-50, in which participants choose tendencies (-0.33, ±0, +0.33) after stating the integer vote might be helpful.

6 Evaluation of energy efficiency

Based on the example of the electric taxi EVA, an exemplary energy and mass flow balance on the car is calculated. The vehicle is defined as an open system, the thermodynamic system boundaries of which envelop the interior of the car, including the central HVAC module and the local HVAC system. To simplify the calculation, transient states are neglected: The control volume is considered to present steady state conditions and the temperature field inside the passenger compartment is assumed to be homogeneous. Within the 'car interior' system boundaries, three more control volumes can be defined: The 'HVAC' unit under the dashboard, the 'local outlet' – if considered a separate system from the central HVAC supply – and the remaining 'cabin interior'.

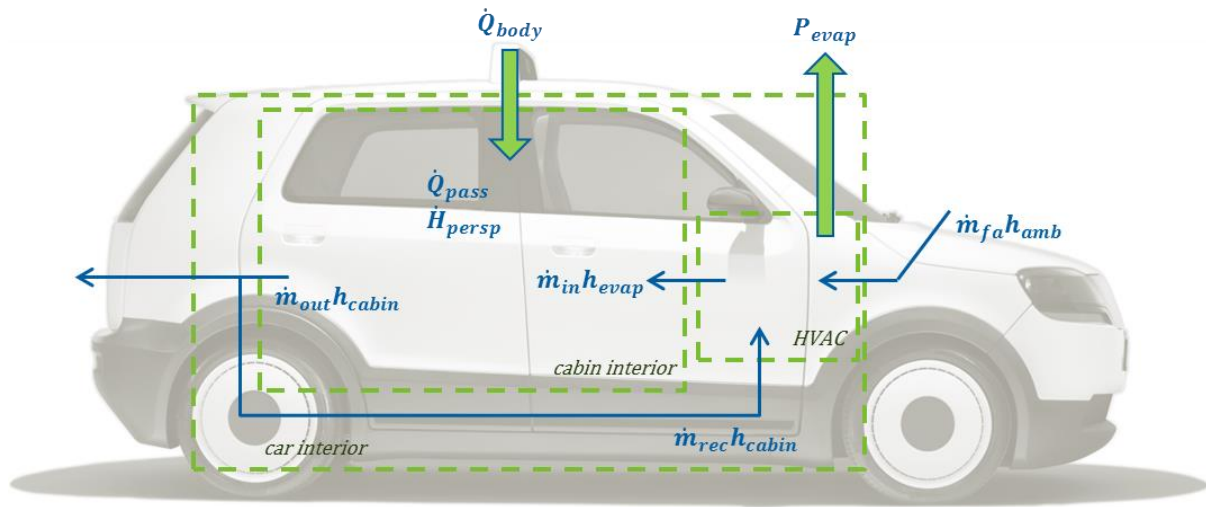


Figure 55: Thermodynamic system boundaries and energy flows in a car

Looking at the system boundary for the cabin interior, the mass flow balance for dry air is as follows:

$$\dot{m}_{air,in} - \dot{m}_{air,out} = 0 \quad (6.21)$$

The mass flow balance for water accordingly:

$$\dot{m}_{air\ moisture,in} + n_{pass} \dot{m}_{persp} - \dot{m}_{air\ moisture,out} = 0 \quad (6.22)$$

$$\dot{m}_{air\ moisture,in} = x_{in} \dot{m}_{air,in} \quad (6.23)$$

$$\dot{m}_{air\ moisture,out} = x_{out} \dot{m}_{air,out} \quad (6.24)$$

And the energy balance inside the car is:

$$\dot{Q}_{body} + \dot{Q}_{pass} + \dot{H}_{persp} + \dot{H}_{in} - \dot{H}_{out} = 0 \quad (6.25)$$

Since the cabin is simplified as a perfectly mixed container, the outward flow is defined by the target state of the cabin (temperature and relative humidity) and the inward flow by the state after the evaporator.

$$\dot{H}_{out} = \dot{m}_{air,out} h_{cabin} = \dot{m}_{air,out} (c_{p,air} T_{cabin} + x_{cabin} (r_w + c_{p,vapour} T_{cabin})) \quad (6.26)$$

$$\dot{H}_{in} = \dot{m}_{air,in} h_{evap} = \dot{m}_{air,in} (c_{p,air} T_{evap} + x_{evap} (r_w + c_{p,vapour} T_{evap})) \quad (6.27)$$

$$\dot{H}_{persp} = \dot{m}_{persp} (r_w + c_{p,vapour} T_{persp}) \quad (6.28)$$

The absolute humidity can be calculated with Equations (6.29) to (6.31).

$$x = 0.622 \frac{p_{vapour}}{p_{amb} - p_{vapour}} \quad (6.29)$$

$$p_{vapour} = p_{sat} \varphi \quad (6.30)$$

$$p_{sat} = \left(\frac{T}{100} + 1.098 \right)^{8.02} 288.68 \quad (6.31)$$

With	T	Temperature of humid air.
	x	Specific air humidity
	p_{vapour}	Vapor pressure
	p_{amb}	Ambient pressure = 101325 Pa (at sea-level)
	p_{sat}	Pressure at state of saturation
And:	$c_{p,air}$	Specific heat capacity of air = 1.006 kJ/kgK
	$c_{p,vapour}$	Specific heat capacity of vapor = 1.86 kJ/kgK
	\dot{H}_{persp}	Enthalpy of the occupants' perspiration, can be assumed to be fully vaporized
	\dot{H}_{in}	Enthalpy of the inward flow
	\dot{H}_{out}	Enthalpy of the outward flow
	h_{cabin}	Specific enthalpy in cabin
	h_{evap}	Specific enthalpy after evaporator
	$\dot{m}_{air,in}$	Mass flow air into cabin
	$\dot{m}_{air,out}$	Mass flow air out of cabin
	$\dot{m}_{air\ moisture,in}$	Mass flow of water contained in inward air flow
	$\dot{m}_{air\ moisture,out}$	Mass flow of water contained in outward air flow
	\dot{m}_{persp}	Mass flow perspiration (per person = 60 g/h) ²
	n_{pass}	Number of occupants
	\dot{Q}_{body}	Heat flow by the warmed car body due to solar irradiation = 0.8kW in case of a sunny day ³
	\dot{Q}_{pass}	Thermal radiation of occupants (per person = 0.15kW) ²
	r_w	Specific enthalpy of vaporization = 2500 kJ/kg
	T_{persp}	Temperature of the occupants' perspiration = 36°C

2 Assumption according to Nadler (2005) in case of physical activity level II (very light physical activity while seating or standing.)

3 Assumptions of solar irradiation in Singapore by Christoph Futter, TUM Create

$x_{evap} = x_{in}$ Specific air humidity after evaporator

$x_{cabin} = x_{out}$ Specific air humidity of the cabin

Three heat flows can be combined to represent the load on the cabin interior:

$$\dot{Q}_{load} = \dot{Q}_{body} + \dot{Q}_{pass} + \dot{H}_{persp} \quad (6.32)$$

The heat load on the cabin's interior is the energy flow that has to be cooled to maintain the cabin temperature on a constant level. It is calculated using Equation (6.32) for a typical sunny day in Singapore and an occupation with four persons and one person respectively:

$$\dot{Q}_{load,1p} = 1.0 \text{ kW} \quad (6.33)$$

$$\dot{Q}_{load,4p} = 1.6 \text{ kW} \quad (6.34)$$

The targeted relative cabin humidity is at 45%. The specific air humidity of the inward air flow is determined by the evaporator. The inward air flow is assumed to exit the evaporator with one uniform temperature in a fully saturated state (relative humidity $\phi = 100\%$).

$$x_{in} = x_{sat,evap} \quad (6.35)$$

The temperature after the evaporator can be calculated by solving Equation (6.21) to (6.31) & (6.35) for T_{evap} . The inward air flow can be calculated by solving Equation (6.22) or (6.25) with the newly found temperature at the evaporator. This is executed for several cabin target states: A representative reference span between 22°C and 24.6°C⁴ and three cabin states from the experiments at 26.5°C, 28.5°C and 30.5°C. For the ambient conditions, a typical hot day in Singapore is chosen: 30°C at 80%r.h (see Figure 56). The results are listed in Table 21.

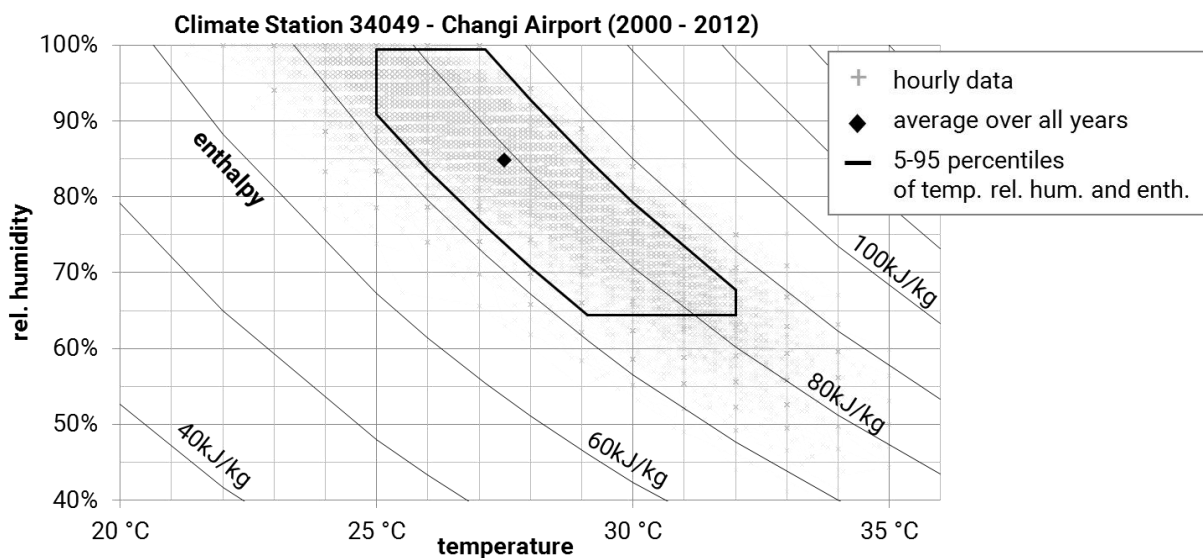


Figure 56: Singapore (Changi Airport) hourly temperature, humidity and enthalpy (NEA Singapore, 01/12/2012)

⁴ Compare values given by Großmann (2013) & Kolb (2004) in Chapter 2.3.5 and the calculated neutral temperature for Singapore in Chapter 2.3.2

cabin target state		22°C - 24.6°C / 45%	26.5°C / 45%	28.5°C / 45%	30.5°C / 43%
1 pass.	T_{evap} [°C]	7.8 - 10.2	11.9	13.7	14.8
	\dot{m}_{air} [kg/min]	3.6 - 3.5	3.4	3.3	3.1
4 pass.	T_{evap} [°C]	4.7 - 7.2	9	10.9	12
	\dot{m}_{air} [kg/min]	4.1 - 4	3.9	3.8	3.5

Table 21: Temperatures at evaporator and corresponding air mass flows⁵

For hygiene reasons, DIN 1946-2:1994 requires a minimum fresh air supply per person of at least 40 m³/h. This results in 0.8 kg/min for one person and 3.2 kg/min for the full occupation with four persons. The divergence from the calculated inward air flows can be recirculated into the HVAC to save cooling power. Recirculation rates can be from 9% for four persons and a target temperature of 30.5°C to 77% for one person at a cabin temperature of 24.6°C. Applying the energy and mass flow balance in the 'HVAC' control volume in Figure 55 provides the equations needed to calculate the power at the evaporator:

$$\dot{m}_{fa}h_{amb} + \dot{m}_{rec}h_{cabin} - \dot{m}_{air,in}h_{evap} - P_{evap} = 0 \quad (6.36)$$

$$\dot{m}_{fa} + \dot{m}_{rec} - \dot{m}_{air,in} = 0 \quad (6.37)$$

$$\dot{m}_{air\ moisture,fa} + \dot{m}_{air\ moisture,rec} - \dot{m}_{condensate,evap} - \dot{m}_{air\ moisture,in} = 0 \quad (6.38)$$

With	h_{amb}	Ambient specific enthalpy
	\dot{m}_{fa}	Mass flow fresh air
	\dot{m}_{rec}	Mass flow recirculation air
	$\dot{m}_{air\ moisture,fa}$	Mass flow of water contained in fresh air flow
	$\dot{m}_{air\ moisture,rec}$	Mass flow of water contained in recirculation air flow
	$\dot{m}_{condensate,evap}$	Water condensing at evaporator
	P_{evap}	Cooling power at evaporator

The power at the evaporator is shown in Figure 57 for the evaluated cabin states and for minimum and maximum occupancy. For comparison, the energy that is needed when recirculation is not active is also plotted. It can be seen, that the influence of recirculation on energy reduction is very high, especially for single occupation and still about 10% for full occupation with four persons. It has to be noted here that the calculation of the heat impact due to solar irradiation was based on a cabin temperature below 24.6°C. Raising the cabin temperature will in turn reduce the heat flow into the cabin (see Chapter 2.1.2). The power needed to cool the interior at increased cabin temperatures will thus be even lower than in this simplified calculation.

⁵ For comparison: According to (DIN 1946-3:1962-06) a typical value to keep a standard car cool in hot ambient conditions (40°C / 40%r.h.) is given with 5kg/min.

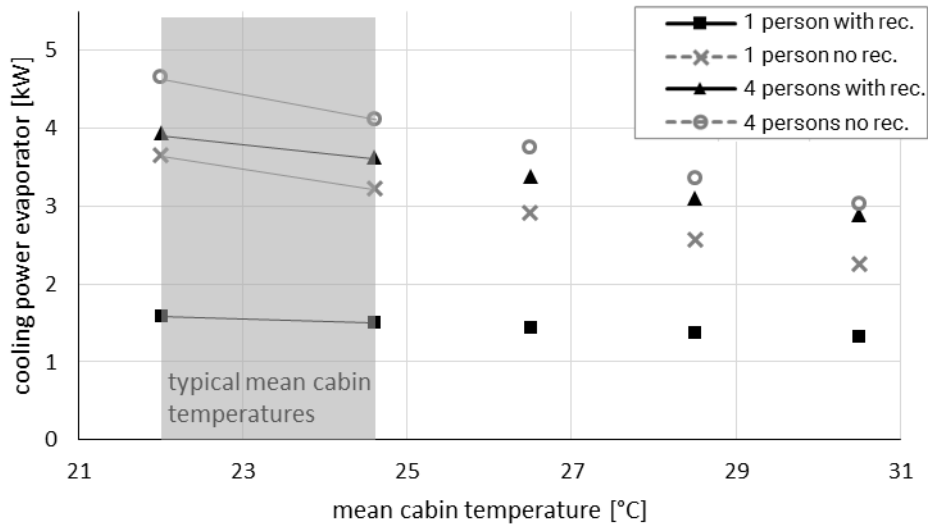


Figure 57: Cooling power at evaporator for one person or four persons, with and without recirculation

The differentiation of the energy balance at a local unit can be made if the energy supply is not provided centrally (as it is the case in the prototype EVA), but locally for example by a small evaporator or a thermoelectric device. If the local outlet is considered separately, the energy balance can be applied on the control volume 'local outlet' in Figure 58.

$$\dot{m}_{loc} (h_{cab} - h_{loc}) - P_{loc} = 0 \quad (6.39)$$

With

- \dot{m}_{loc} Mass flow through local outlet
- h_{loc} Specific enthalpy at local outlet
- P_{loc} Cooling power at local outlet

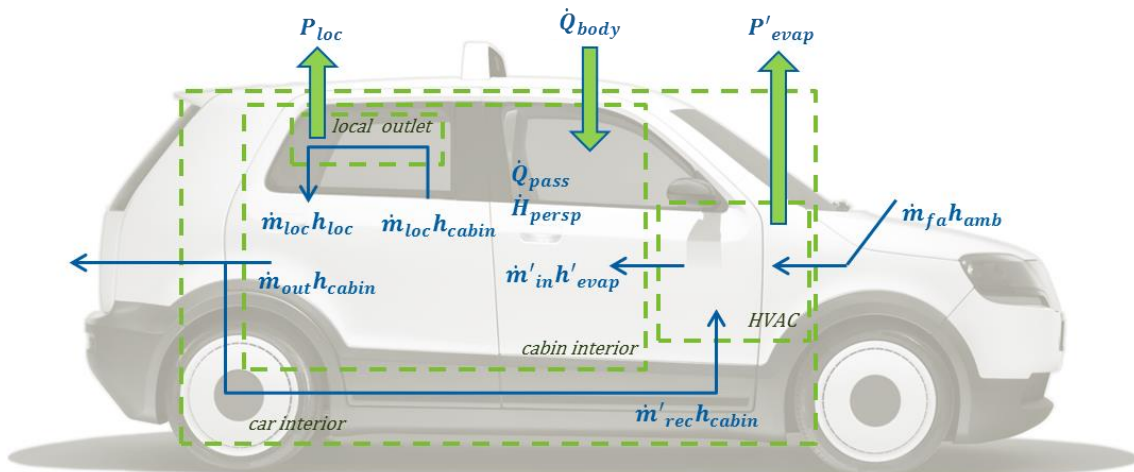


Figure 58: Thermodynamic system boundaries and energy flows in a car with local outlet

The cooling power at the local outlet P_{loc} also contributes to the power needed to maintain the mean cabin temperature and the following equation can be applied:

$$P'_{evap} - P_{loc} = P_{evap} \quad (6.40)$$

Now the energy consumption of the local systems can be calculated using the current, air mass flow and the temperature measurements in the experiment setup. The electric energy consumption of the seat and overhead setup was monitored by measuring both the current through and the voltage drop at the fans and applying Equation (6.41). The heat flow extracted from the air through the overhead outlet is calculated by Equation (6.39) and (6.42).

$$P_{el} = U I \quad (6.41)$$

$$\dot{m}_{loc} = v_{air} A_{outlet} \rho_{air} \quad (6.42)$$

With	P_{el}	Electrical power on the fans
	U	Voltage at the fans = 12V
	I	Current through the fans
	v_{air}	mean air velocity at overhead outlet
	A_{outlet}	Area of overhead outlet
	ρ_{air}	Density of air

	V1.1	V1.2	V2.2	V3.1	V2.4	V3.2	V3.3
cabin temp.	26.5°C	26.5°C	26.5°C	26.5°C	28.5°C	28.5°C	30.5°C
body discomfort	9.3	6.8	7	1.6	9.4	1.5	1.5
OH cooling	on	on	off	on	-	on	on
seat ventilation	off	off	on	on	on	on	on
power fans seat	-	-	6 W	6 W	12 W	12 W	32 W
power OH fans	10 W	10 W	-	11 W	-	23 W	39 W
power OH cooling	57 W	114 W	-	130 W	-	229 W	457 W
sum	67 W	124 W	6 W	147 W	12 W	264 W	528 W

Table 22: Electrical power and energy flow of overhead outlet and seat ventilation in the experiments

The power consumption of the fans in the seat and the overhead outlet is low and will be neglected on the assumption that the main blower in the HVAC consumes comparatively less energy with an active local system. Even at full occupancy, with recirculation and four local outlets active, the power needed locally (~2kW) does not exceed the total power of 3kW needed to maintain the cabin temperature.

The cooling power calculated in Figure 57 shows the potential of local conditioning. If the mean cabin temperature is increased, the possible energy reduction through local conditioning can range from 4% to almost 30%.

cabin target state		26.5°C / 45%	28.5°C / 45%	30.5°C / 43%
1 pass.	T_{evap} [°C]	4 – 9 %	9 – 13%	12 – 17%
4 pass.	\dot{m}_{air} [kg/min]	7 – 14%	14 – 21%	20 – 27%

Table 23: Possible energy reduction by raising the cabin temperature

7 Discussion and outlook

In Chapter 3 three research questions were postulated. In order to address them, a novel interior cooling system was integrated that takes restricting parameters in an automotive environment into account. The system was then rebuilt in a climate chamber to test the sub-systems under controlled conditions with human participant studies. The results and the lessons learned are discussed in this chapter in reference to the research questions.

7.1 RQ1: Is local, vertical cooling feasible in an automotive context?

The work done on the prototype shows that it is reasonable to integrate overhead cooling and seat ventilation in a car. The overhead outlets are flat and integrated in the roof. Due to the conservative dimensioning in the prototype, the air ducts to the roof were led through the B-pillar. A shorter path could lead through the A-pillar, but the cross section of the duct would have to be smaller due to visibility regulations (e.g. (ECE-R125:2)). The result is a higher air velocity in the ducts. Improving the geometry and reducing roughness in the ducts (compared to the prototype version), will reduce unwanted pressure loss and keep noise generation at acceptable levels.

Overhead cooling can present some collisions of interest with car design. One of the pillars has to be thick enough to house the air ducts and the roof has to be at least 1 cm thicker to house the air distribution. Integration in cars with sunroofs and, even more, in convertibles will be difficult.

7.2 RQ2: Does local, vertical cooling improve comfort and efficiency?

Vertical cooling does improve the thermal comfort of the occupants noticeably. To cool the air in the head area, current serial production systems have to use directed spot outlets to cover the distance from the dashboard to the head. The outlet velocity is high and the outlet temperature low (between 5 – 10°C, see Chapter 2.3.5). The overhead outlet provides air with a moderate temperature (around 21 – 22°C) and low air speeds. During the experiments the air flow was seldom noticed and not experienced as uncomfortable. Drying of the eyes, unwanted undercooling or draught, which are common complaints in state of the art systems, did not occur.

The microclimate between body and seat is improved significantly by active seat ventilation. Even when sitting down in hot cabin conditions, the local and overall discomfort votes drop to acceptable limits within 5 – 10 minutes. The impact of the thermal capacity of an overheated seat is reduced by drawing air away from the body through the seat. Immoderate sweat generation was not recorded while the seat ventilation was running.

It was also confirmed that while applying only one local conditioning system (i.e. overhead cooling) discomfort could be reduced noticeably. But the full potential of local conditioning

was effected when local cooling was applied in combination (i.e. overhead cooling and seat ventilation). This is well in correlation with the findings of the FAT studies (Schmidt et al., 2013 and Schmidt et al., 2015), which found that the best results were obtained when combining more than one local heating application e.g. footwell heating, seat heating and heated steering wheel. In the case of cooling, the optimal comfort is obtained by cooling the head and the upper torso while eliminating local hot-spots, as can occur on the seat surface.

The experiments show that vertical cooling has a distinct potential to reduce the energy consumption of the HVAC system (over 20% on a hot day). The calculated potential could even be higher because of the conservative estimation of heat loss at elevated cabin temperatures. The calculated potentials are given for the cooling power. Dependent on the technology used to create the cool air flow these values might vary. The present calculation is based on the assumption that the air is cooled by a refrigerant cycle.

7.3 RQ3: What are the operative limitations of such a system?

Seat ventilation can be operated up to a cabin temperature of approximately 27°C (at 45%r.h.) before becoming uncomfortable. Above this, the risk of unwanted sweating and thus evaporative cooling at the sitting area or the back increases. Overhead cooling by itself can also be operated up to a cabin temperature of approximately 27°C (at 45%r.h.) while the maximum temperature difference at the outlet should not exceed 6K. If both systems are combined, the cabin temperature can be raised to at least 30.5°C (at 43%r.h.). The temperature difference at the outlet in this setting is 9K, which results in an optimal outlet temperature of 21 – 22°C. This value is likely to be confirmed in further experiments by varying the outlet speed and investigating whether higher air speeds can be used to lower outlet temperature difference. A higher cabin temperature might be possible. However one has to bear in mind that the cabin humidity has to be controlled in this case to avoid condensation at the overhead outlet.

7.4 How can the calculation be optimised?

The calculation was based on several simplifications. The biggest being, that the cabin was assumed to be a perfectly mixed container. But even with standard HVAC systems the cabin temperature is set differently for head and leg room. It is already known that adaptive temperature layering for heating and cooling is important for the thermal wellbeing of the occupant (Chapter 2.3.5). However the mean temperature in the cabin in standard systems is lower than what can be achieved with the close-to-body, vertical flow overhead outlet. The exact temperature distribution of a standard system and the new vertical system would prove a valuable input for the energy calculation. This could be done with actual measurements in the car or detailed CFD-simulations. With that input, the heat flow into the cabin due to the surrounding temperature and solar irradiation can be calculated in respect

of rising cabin temperatures. A detailed simulation would prove beneficial for a more realistic efficiency prediction.

Furthermore, the calculated recirculation ratios are based on a guiding value for fresh air per person which is applicable if the air is dispersed within the whole cabin. In case of an overhead ventilation the fresh air can be applied exactly where sufficient oxygen supply is needed. The rest of the cabin could be conditioned with recirculated air. This would impact positively on energy consumption and add to the efficiency potential of the vertical cooling system.

7.5 How can the technical solution be optimised?

Seat ventilation is fairly straightforward and has been implemented in serial production already. What became apparent in the mock-up experiments is that the perforated seat surface width should exceed the width of the seated occupant's body. If the air flow is blocked, the positive ventilating effect is diminished noticeably.

The overhead outlets are supplied with cold air that is generated centrally by the front HVAC unit through a refrigerant cycle. Several other ways of generating cool airflow should also be discussed:

- Positioning the evaporator in the roof. This solution prevents air ducts having to be pillar-located. They can thus be considerably slimmer. The refrigerant pipes would require about a centimetre in diameter. However, added weight has to be taken into account, since metal pipes add more weight than plastic air ducts. Another challenge would be to guarantee lubrication for the compressor. It might be difficult to circulate the refrigerant oil over such a height. The solution to bypass this problem by elevating the whole refrigerant cycle would result in bulky roof attachments. If every outlet were to be supplied with its own evaporator, the weight would increase and the refrigerant cycle control would be more challenging. Additionally, the fans also have to be repositioned at local evaporators, demanding more package space in the roof. At the currently needed mass flow rates the packaging is challenging. Avoiding unwanted noise generation by the fans will add to the complexity in finding a viable solution.
- Cooling by water cycle. Another solution to avoid air ducts in the vehicle columns is to transport the heat by a water cycle. Water pipes would however add even more weight to the system than refrigerant pipes. Also, another system would be needed to cool the water cycle. The final criterion for exclusion would be the need for venting of the coolant system. Positioning of a compensation reservoir at the highest geodetic point is not possible in the roof.
- Cooling locally by Peltier elements. Peltier elements can be built in very compact form. Electrical cabling alone is needed in vehicle pillars and the operation mode can

be switched simply by reversing polarity. The coefficient of performance for Peltier elements is however very low, especially on temperature difference increase. The relatively low power density is another drawback that goes against a solution with Peltier elements.

In summary, the supply of cold air to the roof by air ducts is seen as the optimum in regard of limiting factors and current technical possibilities. The shortest air duct routing in vehicle pillars should be sought and duct geometry should be optimised. Sufficient insulation of the ducts is advised to minimise heat losses.

These considerations derive from findings gained during work on the prototype and during the experiments. They were discussed with experts on automotive air conditioning, both from the university and the automotive industry. Nonetheless it would be beneficial to evaluate in detail the impact of weight (especially on the energy consumption of the overall vehicle) and cost of the different technologies.

7.6 What should be considered for future work?

The scientific findings should be used to parametrise the system built in EVA and then tested in human person surveys on the road. According to the adaptive thermal model (Chapter 2.3.2), the neutral temperature is dependent on acclimatization to the average ambient temperature. The experiments were held in Munich, where the targeted neutral temperature is calculated as 22.4°C⁶. The targeted area of operation is however in a tropical climate zone where the neutral temperature is distinctly higher (+2.2K for Singapore) at much higher humidity. It stands to reason that a population used to higher temperatures will also accept higher temperatures in cars which will again add to the efficiency potential of the vertical cooling system.

The experiments were designed to obtain answers for a near steady state operation of the systems. This was necessary to allow comparison of the votes at a number of cabin temperatures in respect of the efficiency potential. The next step is to evaluate various use scenarios since conditions in cars are seldom at a steady state. The results obtained in Experiment 3 already show very high potential for realistic cooldown performance if the car is already at the targeted cabin temperature. In a next experiment more extreme situations should be simulated. The cabin temperature of a car parked in the sun can climb easily to 80°C, while the dashboard can reach 100°C. A higher gradient between skin temperatures at the front and the back might limit the cabin temperature span in which the vertical cooling has a positive impact. Since the influence of thermal radiation from heated surfaces was not simulated in the experiments, this could be simulated in the mock-up by integrating a heated

⁶ Some experiments that were conducted during the winter months had to be repeated subsequently in summer. The neutral temperature can be adapted with $\pm 1\text{K}$ for the hottest and the coldest months. Cross referencing the results concluded no significant differences between results obtained in summer and in winter.

dashboard. A question that needs answering addresses an important selling point of vertical conditioning: how fast can the cooldown mode of the new system achieve a thermally acceptable state in comparison to state-of-the-art systems?

The rating scales used in the present experiments (CP-50, thermal perception and thermal preference. See Chapter 2.3.6) proved to produce reliable answers. The scales for thermal perception and thermal preference usually needed no explanation. The use of the CP-50 needed some explanation before starting the experiment. It became apparent in the first pre-tests that participants tended to concentrate on the fine tuning of the scale (1-10) before even choosing the category of discomfort (none, very slight, slight,...). This led to unnecessary confusion and slightly distorted answers. When participants concentrated first on the category of discomfort before attempting to state the tendency with a specific number, the results became stable and comparable. It was also helpful to provide some kind of anchoring by explaining that 0 (none) was equivalent to the complete absence of discomfort, while 41-50 (very severe) would represent an almost unbearable scenario (the example of being in a sauna short before heat collapse was often used).

The experiments were all conducted with a homogenous sample: young, male adults with reasonable to good state of fitness. This was done to keep the sample size small while obtaining results that were unbiased by unwanted parameters (such as gender or age differences). Similar person samples for all three experiments were selected. This facilitated comparison of the results. It has to be pointed out again that the sample size allows only an explorative discussion. For a detailed statistical analysis, the sample size should be expanded to at least 25 participants (provided the sample stays homogeneous). Further investigation is needed to establish whether close-to-body conditioning is perceived differently by women, elderly people and children. The influence of overhead cooling on baldness should also be investigated.

The choice for the overhead outlet geometry was mainly driven by anthropometric simulations (in CATIA with the help of the RAMSIS program) to cover possible head positions for a wide variety of physiques and postures. The dimension and spacing of the holes was a decision that evolved through requirements for mass flow, maximum air velocity and interior design and trim issues. Further investigation should go into an optimisation of the outlet geometry in respect of personalisation and adaptability as well as acoustics, air flow distribution and of course the possibilities for design and trim. If the same positive results occur with optimised geometry in which the mass flow can be reduced, the energy efficiency potential of the vertical cooling system could be even higher.

Finally, the review of the state of the art and the findings of a questionnaire on the use of state-of-the-art HVAC HMIs revealed, that people often adjust their system to unsuitable settings. This can result in an energetically disadvantageous state. The HMI concept

integrated in the EVA prototype was an attempt to solve this problem by simplifying the user interface. The feedback gained from the presentation of the prototype showed that the users' perception of the new system is strongly correlating to their possibilities to interact with the system. It would be important to know if people accept the proposed simplification of the HMI. An on-the-road user acceptance study should be conducted with the new system.

Appendix

Fanger's Heat Balance Equation

Fanger refined Gagge's (1936) heat balance equation into the following form:

$$H - E_{diff} - E_{rsw} - E_{resp} - L = K = R + C \quad (7.1)$$

With	E_{diff}	=	evaporation heat loss due to vapour diffusion through the skin
	E_{rsw}	=	heat loss due to evaporation of regulatory sweating from the skin
	E_{resp}	=	respiration latent heat loss
	L	=	dry respiration loss
	K	=	heat transfer from skin to clothing surface
	R	=	radiation loss
	C	=	convection loss

Substituting and refining each value results into the following equation (the step-by-step calculation can be read in (Auliciems & Szokolay, 1997)):

$$\begin{aligned} & \frac{M}{A_D} (1 - \eta) - 0.35 \cdot \left[43 - 0.061 \cdot \frac{M}{A_D} \cdot (1 - \eta) - p_a \right] - 0.42 \cdot \left[\frac{M}{A_D} \cdot (1 - \eta) - 50 \right] \\ & - 0.0023 \cdot \frac{M}{A_D} \cdot (44 - p_a) - 0.0014 \cdot \frac{M}{A_D} \cdot (34 - T_a) \\ & = \frac{35.7 - 0.032 \cdot \frac{M}{A_D} \cdot (1 - \eta) - T_{cl}}{0.18 \cdot I_{cl}} \\ & = 3.4 \cdot 10^{-8} \cdot f_{cl} \cdot [(T_{cl} + 273)^4 - (T_r + 273)^4] + f_{cl} \cdot h_c \cdot (T_{cl} - T_a) \quad (7.2) \end{aligned}$$

With	M	metabolisms energy
	A_D	body surface area (DuBois area)
	η	mechanical efficiency
	p_a	vapour pressure of ambient air
	T_a	ambient air temperature (DBT)
	T_{cl}	clothing surface temperature
	I_{cl}	insulation of clothing
	f_{cl}	ratio of clothed to exposed body surface
	T_r	mean radiant temperature
	h_c	convection conductance

Fanger's PMV

Fanger's Predicted Mean Vote is derived by the following equation

$$\begin{aligned}
 PMV = & \left[0.352 \exp\left(-0.042 \frac{M}{A_D}\right) + 0.032 \right] \left\{ \frac{M}{A_D} (1 - \eta) \right. \\
 & - 0.35 \left[43 - 0.061 \frac{M}{A_D} (1 - \eta) - p_a \right] - 0.42 \left[\frac{M}{A_D} (1 - \eta) - 50 \right] \\
 & - 0.0023 \frac{M}{A_D} (44 - p_a) - 0.0014 \frac{M}{A_D} (34 - T_a) \\
 & \left. - 3.4 \cdot 10^{-8} f_{cl} [(T_{cl} + 273)^4 - (T_r + 273)^4] + f_{cl} h_c (T_{cl} - T_a) \right\} \quad (7.3)
 \end{aligned}$$

Where T_{cl} is found by iteration from

$$\begin{aligned}
 T_{cl} = & 35.7 - 0.032 \frac{M}{A_D} (1 - \eta) \\
 & - 0.18 I_{cl} \{ 3.4 \cdot 10^{-8} f_{cl} [(T_{cl} + 273)^4 - (T_r + 273)^4] \dots \\
 & + f_{cl} h_c (T_{cl} - T_a) \} \quad (7.4)
 \end{aligned}$$

NTC calculation and calibration

Equation (5.18) can be derived by using Ohm's law on the circuit as described in Figure 36:

$$U_{res} = \frac{ANALOG_{IN}}{1024} \cdot 5V \quad (7.5)$$

$$I_{res} = I_{NTC} = \frac{U_{res}}{5110\Omega} \quad (7.6)$$

$$U_{NTC} = 5V - U_{res} \quad (7.7)$$

$$R_{NTC} = \frac{U_{NTC}}{I_{NTC}} \quad (7.8)$$

An easier way to calculate the temperature of a thermistor, other than measuring the values for the Steinhart-Hart-Equation, is by taking the given B- and R25-values (in the data sheet of the sensors) into the equation:

$$\frac{1}{T} = \frac{1}{T_0} + \frac{1}{B} \cdot \ln\left(\frac{R}{R_0}\right) \quad (7.9)$$

This is essentially the Steinhart-Hart-Equation with $C_1 = \left(\frac{1}{T_0}\right) - \left(\frac{1}{B}\right) \cdot \ln(R_0)$, $C_2 = \frac{1}{B}$ and $C_3 = 0$. Comparison of measured results has proven however, that the measuring accuracy can be optimized by using the original Steinhart-Hart-Equation and putting in the effort of a manual calibration.

Questionnaire 1

Fragebogen zur Thermischen Behaglichkeit bei verschiedenen Temperaturen

Alter _____

Geschlecht · m · w

Größe _____

Gewicht _____

Haardichte _____ (1: Vollglatze ... 5: volles Haar)

Fitnesszustand

· Geringe Fitness · neutral · Hohe Fitness

Persönliches Temperaturempfinden (allgemein)

· ich friere schnell · neutral · mir ist schnell warm

Haben Sie schon mal an einem Versuch des Lehrstuhls für Ergonomie teilgenommen? Wenn ja, an welchen Versuchen:

Sitzen Sie komfortabel? · ja · nein

Vielen Dank für Ihre Unterstützung und viel Spaß beim Versuch!

1. Bewertung des momentanen *Diskomforts* des Kopfes und des Körpers:

Kein Diskomfort	Sehr geringer Diskomfort	Geringer Diskomfort	Mittlerer Diskomfort	Starker Diskomfort	Sehr starker Diskomfort
0	1 ... 10	11 ... 20	21 ... 30	31 ... 40	41 ... 50

2. Bewertung der momentanen *thermischen Wahrnehmung* des Kopfes, des Rumpfes und der Beine:

heiß	sehr warm	warm	etwas warm	neutral	etwas kühl	kühl	sehr kühl	kalt
+4	+3	+2	+1	0	-1	-2	-3	-4

3. Haben Sie in den letzten 5 Minuten eine Luftbewegung gemerkt?

ja nein

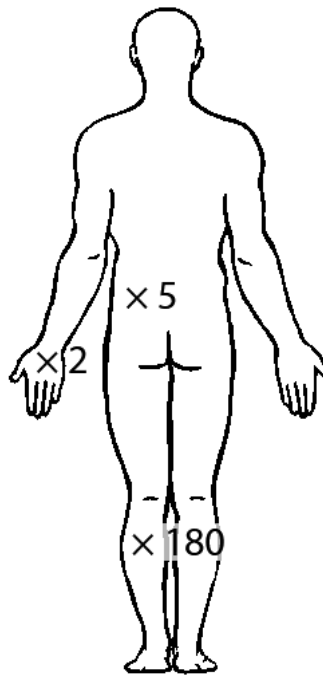
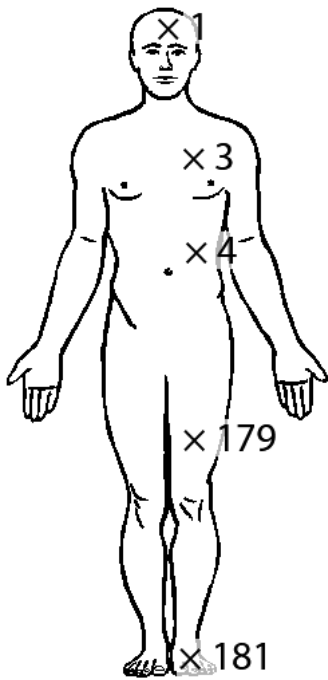
4. Wenn ja, haben Sie die Luftbewegung als unangenehm empfunden?

ja nein

5. Wo haben Sie die Luftbewegung gemerkt?

Gesicht Hals Hände Füße Sonstiges

Positionen Temperaturfühler:



- | | |
|-----|-------------------|
| 1 | Stirn |
| 2 | Handrücken |
| 3 | Sternum |
| 4 | Bauch |
| 5 | Nierenbereich |
| 179 | Oberschenkel oben |
| 180 | Wade |
| 181 | Fußrücken |

Abstand Kopf – Luftauslass: _____ (Soll: 10cm)

Luftgeschwindigkeit: _____ (Soll: 0,2-0,25m/s auf Augenhöhe)

Klamotten: _____

Min	TGebl	D-Kopf	D-Körp	T-Kopf	T-Rum	T-Bein	Luft	Unang?	Wo?	Schweiß
0										
5										
10										
15										
20										
25										
30										
35										
40										

Questionnaire 2

Fragebogen zur Thermischen Behaglichkeit bei verschiedenen Temperaturen

Alter _____

Geschlecht m w

Größe _____

Gewicht _____

Haardichte _____ (1: Vollglatze ... 5: volles Haar)

Fitnesszustand

 Geringe Fitness neutral Hohe Fitness

Persönliches Temperaturempfinden (allgemein)

 ich friere schnell neutral mir ist schnell warm

Haben Sie schon mal an einem Versuch des Lehrstuhls für Ergonomie teilgenommen?

Wenn ja, an welchen Versuchen:

Sitzen Sie komfortabel? ja nein**Vielen Dank für Ihre Unterstützung und viel Spaß beim Versuch!**1. Bewertung des momentanen *Diskomforts* des Rückens, der Sitzfläche, des Kopfes und global:

Kein Diskomfort	Sehr geringer Diskomfort	Geringer Diskomfort	Mittlerer Diskomfort	Starker Diskomfort	Sehr starker Diskomfort
0	1 ... 10	11 ... 20	21 ... 30	31 ... 40	41 ... 50

2. Bewertung der momentanen *thermischen Wahrnehmung* des Rückens, der Sitzfläche, des Kopfes und global:

heiß	sehr warm	warm	etwas warm	neutral	etwas kühl	kühl	sehr kühl	kalt
+4	+3	+2	+1	0	-1	-2	-3	-4

3. Wie würden Sie das Klima momentan ändern?

viel wärmer	wärmer	etwas wärmer	alles passt	etwas kühler	kühler	viel kühler
+3	+2	+1	0	-1	-2	-3

4. Haben Sie in den letzten 5 Minuten eine Luftbewegung gemerkt?

ja nein

5. Wenn ja, haben Sie die Luftbewegung als unangenehm empfunden?

ja nein

6. Wo haben Sie die Luftbewegung gemerkt?

Gesicht

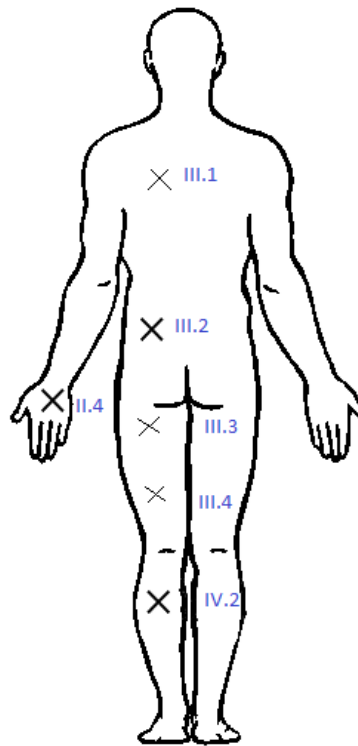
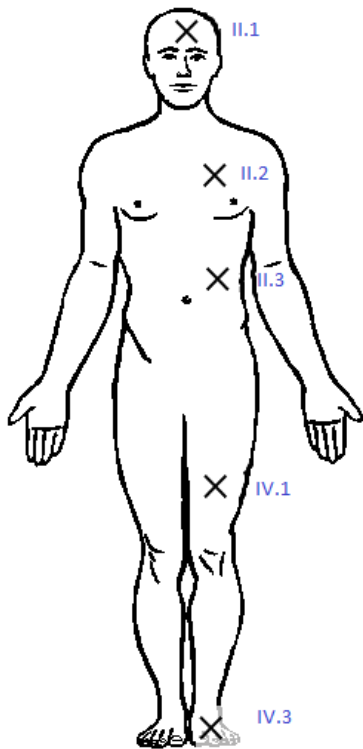
Hals

Hände

Füße

Andere Stelle

Positionen Temperaturfühler:



- I.1 Umgebung Kopf
- I.2 Umgebung Hüfte
- I.3 Umgebung Knie
- I.4 Umgebung Füße

- II.1 Stirn
- II.2 Sternum
- II.3 Bauch
- II.4 Handrücken
- III.1 Rücken oben
- III.2 Rücken unten
- III.3 Sitzfläche hinten
- III.4 Sitzfläche vorne

- IV.1 Oberschenkel
- IV.2 Wade
- IV.3 Fuß
- IV.4 Umgebung

Abstand Kopf – Luftauslass: _____ (Soll: 10cm)

Luftgeschwindigkeit: _____ (Soll: 0,2-0,25m/s auf Augenhöhe)

Klamotten: _____

Durchgang: Temperatur: T-Überkopfbelüftung: Sitzbelüftung:

Fahrer: Luftfeuchtigkeit: Luftgeschwindigkeit: I: II: III: IV:

Datum: _____

Min	D-R	D-S	D-K	D-G	T-R	T-S	T-K	T-B	Tendenz	Luftz.	Wo?	Unang.	Schweiß
0													
5													
10													
15													
20													
25													
30													
35													
40													

References

- Al-Othmani, M., Ghali, K., & Ghaddar, N. (2009). Experimental and theoretical study of transient human thermal comfort response in convective and radiative environments. *HVAC&R Research*, *15*(5).
- Arens, E., Zhang, H., & Huizenga, C. (2006a). Partial- and whole-body thermal sensation and comfort— Part I: Uniform environmental conditions. *Journal of Thermal Biology*, *31*(1-2), 53–59.
- Arens, E., Zhang, H., & Huizenga, C. (2006b). Partial- and whole-body thermal sensation and comfort—Part II: Non-uniform environmental conditions. *Journal of Thermal Biology*, *31*(1-2), 60–66.
- ASHRAE. (2013). *ASHRAE handbook: Fundamentals*. Atlanta, Ga.: ASHRAE.
- Auliciems, A. (1981). Towards a psycho-physiological model of thermal perception. *International Journal of Biometeorology*, *25*(2), 109–122
- Auliciems, A., & Szokolay, S. V. (1997). *Thermal comfort. PLEA notes: note 3*. Brisbane, Qld.: PLEA in association with Dept. of Architecture, University of Queensland.
- Bartels, V. T. (2003). Thermal comfort of aeroplane seats: Influence of different seat materials and the use of laboratory test methods. *Applied Ergonomics*, *34*(4), 393–399
- Bender, S., Pannirsilvam, V., Khoo, R., Lopez Hidalgo, P., Tschochner, M., Sheth, P., ... (2013). Concept of an electric taxi: for tropical megacities. *CoFAT, München*.
- Bhatti, M. S. (1999). Riding in Comfort: Part I: Evolution of Automotive Heating. *ASHRAE Journal*, *41*(8).
- BMW AG. *GIBT DIE BLICKRICHTUNG VOR: Das Design des BMW X6*. Retrieved from <http://www.bmw.de/de/neufahrzeuge/x/x6/2014/design.html>*, Access Date: 11/11/2015.
- Bolinder, E., Magnusson, E., & Nyren, E. (1970). *Risker i jobbet: LO-enkäten: LO-medlemmarnas uppfattning om arbetsplatsens hälsorisker* (in Swedish). Stockholm: PRISMA.
- Brinkkötter, C., & Ackermann, J. (2010). Energiesparendes Wohlfühlklima: Klimakomfort durch "insassenselektives Heizen". *Kundenmagazin der IAV*, *3*.
- Bubb, H. (2003). Komfort und Diskomfort. *Ergonomie Aktuell*, *4*.
- Daly, S. (2006). *Automotive air-conditioning and climate control systems*. Amsterdam, London: Butterworth-Heinemann.
- Dear, R. de, & Brager, G. (1998). Developing an Adaptive Model of Thermal Comfort and Preference. *ASHRAE Transactions*, *104*, 145–167.
- Dear, R. de, Leow, K. G., & Foo, S. C. (1991). Thermal comfort in the humid tropics: Field experiments in air conditioned and naturally ventilated buildings in Singapore. *International Journal of Biometeorology*, *34*(4), 259–265
- ebm-papst. *Fan technology from ebm-papst powers seating comfort in the new S-Class: case study no. 002, seat ventilation*. Retrieved from http://www.ebmpapst.com/media/content/overview_of_industries/automotive/case_studies/CaseStudy_2_seat_ventilation_EN.pdf*, Access Date: 2/12/2015.

- ebm-papst. *Product data sheet 512F*. Retrieved from <http://img.ebmpapst.com/products/datasheets/DC-axial-fan-512F-ENG.pdf>*, Access Date: 4/1/2016.
- Ellermeier, W., Westphal, W., & Heidenfelder, M. (1991). On the "absoluteness" of category and magnitude scales of pain. *Perception & Psychophysics*, *49*(2), 159–166
- DIN EN ISO 9920:2009 (2009). *Ergonomie der thermischen Umgebung - Abschätzung der Wärmeisolation und des Verdunstungswiderstandes einer Bekleidungskombination*.
- DIN EN ISO 7730:2005 (2006). *Ergonomie der thermischen Umgebung - Analytische Bestimmung und Interpretation der thermischen Behaglichkeit durch Berechnung des PMV- und des PPD-Indexes und Kriterien der lokalen thermischen Behaglichkeit*.
- DIN EN ISO 7933:2004 (2004). *Ergonomie der thermischen Umgebung - Analytische Bestimmung und Interpretation der Wärmebelastung durch Berechnung der vorhergesagten Wärmebeanspruchung*.
- DIN EN ISO 15743:2008 (2008). *Ergonomie der thermischen Umgebung – Arbeitsplätze in der Kälte – Risikobewertung und Management*.
- DIN EN ISO 11079:2007 (2008). *Ergonomie der thermischen Umgebung - Bestimmung und Interpretation der Kältebelastung bei Verwendung der erforderlichen Isolation der Bekleidung (IREQ) und lokalen Kühlwirkungen*.
- DIN EN ISO 13732-3:2008 (2008). *Ergonomie der thermischen Umgebung - Bewertungsmethoden für Reaktionen des Menschen bei Kontakt mit Oberflächen - Teil 3: Kalte Oberflächen*.
- DIN EN ISO 13732-1:2008 (2008). *Ergonomie der thermischen Umgebung - Bewertungsverfahren für menschliche Reaktionen bei Kontakt mit Oberflächen - Teil 1: Heiße Oberflächen*.
- DIN EN ISO 13731:2001 (2002). *Ergonomie des Umgebungsklimas - Begriffe und Symbole*.
- DIN EN ISO 10551:2001 (2002). *Ergonomie des Umgebungsklimas – Beurteilung des Einflusses des Umgebungsklimas unter Anwendung subjektiver Bewertungsskalen*.
- DIN EN ISO 11399:2000 (2001). *Ergonomie des Umgebungsklimas - Grundlagen und Anwendung relevanter Internationaler Normen*.
- Fanger, P. O. (1970). *Thermal comfort: Analysis and applications in environmental engineering*. Copenhagen: Danish Technical Press.
- Fanger, P. O., & Christensen, N. K. (1986). Perception of draught in ventilated spaces. *Ergonomics*, *29*(2), 215–235.
- Fiala, D. (1998). *Dynamic simulation of human heat transfer and thermal comfort* (Dissertation). De Montfort University, Leicester, Hochschule für Technik, Stuttgart.
- Fiala, D., Psikuta, A., Jendritzky, G., Paulke, S., Nelson, D. A., Marken Lichtenbelt, W. D., & Frijns, A. J. H. (2010). Physiological modeling for technical, clinical and research applications. *Frontiers in Bioscience*, *S2*, 939–968.
- Frisch, A., Schanda, M., Engelhardt, S., Geisel, T., & Lasi, U. (2013). S-Klasse Interieur: Wellness und Büro vereint. *ATZ extra*, *Juli*, 70–77.

- Gagge, A. P. (1936). The linearity criterion as applied to partitional calorimetry. *American Journal of Physiology*, 116, 656–668.
- Gagge, A. P., Stolwijk, J. A. J., & Nishi, Y. (1971). An effective temperature scale based on a simple model of human physiological regulatory response. *ASHRAE Transactions*, 77(1), 247–262.
- Gatley, D. P. (2013). *Understanding psychrometrics* (Third edition). Atlanta, GA: ASHRAE.
- Gentherm. *Automotive*. Retrieved from http://www.gentherm.com/de/page/automotive?language=de*, Access Date: 2/12/2015.
- GoingElectric. *BMW: Infrarot-Heizung und Wärmepumpe für mehr Effizienz im Elektroauto*. Retrieved from http://www.goingelectric.de/2012/09/20/news/bmw-infrarot-heizung-und-waermepumpe-fuer-mehr-effizienz-im-elektroauto/*, Access Date: 2/12/2015.
- Großmann, H. (2013). *Pkw-Klimatisierung: Physikalische Grundlagen und technische Umsetzung* (2. Aufl. 2013). VDI-Buch. Berlin, Heidelberg: Imprint: Springer Vieweg.
- Hauer, E. (2013). Hydrothermal comfort in car seats. *ATZ*, 115, 36–39.
- Hertle, S. (2015). *Usability gestenbasierter App-Bedienung und Beitrag einer Überkopfbeflüftung zur thermischen Behaglichkeit. Komponenten für effiziente Elektromobilität* (Term thesis). TUM, München.
- Höchenberger, M. (2016). *Influence of passive and active climatisation in car seats on thermal comfort* (Term thesis). TUM, München.
- Houghten, F. C., & Yagloglou, C. P. (1923). Determining equal comfort lines. *Journal of the American Society of Heating and Ventilating Engineers*, 29, 165–176.
- Huizenga, C., Zhang, H., & Arens, E. A. (2001). A model of human physiology and comfort for assessing complex thermal environments. *Building and Environment*, 36(6), 691–699.
- VDI 6032 (2004). *Hygiene-Anforderungen an die Lüftungstechnik in Fahrzeugen zur Personenbeförderung*.
- Jeffus, L. F., & Fearnow, D. (2004). *Refrigeration and air conditioning: An introduction to HVACR* (4th ed.). Upper Saddle River N.J.: Pearson Prentice Hall.
- Jekelius, F. (2013). *Design of the HVAC air distribution box and air ducts for an electric taxi prototype* (Diploma thesis). TUM CREATE, Singapore.
- Klinke, R., Pape, H.-C., Kurtz, A., & Silbernagl, S. (2010). *Physiologie*. Stuttgart: Georg Thieme Verlag.
- Kolb, A. (2004). *Kfz-Klimatisierung*. Lecture notes, Technische Universität München.
- Lorenz, M. (2015). *Reduction of Heating Loads and Interior Window Fogging in Vehicles* (Dissertation). TUM, München.
- Lutz, M. (2013). *Development of a cooling and ventilation system for vehicle seats regarding ergonomic aspects* (Term thesis). TUM CREATE, Singapore.
- Marschall, V. (2015). *Implementation of a mock-up vehicle seat for testing ergonomic cooling options* (Bachelor thesis). TUM, München.
- Mayer, E. (1989). *Anordnung zur Luftführung in Fahrzeugräumen*, European Patent Office: 0312557 B1.

- Mayer, E. (2001). *Verfahren und Vorrichtung zur Klimatisierung von Fahrzeugen und insbesondere von Flugzeugen*, European Patent Office: 1064194 B1.
- Mitchell, D., & Wyndham, C. H. (1969). Comparison of weighting formulas for calculating mean skin temperature. *Journal of Applied Physiology*, 26(5), 616–622.
- Mittag, H.-J. (2016). *Statistik: Eine Einführung mit interaktiven Elementen* (4. Auflage). Berlin: Springer.
- Monteur. (2011). Hydraulische Durchmesser: Kanäle für die kontrollierte Wohnraumlüftung. *SBZ Monteur*, 10, 14–17.
- Morena, M. R., Krahl, R., & Kurz, B. (2012). How users perceive the climate comfort of vehicle seats. *ATZ*, 114, 16–20.
- Nadler, N. (2005). Zur Personenwärme bei der Kühllastberechnung nach VDI 2078. *VDI-Gesellschaft Bauen und Gebäudetechnik: HLH Lüftung/Klima - Heizung/Sanitär - Gebäudetechnik*, 7, 36–40.
- Nall, D. H. (2004). Looking across the water: Climate-adaptive buildings in the United States & Europe. *The Construction Specifier*, 57(11), 50–56.
- NEA Singapore. *Climate Data Changi Airport*. Retrieved from http://www.nea.gov.sg/weather-climate/climate-information/singapore's-climate-information-data*, Access Date: 01/12/2012.
- Olesen, B. W., & Brager, G. (2004). A Better Way to Predict Comfort: The New ASHRAE Standard 55-2004. *ASHRAE Journal*, August.
- Olgay, V. (1962). Bioclimatic evaluation method for architectural application. In S. W. Tromp (Ed.), *Biometeorology. Proceedings of the Second International Bioclimatological Congress held at The Royal Society of Medicine, London, 4-10 September 1960* (pp. 246–261). London: Pergamon Press Ltd.
- Parsons, K. C. (2002). *Human thermal environments: The effects of hot, moderate, and cold environments on human health, comfort, and performance* (Third edition). Boca Raton: Taylor & Francis.
- Pasut, W., Zhang, H., Arens, E., & Zhai, Y. (2015). Energy-efficient comfort with a heated/cooled chair: Results from human subject tests. *Building and Environment*, 84, 10–21.
- Paulke, S., & Kreppold, E. (2008). The Application of Thermal Simulation Techniques for Seat Comfort Optimizations. *SIMVEC, 14. Konferenz und Fachausstellung Berechnung und Simulation Fahrzeugbau*, (VDI Berichte 2031).
- DIN EN ISO 15831:2004 (2004). *Physiologische Wirkungen - Messung der Wärmeisolation mittels einer Thermopuppe*.
- Polifke, W., & Kopitz, J. (2009). *Wärmeübertragung: Grundlagen, analytische und numerische Methoden* (2., aktualis. Aufl.). Ing - Maschinenbau. München [u.a.]: Pearson.
- Prestel, J. (2013). *The dynamic thermal receptor response and comfort in warm and cold environments* (Bachelor thesis). TUM, München.
- Rainer, M. (2013). *Functional development of the thermal management and air conditioning control for an electric vehicle* (Diploma thesis). TUM CREATE, Singapore.

- DIN 1946-2:1994 (1994). *Raumlufttechnik - Teil 2: Gesundheitstechnische Anforderungen (VDI-Lüftungsregeln)*.
- DIN 1946-3:1962-06 (2006). *Raumlufttechnik – Teil 3: Klimatisierung von Personenkraftwagen und Lastkraftwagen*.
- Recknagel, E. R., & Schramek, E.-R. (1999). *Taschenbuch für Heizung und Klimatechnik: einschliesslich Warmwasser- und Kältetechnik* (69. Aufl.). München: Oldenbourg.
- Reimund, I., & Hauptenthal, H. (2014). C-Klasse Komfort: Komfort der Oberklasse. *ATZ extra, Mai*, 90–95.
- Rohles, F. H., Hayter, R. B., & Milliken, G. (1975). Effective Temperature (ET*) as a Predictor for Thermal Comfort. *ASHRAE Transactions*, 81(2), 148–156.
- Rolle, A. (2016). *Influence of over-head ventilation/cooling together with active climatisation in car seats on the overall thermal comfort* (Term thesis). TUM, München.
- RWTH. *Fields of Research, Institute for Automotive Engineering*. Retrieved from <http://www.ika.rwth-aachen.de/en/research/fields-of-research.html>*, Access Date: 10/1/2016.
- Schmidt, C., Praster, M., Wölki, D., Wolf, S., & van Treeck, C. (2013). Rechnerische und probandengestützte Untersuchung des Einflusses der Kontaktwärmeübertragung in Fahrzeugsitzen auf die thermische Behaglichkeit. *FAT-Schriftenreihe*, 261.
- Schmidt, C., Veselá, S., Nabi Bidhendi, M., Rudnick, J., & van Treeck, C. (2015). Zusammenhang zwischen lokalem und globalem Behaglichkeitsempfinden: Untersuchung des Kombinationseffektes von Sitzheizung und Strahlungswärmeübertragung zur energieeffizienten Fahrzeugklimatisierung. *FAT-Schriftenreihe*, 272.
- Schmidt, R. F., Lang, F., & Heckmann, M. (2010). *Physiologie des Menschen: Mit Pathophysiologie* (31., überarb. und aktualisierte Aufl.). Springer-Lehrbuch. Heidelberg: Springer.
- Schmitz, S. (2003). *Vergleichende Messungen und Bewertungen der thermophysilogisch relevanten Parameter an Probanden während des Sitzens auf belüfteten und unbelüfteten Fahrzeugsitzen* (Dissertation). Ludwig-Maximilians-Universität München, Germany.
- Shen, W., & Parsons, K. C. (1997). Validity and reliability of rating scales for seated pressure discomfort. *International Journal of Industrial Ergonomics*, 20(6), 441–461
- Steinhart, J. S., & Hart, S. R. (1968). Calibration curves for thermistors. *Deep Sea Research and Oceanographic Abstracts*, 15(4), 497–503
- Stolwijk, J. A. J., & Hardy, J. D. (1966). Temperature regulation in man: A theoretical study. *Pflügers Archiv (Pflügers Archiv für die Gesamte Physiologie des Menschen und der Tiere)*, 291(2), 129–162
- Stuke, P. (2015). *Vorlesung Elektromobilität: Wärmemanagement*. Lecture notes, Technische Universität München.
- Stuke, P., & Bengler, K. (2013). Interior air conditioning for electric vehicle EVA: New approach on vehicle interior cooling to increase comfort and reduce energy consumption. *CoFAT, München*.

- Tanabe, S.-i., Kobayashi, K., Nakano, J., Ozeki, Y., & Konishi, M. (2002). Evaluation of thermal comfort using combined multi-node thermoregulation (65MN) and radiation models and computational fluid dynamics (CFD). *Energy and Buildings*, 34(6), 637–646.
- Theissen, P. (2015). *Influence of over-head ventilation/cooling on thermal comfort* (Term thesis). TUM, München.
- ANSI/ASHRAE 55-2010 (2010). *Thermal Environmental Conditions for Human Occupancy*.
- TUM. *Main research, Institute of Automotive Technology*. Retrieved from <http://www.ftm.mw.tum.de/en/main-research/>*, Access Date: 10/1/2016.
- TUM CREATE. *EVA - electric taxi for tropical megacities*. Retrieved from www.eva-taxi.sg*, Access Date: 1/12/2014.
- DIN EN ISO 7726:2001 (2002). *Umgebungsklima - Instrumente zur Messung physikalischer Größen*.
- ECE-R125:2 (2013). *Uniform provisions concerning the approval of motor vehicles with regard to the forward field of vision of the motor vehicle driver*.
- Volkswagen. (2002). Der Touareg Heizung und Klimaanlage: Konstruktion und Funktion. *Selbststudienprogramm*, 301.
- DIN EN 27243:1993 (1993). *Warmes Umgebungsklima - Ermittlung der Wärmebelastung des arbeitenden Menschen mit dem WBGT-Index (wet bulb globe temperature)*.
- Watanabe, S., Shimomura, T., & Miyazaki, H. (2009). Thermal evaluation of a chair with fans as an individually controlled system. *Building and Environment*, 44(7), 1392–1398
- Webb, C. G. (1959). An analysis of some observations of thermal comfort in an equatorial climate. *British Journal of Industrial Medicine*, 16(4), 297–310.
- Webb, C. G. (1960). Thermal discomfort in an equatorial climate: A Nomogram for the Equatorial Comfort Index. *Journal of the Institution of Heating and Ventilating Engineers*, 27, 297–304.
- Wellcool. *Spacer fabric products*. Retrieved from <http://www.wellcool3d.com/product/>*, Access Date: 2/12/15.
- Williamson, T. J., Coldicutt, S., & Riordan, P. (1995). Comfort, Preferences, or Design Data? In F. Nicol, M. Humphreys, O. Sykes, & S. Roaf (Eds.), *Standards for thermal comfort. Indoor air temperature standards for the 21st century* (pp. 50–58). London: Chapman & Hall.
- Zhang, H. (2003). *Human thermal sensation and comfort in transient and non-uniform thermal environments* (Dissertation). University of California, Berkeley.
- Zhang, H., Arens, E., & Arens, C. (2002). Using a Driving Game to Increase the Realism of Laboratory Studies of Automobile Passenger Thermal Comfort. *SAE Technical Paper Series*, 2003-01-2710.
- Zhang, H., Arens, E., Huizenga, C., & Han, T. (2010). Thermal sensation and comfort models for non-uniform and transient environments, part III: Whole-body sensation and comfort. *Building and Environment*, 45(2), 399–410.
- Zhang, H., Huizenga, C., Arens, E. A., & Yu, T. (2005). Modeling Thermal Comfort in Stratified Environments. In *Indoor Air 2005. Proceedings of the 10th International*

Conference on Indoor Air Quality and Climate. Beijing, China: Tsinghua University Press.

Zhang, L., Helander, M. G., & Drury, C. G. (1996). Identifying Factors of Comfort and Discomfort in Sitting. *Human Factors: The Journal of the Human Factors and Ergonomics Society*, 38(3), 377–389